AD

USAAVLABS TECHNICAL REPORT 64-68L

HEAVY-LIFT TIP TURBOJET ROTOR SYSTEM
VOLUME XII
FUEL PUMP AND CONTROL SYSTEM DESIGN

CAE REPORT No. 943

October 1965

U. S. ARMY AVIATION MATERIEL LABORATORIES
FORT EUSTIS, VIRGINIA
CONTRACT DA 44-177-AMC-25(T)
HILLER AIRCRAFT COMPANY, INC.
CONTINENTAL AVIATION AND ENGINEERING CORPORATION
CHANDLER-EVANS CORPORATION

BLANK PAGES
IN THIS
DOCUMENT
WERE NOT
FILMED

DDC Availability Notices

Qualified requesters may obtain copies of this report from DDC.

This report has been furnished to the Department of Commerce for sale to the public.

Disclaimers

The findings in this report are not to be construed as an official Department of the Army position, unless so designated by other authorized documents.

When Government drawings, specifications, or other data are used for any purpose other than in connection with a definitely related Government procurement operation, the United States Government thereby incurs no responsibility nor any obligation whatsoever; and the fact that the Government may have formulated, furnished, or in any way supplied the said drawings, specifications, or other data is not to be regarded by implication or otherwise as in any manner licensing the holder or any other person or corporation, or conveying any rights or permission, to manufacture, use, or sell any patented invention that may in any way be related thereto.

Trade names cited in this report do not constitute an official indorsement or approval of the use of such commercial hardware or software.

Disposition Instructions

Destroy this report when it is no longer needed. Do not return it to the originator.

Task 1M121401D14412
Contract DA 44-177-AMC-25(T)
USAAVLABS Technical Report 64-68L
October 1965

HEAVY-LIFT TIP TURBOJET ROTOR SYSTEM

VOLUME XII

FUEL PUMP AND CONTROL SYSTEM DESIGN

CAE Report No. 943

Prepared for

HILLER AIRCRAFT COMPANY, INC.

by

CONTINENTAL AVIATION AND ENGINEERING CORPORATION

and

CHANDLER-EVANS CORPORATION

for

U. S. ARMY AVIATION MATERIEL LABORATORIES
FORT EUSTIS, VIRGINIA

(U. S. Army Transportation Research Command when report prepared)

PREFACE

This report, prepared by Continental Aviation and Engineering Corporation, covers the design of the fuel pump and fuel control for the Continental Model 357-1 tip turbojet engine. This work was accomplished under Hiller purchase order HAC-1-64, Contract DA 44 177-AMC-25(T), and conducted by Chandler Evans Corporation, West Hartford, Connecticut, under subcontract to CAE.

The fuel control system requirements were analyzed, with the most serious attention being given to the extremely high g forces under which the control will operate. A complete system design was prepared after study and design of each of the components.

This report is one of a series of three documents submitted to fulfill the requirements of Hiller purchase order HAC-1-64, Article 1 Statement of Work, Item (3)(e). The reports include:

"Continental Model 357-1 Tip Turbojet Engine - Engine Design," Heavy-Lift Tip Turbojet Rotor System, Volume XI, CAE Report No. 942, U.S. Army Transportation Research Command, Fort Eustis, Virginia, June 1965.

"Continental Model 357-1 Tip Turbojet Engine - Fuel Pump and control System Design," Heavy-Lift Tip Turbojet Rotor System, Volume XII, CAE Report No. 943, U.S. Army Transportation Research Command, Fort Eustis, Virginia, June 1965.

"Continental Model 357-1 Tip Turbojet Engine - Preliminary Model Specification," Heavy-Lift Tip Turbojet Rotor System, Volume XIII, CAE Model Specification No. 2253, U.S. Army Transportation Research Command, Fort Eustis, Virginia, June 1965.

CONTENTS

ILLUSTRATIONS

ILLUSTRATIONS

ILLUSTRATIONS

ILLUSTRATIONS

INTRODUCTION

This report presents the design of a fuel pump and control system for the Continental Model 357-1 tip turbojet engine. At the initiation of this program, it was apparent the problems of designing and developing a fuel control and fuel pump for a tip turbojet application would be severe. The major difficulty was due to the extremely high g field, which rendered many conventional concepts of parameter measurement and system mechanization impossible, as well as the effect of extreme variation in fuel pressure supplied to the engine, which creates structural and sealing problems in itself.

BASIC CONTROL DESIGN

Chandler Evans Corporation was selected to design the control system because of their success with the J69-T-29 engine fuel control (the basic engine from which the Model 357-1 is derived), as well as their experience and familiarity with the fuel control of gas turbine engines in conventional helicopters. Chandler Evans Engineering Report No. R-194, describing the control system design, is included in this report.

FORWARD FLIGHT CONTROL REQUIREMENTS

Engine control during hover conditions is a known art with the exception of operating in a high g field, which is covered herein. Forward flight conditions, however, introduce variables which are difficult to predict and are not encountered in any other application.

During hover, the engine operates at a constant flight speed equal to the rotor tip speed - in this case, 420 knots. During forward flight, the airspeed encountered by the engine varies from this figure through a range of plus and minus 125 knots at maximum flight speed, and this cycle occurs approximately two times per second in the application under consideration. The resulting change in ram effect causes changes in engine pressure ratio and airflow which result in changes in thrust as shown in Figure 1. This figure is derived from Figure 2 by plotting thrust versus airspeed along constant engine r.p.m. lines over the speed range of 420 knots plus and minus forward flight speed.

Inlet losses cause certain additional loss of thrust when the engine axis is not parallel to the direction of flight since the resultant ram into the nacelle is not parallel to the engine axis, and distortions

in pressure and flow result. Tests were run on a J69-T-29 engine to determine the effect of known inlet distortions; test results will be verified when the engine nacelle design is evaluated during wind-tunnel testing. These factors do not affect the maximum and minimum thrust available as a result of forward flight speed and so do not affect the control problem of limiting the magnitude of the change in turbine inlet temperature to values consistent with good engine life.

In order to determine the effect of the change in actual engine flight speed on engine performance, an initial analysis was made to determine the extremes to which the forward flight condition might move engine parameters such as turbine inlet temperature, engine speed, fuel flow, and thrust if no fuel control compensation were affected. For the purpose of these analyses, instant engine response, zero fuel transfer time, and zero inlet loss were assumed, so that the engine is assumed to have reached stable operating conditions instantly at each mode condition.

A set of generalized performance curves of corrected fuel flow and turbine temperature ratio were prepared for the engine and are shown in Figure 3.

The engine inlet conditions at several points of rotor location during the rotor rotation were then computed; that is, for the advancing blade and retreating blade. The mode conditions at fixed engine speed or fixed fuel flow were then imposed and the corresponding parameters calculated from the generalized curves. The results of this process are shown in Figures 4 and 5.

Analyses of the change in turbine inlet temperature at constant engine speed, change in turbine inlet temperature at constant fuel flow, and fuel flow change at constant turbine inlet temperature were made for 100-knots flight speed at 60-percent power (cruise condition) and 125-knots flight speed at 100-percent power (emergency climb condition). These studies, with the assumptions that were made, determined the maximums and therefore present the extreme requirements for fuel flow compensation in order to limit the excursions of turbine inlet temperature to values compatible with good engine life. They show that the change in turbine inlet temperature when fuel flow is constant is too great (plus 156°F to minus 72°F) so that fuel flow changes are required during the cyclic variations in ram. The temperature changes, when engine r. p. m. is held constant, are not excessive and it was decided that fuel control based on holding engine speed

constant would be satisfactory. The governor selected will accommodate the necessary flow variations in the time available for making the change.

It should be remembered that the values shown in Figures 4 and 5 assume instant engine response time. When engine inertias are factored into the analysis they will reduce the magnitude of the change in the parameters which have been plotted. The engine inertia will cause the engine speed to lag behind the instantaneous value assumed and will reduce the amplitude of the speed change. This will in turn reduce the amplitude of the engine airflow change and the amplitude of the turbine inlet temperature change as well.

Fuel transportation time is the length of time required for a change in fuel flow to travel from the control and result in a change in engine performance. In the J69-T-29 engine this time lag is 0.15 to 0.25 second in duration, depending on engine speed, and consists primarily of dwell time in the fuel slinger. The g field at the rotor tip may make significant changes in this value, but the magnitude of the change cannot be determined until whirl testing of the engine is underway. However, transportation lags of this duration are equivalent to a change in rotor position of approximately 100°, and when engine inertias are factored in this phase, lag may approach 180°. This suggests that an anticipatory circuit is required to ensure that the changes in fuel flow required to hold engine speed constant reach the burner at the proper time.

The circuit shown in Figure 6 has been devised to accomplish the necessary anticipation in fuel flow changes. It represents the extreme in control devices which could be required. Regardless of the type of fuel flow variation required and its phase of relationship with rotor position, this system will maintain control of the engine within the desired limits.

The device labeled "Flight Speed Compensator," Figure 6, would measure as input parameters: $P_{total\ hel}$, the total air pressure measured in the direction of flight; $P_{static\ hel}$, the static air pressure; θ_{rotor}, the angular position of the rotor blade with respect to the longitudinal axis of the helicopter; and B_{rotor}, the rotor blade collective pitch setting (as a measure of engine power level). It would then compute the change in fuel flow necessary to keep engine speed constant as a function of blade position. This change in fuel

flow would be superimposed on the engine-controlled fuel flow at the proper time to have the desired effect on engine performance. The computer would be mounted in the aircraft and would furnish its electrical signal to each engine as it reached the significant position.

Should whirl testing reveal that engine response time and reduced fuel transportation time reduce turbine inlet temperature changes as is expected, other simpler circuits are available and will be employed. Since the computer is to be mounted in the aircraft away from the rotor tip g field, development problems are at a minimum and simplification of design can be readily accomplished.

SUMMARY

This report contains the result of a study contract from CAE to design and lay out a fuel control which would operate a rotor tip mounted engine (CAE Model 357-1) in a 235g field.

Based on preliminary tests and analytical design studies, the fuel control system recommended is a combined hydromechanical and electronic control system which includes an engine-driven fuel pump. Figure 7 is a schematic of the control system. Studies indicate that the proposed design can be developed so that production components can be assembled without requiring special whirl-rig-component balancing tests.

The design philosophy is based on power amplifying input signals to high force levels, thereby minimizing the force output requirements of the input signal sensors due to erroneous forces produced by the g field. Also, by power amplifying input signals, precise balancing of linkages, shafts, and so forth is not required. The effect of the g field on the primary sensing and feedback elements can be minimized by proper orientation. Preliminary tests show that springs and bellows can withstand the g field in a lateral direction with negligible change in the axial force. This concept is validated in the appendix of this report.

The proposed design utilizes state-of-the-art components. Therefore, the development effort will be concerned primarily with the details of testing to determine the effects of the g field on control accuracy.

CONCLUSIONS

1. Sufficient design data are presented herein to permit a detail design and fabrication of the fuel control and fuel pump for subsequent whirl testing to substantiate the design in the high g field.

2. A major difficulty in the design of the system has been to ensure operation in the extreme g field at the rotor tip.

3. Engine control difficulties due to the cyclic variation of inlet conditions are difficult to analyze and will require engine test data from simulated operation to determine their magnitude and any requirements for special control system functions.

4. A study of control requirements for operation under conditions of forward flight must be postponed until transient data from engine whirl stand testing is obtained.

1. TECHNICAL BACKGROUND

This report contains the Chandler Evans Corporation findings in a study program authorized by Continental Aviation and Engineering Corporation. The study was conducted to fulfill the following work statement, in accordance with the requirements of Reference 1.

1.1 Work Statement

As provided by the Continental Aviation and Engineering Corporation, the vendor shall furnish the following:

a) A fuel system design report describing a fuel system design in accordance with Reference 1 with discussion covering the reasons for selection of components and type of design, and so forth.

b) A layout of the fuel system design suitable for detailing.

c) Engineering assistance and coordination with CAE personnel in the establishment of satisfactory installation provisions and criteria for the fuel system designed.

d) Monthly progress reports due at CAE the 15th of each month.

1.2 Engine Operating Requirements

The engine operating requirements are specifically stated in the CAE fuel control specification, Reference 1, and excerpts from this specification are provided as a recapitulation of the more important requirements.

To protect the engine from surge and overtemperature and also to permit rapid engine acceleration, the acceleration fuel schedules as provided in Figure 8 are required. The engine required steady-state schedules are depicted in Figure 9. Acceleration schedules are to be maintained within an accuracy of $\pm$ 3 percent or $\pm$ 20 p.p.h., whichever is greater.

Engine speed is to be controlled within $\pm$ 1 percent of the 100-percent speed condition and within $\pm$ 5 percent at the 50-percent speed

condition. As discussed in paragraph 6. of this report, these controlled engine speed requirements will be met for operating conditions wherein the rotor is whirling but the aircraft forward flight speed is zero. A more rigorous nonlinear dynamic analysis must be performed, which cannot be conducted with data now available, to specify and design a control which will hold engine speed constant during forward flight speed of the aircraft.

The fuel control system is to operate in accordance with the requirements of Reference 1 over the following conditions of operation:

a) Altitude - sea level to 25, 000 feet

b) Ram pressure ratio - 1 to 1. 7

c) Ambient temperature - in accordance with Figure 1 of MIL-E-5007B

d) Force field at engine - 0 to 259g

The acceleration force field of (d) will, under normal conditions, be 235g with transient loads to 259g for periods up to 1 minute. The control system shall be designed to withstand peak loads of up to 367g without structural failure.

The fuel control system must be capable of continuous operation when supplied by air at ram or ambient temperatures from -67° to +130°F in the tanks. The effects of the installation on fuel temperature are to be determined.

2. DESIGN CRITERIA

2. 1 Major Control Considerations

Due to the location of the engines at the tip of the rotary blade, an unusually large acceleration force becomes apparent. It has been specified that this loading can range in magnitude from 0 to 367 times gravity in the plane of rotation of the blade. It is this artificial gravitational field which causes major considerations to be given to areas which in fuel control systems of conventional applications would require no special attention.

Any method of signal sensing and conversion for computation purposes which relies upon a force calibration, such as pressure regulators, pressure transducers, and force feedback servo systems must be designed to be insensitive to the artificial g field.

Since fuel will be supplied through the rotor blade to the engines, the blade will act as a centrifugal pump which develops pressures upwards of 3000 p. s. i. at the control inlet. Consideration may therefore be given to the possibility of eliminating the normally required engine-driven fuel pump. In any event, the handling of the high fuel pressure levels with regard to maximum control pressure limits, fuel bypassing capability for hydraulically operated servo systems, and fuel shutoff must be carefully considered.

Structural considerations due to the high force levels and component orientation must also be specially considered.

2.2 Outline of Study

After examining the engine requirements, the basic functions which the control must perform were established. A block diagram representation of the control was prepared as illustrated in Figure 10.

Before the study concerning the component mechanisms and the system considerations was begun, certain limitations and conditions were set up to concentrate the study effort in the most useful areas.

a) A limitation was set up that only present state-of-the-art methods would be considered.

b) A condition was established so that whirl tests to permit balancing of any part of the control for operational purposes would not be required after the control is developed. This would not rule out the whirling of each unit as a test procedure upon final calibration to ensure the control's insensitivity to the g field. In other words, manufacturing tolerance and design technique must in themselves render the control insensitive to the g field.

c) A second simplifying but reasonable condition is that the direction of the g loading can be predicted and will remain within $\pm 2^{o}$ of that direction.

With the limitations and conditions set up, the study was continued on the basis of investigating various methods of sensing, converting, and amplifying the engine parameters to outputs which could be used for computing the required control schedules and yet be sensitive to the g field. Various modes of computing were next investigated along with system studies, and then the combination of elements evidencing the least development effort and most probability for success were joined to form the schematic for the control system, Figure 7. By this reasoning, alternate methods of design which require considerably more development effort may provide a more simplified design. However, it was considered more important to select a design which would provide satisfactory operation as a primary goal, with the capability for simplification as a secondary goal.

A preliminary investigation of the effects of forward flight on engine-control operation was conducted. It was discovered that one of the major engine parameters affecting the system response is the fuel system delay time. This delay time is defined as the time required for a change in fuel flow occurring at the fuel control to be reflected as the initiation of a change in engine speed. The major part of this delay time is the transport time required for fuel entering the fuel tube leading to the fuel slinger to be injected into the combustor. It is anticipated the g field in which operation is intended will have a major effect on this delay time, and that this effect will be unpredictable. Therefore, it was decided that determination of control modifications or additions, if any, which would be required to accommodate forward flight, must be postponed until whirl stand engine testing has been accomplished and transient data is available.

Specific design of the system was then undertaken to a sufficient extent so that a typical layout drawing of the proposed control could be prepared.

3. SYSTEM SELECTION

The schematic diagram of Figure 7 depicts the fuel pumping and control system which has been selected on the basis of the study conducted.

3.1 Functional Description of Control System Selected

The control system design which has resulted from this study is shown schematically, Figure 7. It is a combination of hydromechanical and electronic design, and depends upon servo systems

providing forces which render negligible the effects of the g field, and upon orientation of springs, bellows, and so forth in such a fashion as to nullify the effects of the g field upon the accuracy of the measurements these components are used for.

Referring to the schematic diagram, fuel from the rotor (P_R) enters the control and passes through the upstream shutoff valve. This valve, closed when the power lever is placed in the "off" position, prevents high pressure fuel entering the case under no flow conditions. The fuel then passes through two stages of inlet pressure regulators which function by throttling the incoming flow. These (one coarse and one fine regulator in series) reduce the incoming fuel pressure to a normal value such that conventional hydraulic circuitry can be used in the control, as well as reducing the structural requirements of the control casing. Both regulators are vented to ambient pressure through a safety shutoff valve which will prevent leaks in case of internal failure. Downstream of the regulators is a safety shutoff valve which will prevent high pressure fuel from entering the control in the event of a double regulator failure.

The fuel then passes through a screen into the inlet to the gear pump. The pump is mounted with the gear centerlines vertical to the g field, such that the g forces tend to balance the pressure forces and unload the pump bearings.

From the pump the fuel goes to a metering head regulating valve. This valve is positioned by pump discharge pressure (P_F), operating against the valve end opposed by metered pressure (P_M) and spring force operating against a diaphragm, of area equal to the valve, and maintains a constant metering head (pressure differential) across the metering valve by bypassing excess flow back to pump inlet. This allows the flow delivered by the control to be established entirely by the area of the metering valve. Just ahead of the metering valve is a cross-wash, self-clearing filter which provides clean fuel for the hydraulic servo circuits in the control.

Downstream of the metering valve is a pressurizing valve which maintains the system pressure high enough (above engine back pressure) to ensure adequate functioning of the bypass system. The flow then passes through the downstream shutoff valve and into the engine. This valve, when closed, bypasses metered flow back to pump inlet, and prevents the control from being drained by g forces in the event of in-flight shutdown.

As mentioned previously, the metered flow delivered to the engine is established by the position of the metering valve. The metering valve is positioned by a spring which maintains the valve in contact with a pushrod (unless restrained by maximum and minimum stops which establish maximum and minimum flow settings). The pushrod position is established by a mechanical multiplying linkage as the product of the compressor discharge pressure signal (P_{cd}) and the fuel flow/compressor discharge pressure ratio (W_f/P_{cd}) established by the 3D (three-dimensional) cam acceleration and governing circuits.

The compressor discharge pressure is measured by a bellows opposed by an evacuated bellows of equal area, such that the force produced is a function of the absolute value of the P_{cd}. This force is transmitted by means of a lever to a flapper valve which controls the flow through a half area type of servo. Opening the valve causes flow to pass through the servo piston orifice creating a pressure drop which forces the piston to the left. This, in turn, compresses the feedback spring until the spring forces match the bellows force and moves the valve toward "closed." Closing the valve equalizes the pressure on both sides of the piston, causing the pressure to operate on the area of the piston rod forcing piston and rod to move to the right, reversing the action. Thus, the output of this system sets the position of the double rollers in the W_f/P_{cd} multiplier as a function of the absolute value of the compressor discharge pressure. The roller position in turn establishes the radius at which the W_f/P_{cd} lever from the computer circuit drives the metering valve pushrod.

The computer circuit establishes the position of the W_f/P_{cd} lever as a function of engine speed and inlet air temperature for acceleration limiting (from the surface of the 3D cam), and as a function of engine speed and power lever position (again compared as a second surface on the 3D cam) for governing.

Engine speed is measured with a variable reluctance magnetic pickup and transmitted to an electronic control box. This is compared with the cam position, measured in the same fashion, and the results used to energize a stepper motor which, through a gear train, rotates the 3D cam.

The inlet air temperature (T_1) is measured by a cymene-filled bellows, around which inlet air is induced to flow by a P_{cd} powered ejector. The output of this bulb is the mechanical position of a

lever whose opposite end is attached to the pilot valve of a followup servo, which in turn establishes the axial position of the 3D cam in a manner analogous to the P_{cd} servo system. Thus, the axial position of the cam is a function of the engine inlet air temperature.

For acceleration limiting, the W_f/P_{cd} lever is positioned with its follower in direct contact with the cam (shown on the left side of the cam in the schematic).

For governing, the speed set cam is positioned by the power lever, and measured by a lever having a variable pivot. This pivot is on a second lever in contact with the surface of the cam. The second lever controls the position of the pilot valve in the governor power amplifier. This will cause the amplifier power piston to move to the left if the speed setting is approached by the position of the cam. As it moves to the left, the first lever is contacted by a pin in the piston rod, moving the first lever and its pivot point in a manner which will return the pilot valve to a null position. As this process continues with increasing speed, the power piston and its output rod will move to the left until the W_f/P_{cd} lever is contacted on the left side of the 3D cam. Further movement reduces the W_f/P_{cd} setting and hence the fuel flow.

The selection remains within the original limitations established in (a) and (b) of paragraph 2.2 These limitations were that no special whirl tests would be required to permit balancing of the control components for performance reasons and that only state-of-the-art components would be used.

The system uses components which are accurate with regard to scheduling performance. The 3D cam permits the scheduling of acceleration fuel flow so that optimum engine response may be achieved. Also, fuel schedule changes may be made readily with the replacement of the 3D cam. Governor droop rates and gain changes may be made with minor modifications and linkage replacements.

The number of critical components susceptible to the g field have been reduced to two, and, in addition, their orientation has been so established that the g field effect is minimized. Amplication is provided at high force levels through the use of a readily available servo fuel and electrical power so that the effect of g field on the linkages used in the computation mechanism is of second order.

The components requiring the least development effort, and therefore offering the greatest possibility of success, were selected in all cases.

4. DESCRIPTION AND DESIGN OF SELECTED SYSTEM

A detailed design analysis of the componerts of the selected system has been made in order to ensure adequate performance and permit the preparing of a typical layout drawing. A description of operation for the system and each individual component together with the design analysis is presented in the following paragraphs.

4.1 Description of System Operation

The fuel control system is basically a W_f/P_{cd} scheduling mechanism. The system performs the function of pumping and scheduling fuel flow to the engine to permit starting, acceleration, speed governing, deceleration, and shutoff.

The computer system receives the engine-sensed inputs and provides the intelligence and muscle for positioning the metering valve in the metering section of the control. A relatively constant pressure drop is regulated across the metering valve flow area so that a given valve position represents a given fuel flow.

In the pumping and metering section of the control, the functions of boost pressure regulation, fuel pumping, igniter flow supply, main fuel metering, servo fuel pressure generation, cut-on and shutoff are accomplished.

Engine Start-Up

To start the engine, the igniter flow solenoid is energized and the throttle advanced to the ignite position. The upstream shutoff valve will be open, but the downstream shutoff valve will remain closed. Flow will be admitted to the engine through the igniter-flow solenoid-operated valve. Since there will be difficulty in positively sealing any throttling regulator to maintain a controlled downstream pressure for a "no flow" condition, it is imperative that the igniter flow port be open to permit a leakage path to the engine before the upstream shutoff valve is opened. This is especially true if the rotor is whirling near its top speed. The throttling regulators will be designed to

operate at a minimum leakage value, but this value cannot approximate zero. Concurrently, flow will be circulating through the control to pump inlet through the bypass port in the downstream shutoff valve. This flow circulation will permit generation of sufficient servo fuel pressure to allow positioning of all the hydraulically operated servo systems.

After engine light-off and the correct engine speed is achieved, main flow will be initiated by advancing the throttle to the idle speed or any higher speed setting. This advancement opens the downstream shutoff valve permitting metered flow to be admitted to the engine. The engine will accelerate toward the higher speed setting.

Governing

As the engine approaches the new set speed, the govenor setting will be exceeded by the actual speed and the governor servo system will begin to cut back on the W_f/P_{cd} setting. As the governor-set W_f/P_{cd} reduces to a lower value than the acceleration-set W_f/P_{cd} the governor will be in control of fuel flow. Fuel flow will continue to be reduced in proportion to positive set speed error until the control metered flow is at the engine steady-state required-to-run fuel flow level. At this condition the engine speed remains fixed for the governor setting. The setting of a relatively higher speed will revert control of W_f/P_{cd} back to the acceleration limiter and the engine fuel flow will increase to its maximum permissible level for surge free and temperature-limited acceleration. Maximum engine acceleration will result until a positive set speed error occurs at which time the governor will again take control to maintain a constant engine speed.

Deceleration is accomplished by reducing the throttle lever to any lower speed. Here, the set speed error becomes considerably positive and fuel flow is reduced below the engine steady-state fuel flow to a minimum flow level set by a mechanical stop. This causes the engine to decelerate until the governor set speed error becomes less positive, thereby allowing fuel flow to rise again until a steady-state flow level at the lower speed is achieved. Again, speed will be held constant.

Shutdown

The engine is shutdown by retarding the throttle to the fuel shutoff position. This action first closes the upstream shutoff valve

and next the downstream shutoff valve. Although the shutoff may be executed at any flight condition, it is recommended that for normal shutdown, the rotor speed be reduced to its minimum level before final shutoff is executed. As the pump windmills to a stop after shutdown, fuel will be bypassed through the downstream shutoff valve to pump inlet, thus preventing pump dead heading.

4.2 Design

4.2.1 Inlet Throttling Regulator (Reference Figure 11)

The regulator operates to control the pump inlet pressure (P_B) to a level above ambient pressure (P_o) by throttling through two stages the incoming rotor pressure (P_R). The valves are of the poppet type to minimize leakage and are balanced with a spool and sleeve design. The valves are sized to operate at leakage levels of less than 40 p.p.h. at the high pressure levels which will be encountered during the condition of engine relight while the rotor is whirling. A diaphragm provides the balancing mechanism for regulation and the driving force for positioning the poppet valve in the second stage while an "O"-ring sealed piston is used in the first stage. The g load will be applied in a lateral direction.

In the ambient chamber of each valve a safety vent valve is included. In case of a diaphragm or piston "O"-ring failure, the safety vent valve will be closed by the differential of fuel to ambient pressure applied across the vent valve, thereby containing the high pressure fuel within the regulator housing.

For small valve openings, the equation representing the regulation performance of the second-stage valve is as follows:

$$P_B - P_o = \frac{F_s}{A_D} = \frac{K_s W_f}{59750\ Cd\ Dv\ AD\ \sin\theta \sqrt{(P_B' - P_B)\ Sp\ Gr.}}, \text{ p.s.i.}$$

For the first-stage valve, substitute P_B' for P_B and P_R for P_B',

where for		1st stage	2nd stage
F_s	=	400 lb	33 lb
A_D	=	0.3 $in.^2$	1.0 $in.^2$
Dv	=	0.375 in.	0.375 in.
θ	=	60^o	60^o
K_s	=	2000 lb/in.	150 lb/in.

Specific Gravity = 0.775
Cd (discharge coefficient) = 0.70

Plots of the valve performance, neglecting any flow force effects, for the anticipated flow and pressure ranges are depicted in Figure 12. The maximum flow-force effect calculated for the downstream valve is of the order of 7.0 pounds. Without compensation for the flow force, an additional 7 p.s.i. variation in regulated pressure would be experienced. If proven to be significant, the flow force effects can be minimized by properly flow contouring the valves. The error in regulated P_B pressure due to a $\pm$ 2° variation of direction of the applied g field from the lateral direction is only 1.2 p.s.i. on either valve, an insignificant amount. An axial g load of $\pm$ 5g would contribute an error of approximately 0.7 p.s.i., again, an insignificant amount. The friction effect of the piston in the first-stage valve will contribute a hysteresis in regulation of approximately 60 p.s.i. This is a negligible amount, however, since this stage is only required for approximate regulation. The friction effect due to g loading the valve in the lateral direction is approximately 4.0 p.s.i. in the first stage and 1.2 p.s.i. in the second stage.

An acceptable variation for regulation of the pressure differential $P_B - P_o$ has been set at 70 to 30 p.s.i. The allowable limitation on the variation in regulation of this pressure differential is established on the basis of the minimum servo supply pressure desired and the maximum pump pressure rise at cranking speed. This limitation is explained in paragraph 4.2.5.

The safety shutoff valve is normally open and closes if the regulated P_B pressure exceeds 150 p.s.i. due to the differential area of the piston. Once the valve closes it will remain closed as long as the upstream pressure exceeds 85 p.s.i.

The safety shutoff valve design constants are as follows:

D_P = 0.875 in.
F_s = 40.0 lb.
Dv = 0.50 in.

4.2.2 Fuel Pump (Reference Figure 13)

The pump is of the single-element, positive displacement, pressure-loaded gear type, having a 40-mesh fuel screen at its inlet.

The pump incorporates a bypass return port at its inlet to serve as the sump for the control servo and bypass regulator flows. The shaft seal configuration is of the CECO-designed cartridge type which has proven successful on numerous CECO pump applications. The pump is fabricated from a cast aluminum housing with Nitralloy gears and drive shaft. Bearing material is high-leaded bronze. Because of the compact lightweight design, the inherent ruggedness, and the well-supported drive shaft and seal configuration, no problems are anticipated as a result of the centrifugal forces involved.

For the high centrifugal loads peculiar to this application the pump has been oriented such that the centrifugal forces will increase the journal bearing pressure loading. In this way the low starting requirement can be met with the rotor whirling. Bearing loads have been maintained within safe limits of approximately 600 p. s. i. as demonstrated herein.

Weight of pumping gear - 0. 55 pounds
Centrifugal force, max. - 367g
Bearing load due to CF - 0. 55 x 367 = 200 pounds
Bearing load due to pressure loading = Gear OD x gear width x discharge pressure
= 1. 50 x 0. 816 x 400 = 515 pounds
Total load on bearing = 200 + 515 = 715 pounds

$$\text{Journal UBL} = \frac{715}{0.688 \times 1.6} = 650 \text{ p. s. i.}$$

Note also that the g loading force is greater than the pressure loading area; therefore, had the pump been oriented so that the g loading was subtracted from the bearing loading, there would be a shift in direction of the bearing loading. This shift would produce a loss in pump capacity and detrimental wear on the pump housing which would prematurely limit pump life.

The pump has been designed to operate on fuel which has passed through a 10-micron filter. This filter is not included in the pump design but is to be located in the air frame and will be the airframe manufacturer's responsibility.

The pumping element is designed to meet the starting conditions of 450 p. p. h., 150 p. s. i., and 750 r. p. m. This element will then give rated flows as follows: 6950 p. p. h., 400 p. s. i., and 7500 r. p. m. A plot of the flow-versus-speed curve is shown in Figure 14.

The pump inlet boost requirements are based on the following conditions and assumptions which yield the worst case:

Fuel Type: Aviation Gasoline

Operating Conditions:

T_1 = 20°F at 30,000 feet altitude
T_{max} = 130°F after climb from S. L. hot day
N = 90 percent = 6750 r.p.m., ΔP = 130 p.s.i.
W_f metered = 415 p.p.h.
Metered flow to bypass flow = 5.76 percent
Based on CECO experience, pump rise = 50°F for these conditions.

Therefore,

Temperature of fuel at pump inlet =

+ 115° (assumed 15° net cooling in rotor blades)
+ 15° throttle regulator
+ 50° = 180°F

Pressure required = 30 p.s.i.a. (vapor pressure)
= 10 p.s.i. to charge gears
40 p.s.i.a. boost

A similar analysis may be shown for a locked rotor, 100-percent speed at sea level, and a hot day wherein the required pressure at the throttle regulator inlet is 40 p.s.i.a.

Adding a safety factor, then the tank-mounted boost pump should supply a minimum of 30 p.s.i.g. to the throttle regulator inlet. The throttle regulator will then be designed to operate at a minimum regulated pressure level of 30 p.s.i.g. and permit a maximum of 10 p.s.i. pressure drop through the valve at a flow of 1275 p.p.h. when not regulating.

4.2.3 Metering Head Regulator (Reference Figure 15)

The regulator maintains an essentially constant pressure drop across the metering valve by bypassing pump discharge pressure back to the pump inlet (P_B). The valve is of the poppet type, its shaft supported on a ball bushing. A diaphragm opposed by the poppet valve

provides the pressure differential sensing area and also the pressure force for positioning the valve.

The equation describing the valve regulation for small openings follows:

$$P_F - P_M = \frac{F_{PL}}{A_D} + \frac{K_s W_f}{59670 \text{ Cd Dv Sin } \theta \sqrt{(P_F - P_B) \text{ Sp. Gr.}}}$$

where, for the selected design

A_d = 0.785 in.^{2}
Dv = 1.00 in.
θ = 60°
K_s = 50 lb/in.
Cd = flow discharge coefficient = 0.7
Sp. Gr. = 0.775

The performance of the regulator to these design constants is plotted in Figure 16. The metering head has been selected to be 40 p. s. i. and the error in metered flow due to the metering head error is desired to be less than 1 percent. Since error in metered flow is proportional to metering head error in the following manner,

$$\text{Error in percent metered flow} = \frac{50 \Delta \text{ MH}}{\text{MH}},$$

then the error in metering head can be $\pm$ 0.8 p. s. i.

The variation in metering head regulation indicated in Figure 16, if taken at face value, would be too great for accuracy purposes. Since, at any given metered flow, the variation in bypass flow and pressure differential ($P_F - P_B$) is limited and predictable, it is therefore possible to contour the metering valve accordingly to the average metering head value which will occur due to these variations at any given metered flow. By this means, the performance depicted in Figure 16 is acceptable with an adequate safety factor for meeting the control acceleration and governing limits.

The valve will be oriented such that the high g field will be directed laterally to the axis of the valve, spring, and diaphragm. The ball bushing will minimize any friction effects which will be introduced by the g field to negligible amounts.

Due to the weight of the valve, spring, and diaphragm, a directional change of the g field by $\pm 2^{o}$ will cause a metering head error of approximately $\pm$ 0.5 p.s.i. at 259g. In addition, a loading of 5g in the axial direction would cause approximately $\pm$ 0.2 p.s.i. If all the errors mentioned above were cumulative, which is not a likely situation, then the metered flow could be in error by approximately $\pm$ 1.5 percent as a result of the metering head regulator.

4.2.4 Metering Valve

The valve is of the sleeve type design with a slab cut to provide the required area versus stroke. In conjunction with the design of the multiplier described in paragraph 4.2.10 the valve is spring loaded in the open direction and is driven closed by the power of the servo systems (compressor discharge pressure and 3D cam). The valve is essentially pressure balanced to more closely control the servo system applied forces although this is not absolutely necessary.

The valve area will be contoured in accordance with the 40 p.s.i. nominal metering head to provide an essentially constant flow-versus-stroke relationship of 10 p.p.h. per 0.001 inch. Minor deviations from this relationship will be made as necessary based on the discussions in paragraphs 4.2.3 and 4.2.8. The profile of the valve will be essentially as depicted in Figure 17.

The spring force loading the valve in the open direction will vary about 4 pounds as the valve strokes, with the maximum being of the order of 10 pounds. Orienting the valve so that the g field will be applied laterally to the axis of the valve will introduce some frictional effects to resist the motion of the valve. However, the friction will be of the order of 1.0 pound at 367g and will, therefore, be of negligible consequence in the ability to position the valve.

4.2.5 Pressurizing Valve (Reference Figure 18)

The function of the pressurizing valve is to raise the level of fuel pressure within the control to ensure that a minimum positive differential of $P_F - P_B$ equal to 100 p.s.i. exists under all operating conditions. This is required to operate the servo systems and the bypass metering head regulator.

For the worst operating condition, the cracking pressure (ΔP_V) must be approximately 115 p.s.i. to satisfy the required relationship

of $P_F - P_B$. For any condition, then, neglecting the change in ΔP_v due to flow variations, the following applies.

$$P_F - P_B = P_{cd} - P_o - 105 \pm 20 \text{ p. s. i.}$$

where P_{cd} and P_o are in p. s. i. These values are based on P_B regulated to 50 $\pm$ 20 p. s. i.

The pressure drop-versus-flow relationship for the valve is plotted in Figure 19. The design constants are as follows:

Dv	=	0.4 in.
θ	=	60^o
K_s	=	40 lb/in.

The orientation of the valve with regard to the g field will be similar to that of the metering head regulator and high pressure throttling regulators. A ball bushing supporting the valve shaft will also be used with this valve. However, the development tests may indicate this to be unnecessary since the regulation of this valve is not critical. The effect of friction could probably be tolerated as it would result in approximately an 8.0 p. s. i. shift in cracking pressure at 367g. The effects of a $\pm$ 2^o change in direction of the laterally applied g loading and a $\pm$ 5g load variation in the axial direction would be negligible with respect to the required performance of the valve.

4.2.6 Igniter Solenoid Valve

The valve will be oriented in the g field such that the g forces tend to close the valve. The solenoid is designed to overpower the effects of the g forces as well as the pressure forces.

The igniter flow port is taken off upstream of the fuel pump at which point the pressure will be regulated by the throttling regulator when the rotor is whirling or by the tank-mounted boost pump when the rotor is not whirling. With locked rotor blades the pressure for igniter flow will be approximately 25 p. s. i. g. However, with the rotor whirling at 15 percent of its normal rated speed the pressure will be of the order of 60 p. s. i. The pressure at the two different conditions could be made identical at a maximum of 60 p. s. i. if the boost pump pressure were raised to 70 p. s. i. g. from the now specified 25 p. s. i. g. In this event the throttling regulator would be operating in either case to maintain the constant pressure level.

4.2.7 Inlet and Outlet Shutoff Valves

Two shutoff valves are required for this application. The inlet valve protects the control and pump housing from the high pressure level during normal engine shutdown when the rotor is whirling. The downstream valve permits igniter flow and pump flow circulation without main flow, and also contains fuel within the control housing during shutdown. To accomplish these two functions, the downstream valve contains a port to bypass metered flow back to pump inlet when the valve is in the shutoff position.

The valves are sized to open rapidly during the first few degrees of throttle travel, thereby providing the minimum restriction to flow. Both valves are pressure balanced to minimize the pressure effect on throttle torques. To permit drop tight operation, both valves close against resilient seats.

The orientation of the valves is such that the high g field is applied lateral to the valve axis. This causes a fairly high friction force which finally results in throttle torque. The friction force could be of the order of 8 pounds per valve. For the lever arrangement considered, this would result in 6.9 inch-pounds of throttle torque. Additional torque due to normal "O"-ring friction could increase the throttle torque up to about 15 inch-pounds.

4.2.8 P_{cd} Amplifier (Reference Figure 20)

The P_{cd} amplifier is a force balanced system incorporating a sensing bellows assembly, feedback spring, force bar and flapper valve, and a hydraulic amplifier. The bellows assembly consists of back-to-back, equal area bellows. One bellows senses P_{cd} and the other bellows is evacuated. Thereby, the assembly senses P_{cd} absolute, and since the bellows have equal area, the assembly is insensitive to variations in case pressure.

The force produced by the pressure in the bellows is balanced on the force bar by a force feedback from the actuator. A change in P_{cd} will disturb the force balance. This results in a deflection of the flapper valve, and thereby the flow into the piston chamber changes. This causes the piston to move and deflect the feedback spring in a direction which will restore the force balance. The system thereby generates a position output as a function of P_{cd}.

Design and Performance Data

The following table summarizes the design and performance of the system. The nomenclature is defined in Figure 20.

P_{cd}	0 to 140 p. s. i. a.
X	0 to 0.8 in.
A_b	0.5 $in.^2$
K_b	15 lb/in.
K_s	224 lb/in.
ℓ_1/ℓ_2	1.6
ℓ_4/ℓ_3	1.6
ℓ_5/ℓ_1	1.5
A_1	0.70 $in.^2$
A_2	0.90 $in.^2$
A_u	0.002 $in.^2$
A_d	0.004 $in.^2$

Accuracy

Figure 21 is a plot showing the P_{cd} error due to load variations on the actuator. The data are plotted as a function of P_{cd} and supply pressure (P_F).

The feedback spring in the amplifier produces a load on the actuator which is proportional to P_{cd}. Therefore, the resulting error can be compensated for by biasing the 3D cam.

The force levels required to operate the W_f/P_{cd} multiplier are shown in Figure 22. The maximum load occurs at the minimum values of P_{cd} and is equal to 5 pounds. It will produce a P_{cd} error equivalent to 0.2 p. s. i.

To minimize the error due to load variation caused by the g field, the system will be oriented as shown in Figure 20. As indicated, the g field acts normal to the bellows assembly and associated linkages and along the output of the actuator. The actuator and linkages will be designed to approximate g load balancing. Thereby, g field force will be minimized and reflected at the pivot bearings as friction loads.

In addition to the friction loads caused by the g field, piston shaft and cup seals will produce friction. It will be possible to keep

the total load due to friction under 10 pounds. This will cause a 0.27 p.s.i. error in P_{cd} at 100-percent speed (0.4-percent error).

Leakage Flow

Figure 23 shows an estimate of the flow required during steady-state operation as a function of P_{cd}.

Piston Force Levels

Figure 24 shows an estimate of the force output capability of the system as a function of CDP. The dashed lines indicate the force output requirements. The force output levels are therefore sufficient to ensure proper operation. The estimated force level output assumes 5-percent leakage and $P_F \approx 100 + P_{cd}$.

Time Response

There are two first-order lags in the system: a pneumatic lag due to the time required to pressurize and depressurize the P_{cd} sensing bellows and a hydraulic lag due to the time required to move the piston. Based on a linearized analysis, and assuming the P_{cd} inlet line is a lumped resistance, the pneumatic time constant is negligible in comparison to the hydraulic lag. The transfer function from P_{cd} to X can therefore be approximated by a first order system given by:

$$\frac{\Delta X}{\Delta P_{cd}} = \frac{0.00572}{0.007\,S + 1}$$

4.2.9 3D Cam Acceleration Schedule Contour

The 3D cam is rotated as a function of engine speed and translated as a function of compressor inlet temperature. The cam contours thereby generate the W_f/P_{cd} input to the multiplier.

Cam Contours

Figure 25 is a plot of cam radius versus cam angle and compressor inlet temperature.

Accuracy

To minimize fuel flow scheduling errors due to errors in positioning the 3D cam it is necessary to minimize the cam rise. This may be accomplished by increasing the cam radius and/or the amount the cam is rotated per unit speed change and translated per unit temperature change. However, practical considerations limit minimizing the cam rise, and based on the cam contours of Figure 25, the percent error in fuel flow due to a 0.001-inch error in the rotational position of the cam is given by

$$W_{f_e} = \frac{9.53}{W_f/P_{cd}} \tan \phi_N \qquad (1)$$

Similarly, a 0.001-inch error in the translational position gives a fuel error of

$$W_{f_e} = \frac{9.53}{W_f/P_{cd}} \tan \phi_T \qquad (2)$$

where

ϕ_N = cam slope with speed - degrees
ϕ_T = cam slope with temperature - degrees

The cam radius and speed input signal ensures that the cam slope (ϕ_N) never exceeds 30°. The maximum slope occurs at 10-percent speed. The W_f/P_{cd} value at this speed is approximately 12 p.p.h./p.s.i. From equation (1), the fuel flow error is therefore 0.66 percent. At any other operating point, the error will be significantly less than 0.66 percent. For example, at 100-percent speed the error will be 0.13 percent. The maximum cam slope (ϕ) with temperature is 21° and occurs at 70-percent speed. The fuel flow error due to a 0.001-inch error in the position of the cam at this point is approximately 0.16 percent.

4.2.10 W_f/P_{cd} Multiplier

The W_f/P_{cd} multiplier mechanically multiplies two position inputs; the product is a position output. The input signals correspond to P_{cd} and W_f/P_{cd}. The output positions the main metering valve and therefore is a function of fuel flow.

With reference to Figure 26, which is a schematic of the multiplier, the method of operation is described by the following equation:

$$Z = X\ (\text{Tan}\ \phi + \text{Tan}\alpha) \qquad (1)$$

where

Z = main metering valve position
X = output of P_{cd} amplifier
α = angle corresponding to value of W_f/P_{cd}
ϕ = constant angle

Substituting the design relationships

$$X = K_1 P_{cd} \text{ and} \qquad (2)$$
$$Z = K_2 W_f \qquad (3)$$

it can be shown that:

$$\text{Tan}\,\alpha = \frac{K_2}{K_1}\ \frac{W_f}{P_{cd}} - \tan\phi \qquad (4)$$

Substituting 2, 3, and 4 into equation 1 gives

$$W_f = P_{cd}\ \frac{W_f}{P_{cd}} \qquad (5)$$

which indicates the required multiplication.

Design and Performance Data

The following table summarizes the design and performance of the system:

P_{cd}	0 to 140 p. s. i.
X	0 to 0. 8 in.
W_f/P_{cd}	2. 86 to 28. 6 p. p. h. /p. s. i.
α	13. 1° to -12. 3°
Y	0. 030 to 0. 30 in.
ℓ_2	0. 6 in.
ℓ_1	3. 375 in.
θ	15°
W_f	Min. stop to 4000 lb/hr.
Z	Min. to 0. 14 in.

Accuracy

The following equation gives the percent error in fuel flow for a 0.001-inch error in X:

$$W_{f_e} = \frac{17.5}{P_{cd}} \tag{6}$$

Similarly for a 0.001-inch error in Y

$$W_{f_e} = \frac{9.53}{W_f/P_{cd}}$$

As the angle α changes, an error in X is introduced due to the radius of curvature of link ℓ_1. This error results in a maximum fuel flow error of 0.37 percent. However, if required, it is possible to partially compensate for this error by biasing the P_{cd} amplifier. Also, it should be mentioned that as α changes, the radius of curvature in ℓ_2 and the change in the contact point between the roller and upper track do not produce errors. Both these effects are functions of W_f/P_{cd} and therefore can be cammed out of the system.

Force Levels

The force levels required to operate the multiplier are shown plotted in Figure 22. As indicated, the forces are reflected to the P_{cd} amplifier and W_f/P_{cd} cam.

g Field Orientation

The multiplier linkage will be oriented to ensure that g loads act on the powered inputs.

4.2.11 T_1 Sensor and Amplifier

A schematic of the T_1 sensor and hydraulic amplifier is shown in Figure 27. The system incorporates a liquid cymene-filled bellows assembly, a sleeve-type servo valve, and a hydraulic amplifier.

The cymene bellows assembly includes two concentric bellows, one inside the other. The cymene is trapped between the two bellows.

T_1 inlet air is induced to flow through the assembly so that the inside of the inner bellows and the outside of the outer bellows are exposed to T_1. This increases the heat transfer surface thereby decreasing the time response of the system. For an application in which operation with a locked rotor is a required condition, an aspiration will be utilized to induce engine inlet airflow to pass over the T_1 sensor. The primary airflow for operating the aspirator will be supplied from the compressor discharge section of the engine. Where operation with a locked rotor is not a required condition, air scoops may be provided at the engine inlet to provide the necessary flow to the T_1 sensor bulb. Here, an aspirator will not be necessary. An aspirator has not been included in the design of the recommended fuel control system. However, there are no anticipated problems of operating the aspirator in the environment under consideration if one is required.

Method of Operation

An increase in the inlet temperature T_1 causes the cymene to expand. The inner bellows is thereby compressed and through the output rod causes a deflection of the lever. This results in a deflection of the spool valve which for an increase in T_1 will cause a decrease in A_d. Neglecting load variations on the actuator, a decrease in A_d causes the net flow into chamber P_a to increase and thereby move the actuator in a direction to increase A_d back to its original value.

The net result of the operation described above is a hydraulic powered output position which is a function of T_1.

Design Summary

The following data summarize the design and performance of the T_1 sensor and amplifier:

T_{T1}	-75 to 250°F
X	0 to 0.325 in.
A_{bo}	0.341 $in.^2$
A_{bi}	0.159 $in.^2$
ℓ_1/ℓ_2	1.0
A_s	0.405
A_2	0.552
A_u	0.0007 $in.^2$
A_d	0.785 ΔX

Accuracy

Variations in the piston load will produce errors in the output position of the T_1 system. The error caused by piston load variations reference to T_1 temperature is given by

$$\frac{\Delta T_1}{\Delta F_L} = \frac{5 \times 10^{-3}}{P_F}$$

Variations in the piston load are caused by the g field piston and piston rod seal friction, and the force required to move the 3D cams. The effective load due to g forces will be held to less than 5 pounds by balancing the actuator and linkages, and orienting the components so that g load forces will act on bearings and thereby be reflected to the actuator as friction loads. The total load due to friction will be less than 10 pounds. The maximum force required to move the cams is approximately 9 pounds and occurs at P_F = 240 p. s. i. The total error due to the resultant 19-pound load is therefore less than $1^{\circ}F$.

The temperature error due to g forces acting on the bellows assembly is $\pm$ 1. $5^{\circ}F$ maximum.

Steady-State Flow Requirements

The maximum flow required to operate the T_1 amplifier at starting conditions is approximately 50 p. p. h.

g Field Orientation

The g field will act along the output of the amplifier. However, as previously mentioned, linkages ℓ_1/ℓ_2 will be balanced and the actuator mass will be g load balanced to hold the resulting force levels below 5 pounds. The T_1 bellows assembly will be oriented so that the g field acts along the output rod. It is not necessary to g load balance the T_1 bellows assembly because the error due to the g field is negligible.

4. 2. 12 Speed Sensor and Amplifier

Function

The speed sensor and amplifier is a computer servo whose function is to position the 3D cam as a linear function of engine speed.

The output of this device must conform to the accuracy (resolution), speed of response, and torque capabilities required for successful computing of fuel flow in the specified operating environment of the proposed fuel control. In addition, size and weight must also be in conformance with design requirements.

Operation (Reference Figure 28)

The operation of the speed computer servo is based on measuring the time required for a gear tooth, which is rotating in proportion to engine speed (KN), to rotate the angle (θ) between a fixed position pick-off and a variable position pick-off. This time period (θ/KN) is compared with a fixed reference (T_R). The difference between θ/KN and T_R generates a command signal (Σ) which drives a (P. M.) step motor. The output shaft of the step motor positions the variable position pick-off so that θ/KN = T_R. Therefore, during steady-state operation the angular position of the step motor is a direct measure of engine speed.

Figure 29 is a timing diagram illustrating the detail operation of the computer servo. Signals θ_O and θ_T are generated at their respective pick-offs by reluctance variations produced when a tooth on a rotating gear passes the pick-offs. The tooth is rotating at a speed proportional to that of the engine. The θ_O signal is obtained from the fixed position pick-off, and θ_T is obtained from the pick-off whose angular position is adjusted by the step motor. The arrangement of the pick-offs ensures that θ_O always leads θ_T on the timing diagram. The time between them is directly proportional to the angle between pick-offs.

The speed computation program is initiated by the leading edge of θ_O which trips register N_6 and N_{11}. The output signal of N_6 switches from 1 to 0, thereby "gating" the clock oscillator pulses into the binary counter. The binary counter counts the period following the arrival of the leading edge of θ_O. When the time period T_R is counted down, signal T9 will be switched from 0 to 1 and $\overline{T9}$ from 1 to 0. The leading edge of θ_O also sets registers N_7, N_{12}, and N_{17}, N_{23} switching signals M_T and M9, respectively, from 1 to 0, thereby enabling the error signal gates N_9 and N_{14} to be switched by their respective signals $\overline{\theta_T}$ and $\overline{T9}$. If the leading edge of θ_T should arrive before the end of the reference period T_R (see broken lines on the timing chart) T9 will remain "0," $\overline{T9}$ will remain "1" and θ_T will be switched at N_{15} from "1" to "0." Simultaneously, register N_7, N_{12}

is reset, switching M_T back to "0." The above action will switch Σ -. at N_9 from "0" to "1" while at the same time disenabling N_{14} so that Σ+ signal cannot be generated until after the system is reset. Σ - is switched back to "0" when T_9 is switched to "1" at the end of the countdown. Σ - is supplied directly to the translator which through its decoding circuits supplies signals to the step motor causing it to step the θ_T pick-off (θ_o). The delay in the arrival of the θ_T is decreased, and the interval between the arrival of T_9 and θ_T is reduced.

The completion of the reference period count by the binary counter before the arrival of the leading edge of θ_T causes T_9 to switch from "0" to "1" (see solid lines on timing chart). $\overline{T_9}$ switches from "1" to "0," causing N_{14} to switch Σ+ from "0" to "1." Simultaneously, register N_{17}, N_{23} is reset, switching M_9 back to "0," thereby disenabling N_9 so that Σ- will remain zero until the system is reset. The arrival of the leading edge of θ_T switches Σ+ back to "0." Σ+, unlike Σ-. is not supplied directly to the translator but is placed at the input of the "dead zone" generator comprising the circuits from N_{20} to N_{22}. Here the leading edge of Σ+ triggers one shot 2 to produce a pulse of width T_b while the lagging edge of Σ+ triggers one shot 1 which produces a pulse of width T_A. Both pulses are supplied to the input of N_{22}. If pulse width T_b exceeds the sum of pulse width T_A and the width of Σ+, then the output of N_{22} remains "0" and no signal is supplied to the translator. If T_b is less than the sum of T_A and the width Σ+, then a signal will be generated by A_{22} following the termination of the T_b pulse and lasting to the end of the T_A pulse. This signal is transmitted to the translator which through its decoding circuits commands the step motor to step in a direction that will reduce the angular displacement between θ_T and θ_o pick-offs. The delay in the arrival of θ_T is decreased and the interval between the arrival of T_9 and θ_T is reduced.

The lagging edge of either the T_9 or θ_T signal triggers one shot 3 or one shot 5 which generates a short duration pulse, T_{RE}, to the output amplifier. The output amplifier, on receiving this pulse, provides a reset signal, R, to the counter and to all the registers in the system. This reset pulse clears the counter of its accumulated total and restores the registers to their initial condition. In addition to the reset signal the lagging edge of Σ+ or Σ- triggers one shot 3 which generates pulse T_D. T_D will disenable both N_9 and N_{14}, thereby preventing either and Σ+ or Σ- signal from being generated while this signal is on. The period of T_D is selected to prevent the computer from pulsing the step motor at a rate exceeding its maximum response rate.

The overall effect of the computer servo control action described above is to maintain the adjustable pick-off in a position which for a given gear speed produces a θ_T signal whose leading edge follows that of T_9 and is separated from it by an interval not greater than the difference between pulse width T_b and T_A. T_9 of course signifies the completion of the reference period T_R while $T_b - T_A$ is the maximum allowable quantum timing error in the system.

Figure 30 is a block diagram of the speed computer servo translator, and Figure 31 provides a timing diagram describing translator operation. The purpose of the translator is to accept bidirectional command pulses (cw or ccw) corresponding to $\Sigma+$ or $\Sigma-$ errors in 3D cam position, and to convert these to output signals $\emptyset_1$, T_1, $\emptyset_2$, and T_2, which when amplified will result in incremental stepping of a step motor in exact correspondence with the command. Our significant output signals are provided by FF_1 and FF_2 through their associated amplifiers N_{12}, N_{13}, N_{14}, and N_{15}. Each of the four possible combinations of $\emptyset_1$ and $\emptyset_2$ represents one of four unique positions of the step motor. A sequential step in either direction to the next adjacent position requires a change of state of FF_1 and/or FF_2. The exact change required is dictated by the command direction and the initial states of FF_1 and FF_2. The network composed of N_1 through N_9 and N_{16} and N_{17} generates this decision and transmits it through the delay comprised of N_{10} and O_{S1} and/or N_{11} and O_{S2}. These delays are required in order to avoid generating a signal whose constituent components are in a transient state.

System Performance and Design Requirements

The computer servo is designed to perform in accordance with the following specifications:

1) Accuracy: The maximum allowable error in positioning the 3D cam as a linear function of engine speed is 1/3 percent of full scale (100-percent engine speed).

2) Speed of Response: At 100-percent engine speed, the computer servo must be capable of following with negligible attenuation and phase lag a 4-percent peak-to-peak, 2-c.p.s. variation in engine speed.

3) Stability: The computer servo must not "limit cycle" (hunt) under steady-state conditions.

4) Torque Output: The maximum torque the computer servo is capable of applying at the 3D cam shaft must be at least twice as large as the maximum driving torque requirements of the 3D cam mechanism.

5) Environmental: The computer servo must provide its required performance under the environmental operating conditions of the fuel controller (see Reference 1).

In order to ensure that the selected system, Figure 28, meets the above specifications, the operation of each component comprising the system must be compatible with the overall system operating requirements. System specifications must therefore be translated by the system designer into component (or subsystem) specifications which will ensure compatibility.

The operation of the engine speed computer servo can be subdivided into three major functions, that is, sensing, computing, and signal processing, and actuating. Figure 32 is a simplified functional block diagram of the computer servo system which includes the above functions and illustrates their interrelationships.

In the selected system, computing is performed digitally, actuation is provided by a step servo motor which is operating essentially as a digital to analog transducer as well as a positioning device, and sensing, which is performed for both engine speed and shaft position by a single device, also provides analog to digital conversion. In this digital type of system, accuracy is determined by the device providing the largest quantum error rather than by the RMS sum of the component errors characteristic of analog systems.

The step servo motor is capable of positioning the 3D cam to within an increment of its output shaft angular position, thus contributing a quantum of error in generating the reference period, T_R. It times this period by a binary count of discrete clock pulses; therefore, the interval between successive pulses cannot be measured. This contributes a quantum error to the system. The magnitude of this error will depend on the clock pulse frequency in the computer, the error being inversely proportional to clock frequency. The sense provides the computer with a pulse position modulated signal in which the shaft position error is proportional to the time interval between the fixed pick-off pulse and the adjustable pick-off pulse that follows it. The error in this signal is due primarily to pulse "jitter."

If the actuator contributes the largest quantum error and if this is not excessive (less than 1/3 of 1 percent of full scale) the 3D cam error will not exceed it and the system will meet its specification for accuracy. However, it will fail its stability specification because the computer, responsive to errors of lesser magnitude, will continually command the actuator on the basis of errors it cannot correct, resulting in "hunting" during steady-state conditions. To ensure stability, the actuator quantum error must not exceed that of the computer. The peak error generated by jitter in the transducer output signal must also be less than the quantum error of the computer. If this condition is not satisfied, then the system will tend to oscillate in response to the jitter in the error signal. In conclusion, both system accuracy and stability specifications can be met by designing the system so that the computer provides the maximum error and that the magnitude of this error does not exceed 1/3 of 1 percent of full scale.

The response speed of the system is determined primarily by the actuator since it is the slowest acting device. Since actuators cannot act until signalled by the computer, the delay in sensing and computing the control signal must be added to that of the actuator. The sensor and computer delays overlap each other during most of their operating period, since the fixed pick-off pulse from the sensor initiates the computer operation and the computer control signal is generated shortly after the arrival of the adjustable pick-off pulse. The computer's operating speed capabilities are much higher than that of the sensor which is limited by mechanical design considerations. The response speed of the sensor is therefore the limiting factor in determining computer speed of response.

In a digital operating system, the speed of response is essentially given by the stepping rate that the system can develop in stepping from an initial to a final steady-state position. The stepping rate required of the system to enable it to provide simultaneously the specified accuracy and speed of response (see above) is given by the equation below:

$$P = \frac{\pi F f}{Q}$$

where

P = system stepping rate (steps/sec.)

F = Peak-to-peak amplitude of input signal
f = Frequency of input signal
Q = Quantum error of system

For a system which satisfies both the accuracy and response speed requirements, the stepping must be equal to or greater than:

$$P = \frac{\pi \times 4 \times 2}{1/3} = 75 \text{ steps per second}$$

This corresponds to a step period of 13 milliseconds. The system must be capable of supplying this stepping rate or better under full output torque conditions.

The torque and power output capabilities of the system are determined entirely by the step servomotor. The maximum driving torque requirement of the 3D cam is not expected to exceed 5 inch-pounds. The step servomotor must be capable of supplying at least twice this load (10 inch-pounds) at the 3D cam, while maintaining its stepping speed above the minimum rate of 75 steps per second. The stepping speed of the motor at maximum load must exceed the minimum system stepping rate sufficiently to allow time for the computer and sensor operations.

As far as environmental specifications are concerned, there appears to be no problem in providing components capable of operating in the specified temperature range of the fuel control. The computer transistor modules are the elements in the system most affected by temperature rise, but with proper packaging it will be possible to operate them without failures. Acceleration and vibration have the greatest effect on the mechanical components: the sensor and actuator; however, since these are low inertia devices the effect of acceleration (and vibration) on their operation is expected to be second order in magnitude.

System Component Design Considerations

The actuator which was selected for the proposed system is commercially available and can provide a maximum stepping rate at no load of 145 steps per second while its maximum running torque is 3.7 inch-ounces at less than 5 steps per second. It is a four-phase machine with a maximum power dissipation of 18.5 watts per phase at 28 v.d.c.

supply. This device provides four steps in a single rotation and is capable of positioning its rotor within a 90^{o} segment providing its stall torque is not exceeded.

The maximum driving torque of the 3D cam is 5 inch-pounds at the 3D cam and the allowable error in cam position must not exceed 1/3 percent of full scale. The full-scale pick-off displacement is 36^{o} and corresponds to 100-percent engine speed. Therefore a speed reduction is required between the step servo motor output shaft and the 3D cam to convert the step motor motion and torque output into that required by the cam. The gear ratio of the reductor can be calculated from the equation below:

$$R = \frac{360}{4 \alpha Q}$$

where

R = reductor gear ratio
α = is the full pick-off displacement = 36^{o}
Q = allowable percentage of quantum error = 1/3 of 1 percent of full scale

On the basis of the above parameter values, the gear ratio should be

$$R = \frac{360}{4 \times 36 \times (1/300)} = 750:1$$

The load torque (T_L) on the motor at maximum cam driving torque is therefore

$$T_L = \frac{5 \text{ in./lb} \times 16 \text{ oz/lb}}{750} = 0.12 \text{ in-oz.}$$

If we assume that the relationship between motor torque and speed is linear (a valid assumption in a first-order approximation), then the stepping rate of the motor at maximum driving torque is computed from the equation below:

$$\frac{P_{max}}{T_{max}} = \frac{P_{max} - P_L}{T_L}$$

$$P_L = P_{max} \left(1 - \frac{T_L}{T_{max}} \right)$$

where

P_{max} = no load step rate = 145 steps/sec.
T_{max} = maximum running torque = 3.7 in-oz.
T_L = maximum output torque = 0.12 in-oz.
P_L = step rate at maximum output torque

For the above parameter values, P_L is:

$$P_L = 145 \left(1 - \frac{0.12}{3.7} \right) = 145 \, (0.9675) = 140 \text{ steps/sec.}$$

Therefore, the maximum delay in stepping through a single quantum is about 7 milliseconds.

The sensor, Figure 28, is a variable reluctance tachometer (see above and paragraph 5.1.2.2) which is to be developed for this application. Its operation is in principle the same as any of the conventional reluctance tachometer devices except that the teeth are cut on the inner circumference of the gear and the two pick-offs are placed inside the gear. The gear rotates around the pick-offs in proportion to engine speed. This is a phase measuring device which for a single tooth gear would generate two pulses, one from the fixed pick-off followed by a pulse from the pick-off whose angular position is adjusted by the step servomotor. The time interval between these two pulses is a measure of the 3D cam position while the pulse repetition rate is a measure of engine speed. The computer and sensor are designed to operate together and the computing period is included in the time interval separating successive fixed pick-off pulses. Since this interval must be added to the step servomotor delay (7 milliseconds) discussed above, it must not exceed 6 milliseconds if the maximum system delay of 13 milliseconds is not to be exceeded. A single-tooth gear would require better than 100 c.p.s. (6000 r.p.m.) of the gear to generate a computing time interval less

than 10 milliseconds long. Speeds in excess of 6000 r.p.m. are generally not desirable in engine fuel control devices (largely because of gyroscope and dynamic balancing problems), particularly where a large g field is present and are best avoided. This problem is overcome by running the gear at 100 c.p.s. at 100-percent engine speed and providing a multitooth gear. In this device, a ten-tooth gear is provided which gives a computing interval of 1-millisecond duration. The total delay in the system is therefore about 8 milliseconds or almost half of the maximum allowable delay of 13 milliseconds. This system is to be designed with the capability of stepping almost twice as fast as its specifications require. A 1-millisecond pulse repetition rate generated by a ten-tooth gear whose outer diameter is about 1 inch imposes a number of constraints on the design of the sensor. This particular configuration has been selected because it provides a compact device with efficient utilization of space for a given outer dimension. A multitooth-gear reluctance generator requires a good deal of control over gear-tooth pitch variations in both the sensor gear and the speed reductor which couples it to the engine shaft. Antibacklash gears are also required in the construction of the reductor, coupling the step-servomotor to the sensor. The primary effect of backlash and variations in gear tooth pitch is the introduction of jitter in the sensor signal (see above). Another source of jitter is noise in the signal generated by air gap variations (due to vibration) and thermal activity in the electronic components. Their effect on the signal can be minimized by designing the pick-offs to generate sharp-edged pulses. To achieve this, the pick-offs must be designed for minimum inductance, leakage flux, and fringing at the poles. These are affected in the design by restricting the number of turns of the pick-off coils, providing a relatively thin coil compared to core diameter and by careful attention to the shaping of the poles (gear teeth). The RMS sum of the jitter introduced from each separate source must not exceed the system quantum error if the system is to remain unresponsive to jitter. For a quantum error of 1/3 of 1 percent of full scale, this indeed a stringent but not impractical design requirement for the sensor.

The computer which generates and translates the error correction signals provided at the input of the actuator drivers is described in detail in the first part of this section. Some of the operations described above become more meaningful when examined in terms of the operation of its input and output components and the overall system. The rapid speed of the computer requires that it be provided with a dead zone time delay to prevent hunting, as discussed above.

In addition, a time delay must be provided which will disable the computer for at least 7 milliseconds following the generation of a command signal to the actuator. This is required because any signaling from the computer demanding a faster step rate from the actuator than its maximum response will not result in actuator motion, and in all likelihood will result in overheating of this device. The computer action is therefore to command a single quantum correction of the error 1 millisecond after it has occurred and then to delay the next correction 7 milliseconds.

The control signal supplied to the actuator is in the form of a short duration pulse which switches a flip-flop (see Figure 33). Each half of the flip-flop supplies current to a single phase of the motor winding. The current will remain on or off in a given winding until another control pulse is received from the computer translator at the input of the flip-flop. In this way torque current can be supplied to the motor winding without requiring a steady-state error in the system. Because this is a closed loop system, inadvertent switchover or failure to switch in any of the four flip-flops is self-corrective and tolerable if it does not occur too frequently. In Figures 33 and 34 are examples of typical circuitry used to perform the logical operations in the computer and translator. These circuits require regulated power supplies to operate properly (about $\pm$ 5 percent or better). A typical power supply circuit which would be provided in this system is illustrated by Figure 35. It should be noted that aircraft d.c. power (+ 28 volts) is the basic source of electrical power in this system and is supplied directly to the motor windings as well as to the regulated voltage supplies. The maximum load current from this supply is not expected to exceed 2 amperes at any time during the operation.

4.2.13 Speed Governor Amplifier

A schematic of the speed governor amplifier is shown in Figure 36. The system incorporates a floating summation linkage, a four-way spool valve, and a hydraulic power piston.

There are two position inputs to the system: X input which is a measure of the engine speed, and Y input which is a measure of the desired cut-in speed. The output is the position signal Z which during governor operation positions the main metering valve.

Method of Operation

The summation linkage compares the desired cut-in speed with the actual speed. If the actual speed is less than the cut-in speed, the servo valve will be to the left of its null position. Therefore, P_1 will be ported to boost pressure, P_2 will be ported to supply pressure, and the actuator will be hard over to the right. As the engine speed increases, X moves to the left and through linkage ℓ_1/ℓ_2 causes the servo valve to move to the right. When the engine speed is equal to the cut-in speed the servo valve will be at its null position. As the engine speed continues to increase, the servo valve will be deflected to the right side of its null position. This ports supply pressure to P_1 and boost pressure to P_2. The piston therefore moves to the left and due to the feedback link ℓ_4/ℓ_3 will move a distance which is proportional to the difference between the cut-in speed and the actual speed. The net result of the operating sequence described above is a hydraulic-powered, null-type position system wherein the output position is proportional to the difference between the cut-in speed and the actual speed.

Design and Performance Summary

The following table summarizes the design and performance of the system. Nomenclature is defined in Figure 36.

A_P	0.5 $in.^2$
ℓ_1/ℓ_2	1.33
ℓ_4/ℓ_3	6.0
$\Delta X/\Delta N$	0.0045 in./percent
$\Delta Y/\Delta N$	0.0095 in./percent
$\Delta Z/(N-N^*)$	0.0135 in./percent

governing range 40 to 106 percent speed

Accuracy

Previous experience on this type governing system shows speed accuracies of 1/4 of 1 percent. However, based on the assumption that the steady-state fuel schedules correct as a function of $\sqrt{\theta}$, the speed accuracies specified cannot be met. It is therefore necessary to bias the governor cut-in speed as a function of compressor inlet temperature. Figure 37, which is a plot of speed error versus inlet temperature for 100- and 50-percent speed, shows that this method of biasing cut-in speed reduces the speed error to within the specified limits.

Force Output Capability

The maximum force output of the piston is 0.5 P_F. Therefore, (P_F = 100 p.s.i. minimum) the minimum force occurs at P_F = 100 p.s.i. and is 50 pounds. The maximum force required to move the metering valve is 25.6 pounds. Allowing 10 pounds' force for friction leaves a 15-pound safety factor.

g Field Orientation

The speed governing system will be oriented in the g field so that the powered components support the g loads. Linkages will be rough balanced to minimize g field forces.

Time Response

The transfer function from input X to output Z, based on a linearized analysis, is given by

$$\frac{Z}{X} = \frac{3}{0.007s + 1}$$

5. COMPONENT STUDIES

Various methods of accomplishing the required functions are examined in this section of the report in order to permit an overall system selection. The functions to be accomplished have been assigned tentative accuracy requirements upon which to judge the usefulness of the design. It will be noted that the accuracies differ depending upon the system with which they would be integrated.

Parameter sensing and amplifying, mode of computing, metering system, and pumping systems will be discussed in this section of the report.

5.1 Parameter Sensing and Amplifying

For the accomplishment of the control function in accordance with the block diagram, Figure 10, three parameters must be sensed and amplified, these being compressor discharge pressure, engine

speed, and compressor inlet temperature. The basic problem in all three cases is that of making the components insensitive to the varying g field.

5.1.1 Compressor Discharge Pressure

It is required to sense the signal pressure and provide an output, powered or otherwise, which will be insensitive to g loading. Any practical method of sensing pressure involves a force and a displacement and, therefore, may be sensitive to g loading depending upon the load orientation. An overall accuracy from sensed signal to output of the order of 1 percent of full scale has been assigned this component.

Hydromechanical, electromechanical, and electropneumatic methods are investigated, with the former appearing the most desirable.

5.1.1.1 Hydromechanical (Reference Figure 20)

This method utilizes a pair of opposed bellows, one being evacuated, a three-way servo valve, a power piston, and a feedback spring. A powered output is provided as a linear function of the input pressure. The system is called a force feedback servo amplifier.

It is assumed for this application that the error just due to sensing must not exceed $\pm$ 1/4 of 1 percent, thus leaving $\pm$ 3/4 of 1 percent for amplifier. Orientation to the g load is considered of prime importance for this application. As pointed out in the Appendix, a spring or bellows can be designed to exhibit a negligible change in force in the axial direction when subjected to purely lateral acceleration forces. If the spring or bellows is g loaded such that a force component lies along the axis, then the force applied to a system by the spring will vary in proportion to the g load. Since the g load is considered to be applied in a fixed direction and lateral to the spring axis, then the sensing and feedback portion of the system depicted by Figure 20 should be relatively insensitive to the g loading.

A servo system is capable of supporting extraneous forces without appreicable error; and, therefore, if the power piston is loaded along its axis, all the linkages connected to the power piston, up to and including the spring support, can be supported by the hydraulic force of the power piston. This will cause an error of the

second order in the signal amplification, but this can be minimized with the use of a high gain servo valve. To minimize the error due to the g loading on the power piston, the piston may be balanced within the limits permitted by ordinary manufacturing tolerance. Exact balancing would not be necessary.

A half-ball-type servo valve, although not conducive to permitting extremely high gains, must be used so that there is no extra hardware attached to the force balance lever to allow erroneous force inputs due to g loading. Errors on the force balance lever would cause an output error of the first order. Any type of servo valve that is attached to the force balance lever would require precise balancing on a whirl rig. If the required accuracy cannot be achieved with a single three-way valve, two three-way valves could be used. In this case, the piston areas would be equal.

The force balance lever is supported on a pair of ball bearings which can be sized to support adequately the torque load applied by the g loading.

5.1.1.2 Electromechanical/Electropneumatic Pressure Transducers

The most common transducers which provide an electrical output as a measure of input pressure are conventional types of pressure sensors (bellows, diaphragm, and so forth) equipped with a transducer that converts their mechanical output (displacement force, strain, and so forth) into a proportional electrical signal (usually voltage). These transducers are characteristically analog in that the pressure level information, at any instant of time, is found in the amplitude of the output signal.

This type of output can be supplied directly and without further signal conditioning to analog computer circuitry described in paragraph 5.2.4 of this report. In paragraph 5.2.4, however, it is concluded that digital computing techniques are preferable to analog in this application. Digital computing methods operate on the basis of counting discrete quantities (called quantums) and therefore require signal inputs in the form of pulses rather than a continuously varying signal lever.

The pressure level information now resides in the frequency or pulse repetition rate of the transducer output signal. Therefore, the function required of the "Compressor Discharge Pressure" (P_{cd}) transducer in a digital application illustrated in Figure 38 is, preferably, a single device which can receive P_{cd} as an input and supply an F.M. signal in which frequency deviation is proportional. The existence of a single device (defined as composed of elements which by themselves are incapable of transducing pressure) providing an F.M. output signal is unknown to the author. However, an F.M. signal can be obtained from an analog type pressure sensor by coupling its output to the input of an F.M. oscillator as illustrated in Figure 39.

If the output of the analog pressure sensor is a voltage proportional to pressure, it can be utilized in frequency modulating the carrier frequency of a standard voltage-controlled oscillator (VCO) which is frequently used in telemetering systems. An F.M. signal can also be obtained by having the pressure sensor change the inductance (or capacitance) and therefore the tuning of an oscillator's tank circuit.

A number of analog pressure-sensing devices have been reviewed and the results are given in Figure 40. Indications are that the best accuracy that can be expected from the approach of Figure 39 using "off the shelf" or presently operational pressure sensors and F.M. oscillators is $\pm$ 3 percent of full-scale error, or greater, under the given environmental conditions. This error is more than three times the maximum error in pressure transducing that can be tolerated in this system ($\pm$ 1 percent).

Because of the error inherent in the analog type of pressure sensor, other forms of F.M. pressure transducing, such as the vibration (which uses a vibrating string in which F.M. is obtained by varying string tension with a pressure transducer) are expected to possess equally large errors.

A number of manufacturers of pressure transducers have been contacted and some have indicated an interest in reviewing the possibility of extending the accuracy and operating environmental range of their devices to meet our requirements. This would require some development as well as redesign of existing devices.

Figure 41 represents a radically different approach to the problem. Here, a device is provided in which P_{cd} is transduced

into an F. M. pressure wave which is sensed and transduced into an F. M. output signal by a dynamic pressure sensor such as a crystal. The pressure sensor in this configuration would contribute negligible error to the output signal since the P_{cd} information is in the frequency of the signal and not in its amplitude. It would therefore have to be capable only of response in the operating frequency range at an acceptable power level.

A commercially available dynamic pressure transducer such as is included in Figure 40 could satisfy this requirement.

The difficulty in the scheme represented by Figure 41 is the procurement of a suitable F. M. pressure transducer. Theoretical considerations and experimental data indicates that a bistable pure fluid device, commonly referred to as a DOFL valve, can be utilized as an F. M. pressure transducer. However, a good deal of development will be required before this device will be able to supply the accuracy required in the pressure and environmental range of the proposed fuel control.

Because of the inherent simplicity and economy of this approach, a program of continuing study into the feasibility of the DOFL valve as an F. M. pressure transducer is recommended.

Figure 42 represents a system of pressure sensing in which a feedback system utilizing an instrument servo and a regulated pressure supply is provided with a conventional dynamic (crystal) pressure sensor to measure P_{cd}. This system, by its very nature, is a good deal more complex than the previous three and can therefore be expected to be more costly and less reliable. Its feasibility depends primarily on:

a) The ability to procure or design a two-part pressure valve capable of being oscillated at a frequency of several cycles per second without appreciably attenuating pressure response at the dynamic pickup.

b) The accuracy and repeatability of the regulated pressure supply as a function of servomotor shaft position.

c) The threshold sensitivity of the dynamic pressure sensor.

The system operates in the following manner: The pulsated pressure valve switches the pressure applied to the pickup continuously between P_{cd} and reference pressure at some desirable frequency (as determined by the astable multivibrator). The output is therefore a pulsating signal in which the peak-to-peak amplitude is proportional to the difference in pressure between the P_{cd} and reference sources. This signal is amplified, demodulated, and then supplied to the control winding of a servomotor. The motor, which controls the regulated pressure supply will turn in a direction which will cause the reference pressure to approach the P_{cd} level. When this occurs, the peak-to-peak amplitude of the pulsating signal is reduced to zero and the motor stops turning. The motor shaft is connected to an F. M. oscillator where it can adjust the tuned frequency of an oscillator proportional to its position, thereby producing an F. M. output signal in which frequency deviation is a function of P_{cd} level.

This system is independent of temperature and acceleration effects on signal null and gain because of two factors:

a) The dynamic pressure pick-offs are insensitive to static effects such as null shift produced by temperature and acceleration loading.

b) The variation of pressure pick-off gain with temperature has no effect on the steady-state output of the F. M. signal transducer since this is a closed-loop, null-seeking system.

Because the system of Figure 42 is a closed-loop instrument-type servo, attention must be given to its dynamic response and stability in its development.

The feasibility of this system is dependent upon the improvement in P_{cd} measurement accuracy obtained through its use as compared with the accuracy obtainable from the systems of Figures 39 and 41. A significant reduction in P_{cd} error must be expected to justify the increased complexity and cost of the system illustrated in Figure 42.

Of the several methods of transducing pressure into a frequency modulated (F. M.) signal that have been investigated in this report and which are represented as "black box" diagrams in

Figures 38, 39, 41, and 42, the results indicate that no off-the-shelf or presently operational devices exist to the knowledge of the author that will meet all the performance and environmental requirements listed in Figure 38. On the basis of available information, it is concluded that a suitable electrical pressure transducer for our application requires development. The approaches described in Figures 39 and 41 appear to offer the greatest potential for development of a relatively simple, inexpensive, yet reliable device capable of providing high accuracy under severe environmental conditions. A program of continued study of both types of pressure transducers to determine feasibility and relative merits is therefore recommended.

5.1.2 Engine Speed

It is necessary to sense engine speed and provide a usable stroke or rotational output, powered or otherwise, which will be insensitive to the g loading. The output will be used to position a 3D cam upon which contours will be provided for scheduling the acceleration fuel flow. It has been decided that no matter what mode of computing is used, the 3D cam provides the best means for scheduling a single output as a function of two other variables. Considerable equipment would be required to replace the 3D cam with electronics. For contouring purposes on the 3D cam, it would be desirable, although not necessary, that the output be linear with speed.

An overall accuracy of $\pm$ 0.25 percent of full scale from sensed signal to cam position has been assigned to this component. For acceleration fuel scheduling alone, the accuracy would not have to be this stringent; however, it is anticipated that the cam position will be used as the speed signal for governing purposes.

Hydromechanical and electrical methods for performing the required function were investigated. The latter, using a stepping motor, appears the most desirable.

5.1.2.1 Hydromechanical

Under this category of design, flyweights would be used as the sensing element. The methods of amplifying the signal are several, but the most important aspect of this type of design is the interface between the signal and amplifier. A balancing problem concerning the force extracting linkage and the rotary to linear position mechanism exists (Reference Figure 43). The tolerances on these mechanisms

would have to be carefully controlled and, in addition, the parts would require precise weighing and balancing before assembly. For instance, on a flyweight system developing a force output of 20 pounds at 100-percent speed, an unbalanced force of only $\pm$ 0.00017 pounds as seen at the flyweights would be permitted before a sensing error of $\pm$ 0.1 percent is evidenced, thus leaving $\pm$ 0.15-percent error for the amplifier. This is indicated by the following equation:

$$F = 20 \times 10^{-4} (N)^2 \text{ lb}$$

where N is in percent speed.

Differentiating,

$$\frac{dF}{dN} = 40 \times 10^{-4} N \text{ lb/percent speed}$$

and therefore for dN = 0.1-percent speed change about N equal to 100 percent

$$dF = 0.04 \text{ lb}$$

Therefore, at 235g

$$\text{Unbalanced weight (W)} = \frac{0.04}{235} = 0.00017 \text{ lb}$$

Although this unbalanced weight seems very small, it is conceivable that the system could be properly balanced without special whirl tests. Parts could be weighed and balanced at bench tests. The recommended arrangement of the flyweights is depicted by Figure 43 with the g load being applied through the center of rotation. With this arrangement and direction of g load, the flyweights themselves are insensitive to the g field.

The gyroscopic couple developed by a system of this design has been calculated using the formula listed herein and essentially no effect is produced on the system.

$$T = I \omega \Omega \text{ ft-lb}$$

where

ω = rotor speed, rad/sec.
Ω = flyweight speed, rad/sec.
I = polar moment of inertia of flyweights, slug-ft^2

Bearing forces also are within normal levels.

Several opportunities exist with the use of a hydraulic servo system for providing the amplification of the speed signal. The same philosophy as presented for the compressor discharge pressure amplifier described in paragraph 5.1.1 would apply. It would also be possible to use a nonlinear hydraulic servo amplifier to compensate for the nonlinear force output of the flyweights such that a nearly linear relationship between the output and speed would exist.

5.1.2.2 Electronic Engine Speed Computer

The engine speed may be sensed and amplified electronically. The system may be divided into three functional activities: input signal generation, signal processing and computing, and output actuation. A block diagram of the basic system, Figure 32, illustrates the relationship of the major functions to each other and to the input and output.

This system must accept an analog input (engine rotational speed) and also provide an analog output (3D cam shaft position). The system may therefore be designed to operate as a purely analog system utilizing an analog computer, with a torque motor providing actuation. However, an analysis of electronic computing techniques (see paragraph 5.2.4) indicates that analog computing is more severely limited in our application than comparative digital techniques, and it is strongly recommended that the computing function be performed digitally. Though utilizing a digital computer, the system input and output remain analog in character. This condition can result in serious interface problems at the input and output of the computer. The computer can operate only on digital signals (discrete pulses) at its input while its output will be presented in a digital form. Therefore a digital transducer is required for sensing engine speed while the computer output signal must be translated into a form which is acceptable to the actuator. Fortunately, a number of proven devices exist which can transduce rotary motion into a pulsed or a sinusoidal signal in which the frequency (pulse repetition rate) is proportional to engine speed. The problem of processing an actuating device with acceptable torque output that can translate digital signals into shaft position is somewhat more troublesome and usually requires some signal

processing of the computer output before it can be used in controlling the actuator. A discussion of the hardware requirement and availability is given below for the speed sensor and actuator. The computer is discussed in detail in a later paragraph (5. 2. 4).

5. 1. 2. 2. 1 Engine Speed Sensors

The following types of speed transducers are applicable in providing the computer with an input signal in which the frequency of the sinusoidal signal or the repetition rate of the pulse train is proportional to engine speed:

a. Photo Electric Pickup

This is a device intermediate in cost, which utilizes a photo electric cell and a beam of light. The beam of light is periodically interrupted by irregularities in the rotating member (which can be a gear). As a result, a pulse modulated electrical signal is generated in which the pulse repetition rate (frequency) is proportional to rotational speed. As a sensing device it is readily subject to failure under environments which expose it to dirt, vibration, and high temperatures.

b. Vibration Pickup

This is an intermediate cost electro-acoustical device which couples acoustical energy through a resilient member into an inductive pickup. Because of its nonselective nature it is prone to transmit erroneous information.

c. Switching Pickup

This is the heart of a low-cost, very accurate system based upon the enumeration of switch closures of a set of breaker points driven by a cam on the rotating member. It is, however, limited to low-speed operation in clean environments.

d. Permanent Magnet Field Generator

This is an electromagnetic device whose output is a sinusoidal signal with both amplitude and frequency proportional to the speed of its rotating member. In a digital application, only the frequency of the signal is utilized by the computer. P. M. field generators are capable of relatively high level output signals and require no input power; however, they are fairly high in cost ($50-$100).

e. Variable Reluctance Generators

This is a low-cost (less than $20.00) inductive pickup whose output is a pulse train with a pulse repetition rate (frequency) directly proportional to the product of the rotational speed and number of teeth on a gear passing under it. As a speed sensor device it is not only comparatively inexpensive, but is also capable of high resolution and high signal-to-noise ratio. These devices have a history of successful application in high resolution speed transducing.

f. Magnetic Recording Disk

This approach to digital speed transducing utilizes magnetic drum recording techniques and practices now current in the computer field. Its operation is based upon the elapse in time between the recording of a magnetic pulse and its readout. This period is of course inversely proportional to disk rotational speed and, when compared with a fixed and known clock period, provides a measure of that speed. As a speed-measuring technique, its accuracy is potentially as high as (or higher than) the inductive pick-off and, in addition, it can be easily synchronized with the time reference (clock) when this is necessary or desirable. It is also more flexible as a speed-measuring technique since it is not preprogrammed as in the case of the variable reluctance generator.

Its disadvantages, when compared to a variable reluctance transducer, are greater complexity (since recording and erasure operations are required in addition to readout) and higher sensitivity to air gap fluctuations. Magnetic recording heads range from under $20.00 for commercial magnetic tape recording types to several hundred dollars for digital computer recording heads. Although the cost of a magnetic recording speed device can be expected to exceed that of the variable reluctance generator, its capability for synchronization with the reference clock can allow for a simpler and therefore less costly computer.

The writer knows of no previous application of magnetic recording technique in speed transduction.

All of the aforementioned transducers are similar in function in that they generate a pulsating signal whose frequency (or period) is proportional to rotary speed. A common criterion can therefore be established for purposes of comparison .

Our requirements are that a transducer be provided at acceptable cost, with a resolution error not exceeding 1/300 of full scale whose speed of response (information rate) is not greater than 1 millisecond and whose outside diameter is in the order of 1 inch. This device must provide the above performance levels in the range of 8 to 100 percent of full engine speed and under the stated environmental conditions.

Speed can be measured digitally either by counting the number of pulses in a given period or by "clocking" the elapsed time between two successive pulses. The former technique is more commonly used than the latter in transducer types 1 through 5 whereas in the magnetic disk recorder, the latter approach is more directly applicable.

In the counting technique, to obtain a resolution error (quantum) of 1/300 with response time of 1 millisecond would require 300 irregularities (example, gear teeth) about the circumference of the rotating member if its maximum speed were 1,000 c.p.s. or 3,000 irregularities if the speed of rotation were limited to 100 c.p.s. For mechanical reasons, the latter speed limit is desirable. However, a rotary member with 3000 irregularities on the perimeter of a disk with an outside diameter no greater than 1 inch would be quite difficult to design within the required tolerances. The need for a large number of irregularities, or poles in the case of the p.m. generator, is obviated by utilizing the technique of measuring speed by clocking the elapsed period between successive pulses. In this case, only ten irregularities (or poles) are needed when the rotating member is limited to 100 c.p.s. in speed. Each of the six devices described now requires two pickups for measuring the time required by the rotating member to transverse 1/10 of its perimeter against the reference clock oscillator. In order to provide the required accuracy, the device must be constructed with close tolerances on the angular separation between irregularities. Error can also be introduced in the form of pulse jitter due to noise pickup and gear train irregularities. Pulse jitter can be minimized by designing the digital transducer to provide sharp-edged pulses and by careful control of gear pitch. Elapsed time may be measured by either counting the number of pulses generated by the clock oscillator between the occurrence of the two recorded pulses or by timing the interval with a reference multivibrator which generates a signal with a known pulse width when triggered by the first pickup's signal. The former is preferred because it can provide a more accurate and stable measure of time under our environment conditions.

Of the six techniques reviewed above, the variable reluctance generator is preferable. Preliminary design and feasibility studies indicate that this type of digital speed transducer, if properly designed and constructed, should be capable of providing reliably the high resolution and speed of response discussed above without exceeding cost and size limitations. Although the photo electric and vibration pickup technique also appear to be capable of high resolution and response speed, their inherent lack of reliability in the fuel control environment makes then unacceptable as speed transducers. Technique number three was rejected because the low operating speeds of switching devices limit their speed of response excessively for our application. In addition, the space requirements of this type of device can be expected to be considerably larger than that required by a reluctance type of transducer providing the same function. Some improvement in speed of response can be realized by use of magnetically operated reed contacts for switching; however, this improvement is not expected to make the switching pick-off competitive with the variable reluctance generator approach.

The permanent magnet (p. m.) field generator was rejected principally because a ten-pole 1-inch-diameter device is expected to be high in cost when compared with a reluctance-type generator. A secondary consideration was the possibility of obtaining sharp pulses from the reluctance generator as compared with the sine-shaped output signal of the p. m. generator.

The magnetic disk recording technique offers some definite advantages in speed transducing not obtained from a variable reluctance device. The chief advantage is that it allows for convenient synchronization with the clock oscillator, thereby reducing computer complexity. Despite these advantages it was rejected primarily because its development is expected to involve greater risk and time than that incurred in developing a reluctance-type transducer. The development of a magnetic-disk recording device which is operational in our environment and provides the required accuracy will encounter most of the problems involved in the development of an equivalent functioning variable reluctance generator in addition to problems of recording and erasing which are not encountered in the latter device. Air-gap variation induced by the high vibrational level of the environment can seriously degrade the recording, thereby producing serious and repeated errors in speed measurement. Air-gap spacing can be stabilized by a head positioning control such as is utilized in computer magnetic storage drums; the addition of this control to the system will of course

result in greater cost, size, and complexity. The magnetic recording technique also provides some difficulties in packaging and size reduction not encountered in reluctance devices. This results from the necessity to record and read-out magnetic pulses in the same plane.

In conclusion, it is recommended that a variable reluctance digital speed transducer be developed along the lines outlined in paragraph 4.2.12 of this report. Development is believed necessary because it appears unlikely that a device can be procured commercially which will provide the required performance under the severe environmental conditions and space limitations encountered in the fuel control system.

5.1.2.2.2 Output Actuators

There are a number of devices which can be used in the electronic speed computer to provide output actuation of the 3D cam shaft. Those described below are representative of the more commonly applied techniques. A comparison of their merits appears to favor the step-motor type as the most applicable actuating device for this system.

a. Proportional Solenoids and Torque Motors

These two devices may be lumped together with respect to characteristics; they both give a position output proportional to input signal. They range in price from $30 to $300 depending upon the severity of the specifications they must meet. These specifications include output power, efficiency, hysteresis, speed of response, durability, and linearity. Proportional devices require a digital to analog conversion circuit for compatibility with a digital computer output.

b. Stepping Relay and Rotary Solenoids

These are low torque devices which provide true digital actuation since they can respond directly to a pulsed input signal. Functionally, they are ring counters in which the output, and angular displacement of the shaft, is the sum of the number of pulses received at the input of the device. Stepping relays and rotary solenoids are slow in operating speed, being limited perhaps to less than 50 pulses per second and their life is severely limited in this type of application. They are low-cost devices ranging from $10 to $20, depending on size.

c. Step Servomotor

A step servomotor is a device that, when energized by d.c. voltages in a programmed manner, indexes in given angular increments. Its angular displacement is either clockwise or counterclockwise and is determined by the sequence in which the windings are pulsed.

Step servomotors have a number of advantages over linear devices. They offer:

- fast response
- insensitivity to linear vibration and shock
- long life (up to 1 billion cycles)
- insensitivity to voltage and pulse amplitudes
- higher stability

These devices are moderate in price; they can be purchased for less than $100 per unit.

d. Magnetic Proportional Clutches

This device is essentially a proportional actuator which operates on the basis of coupling two rotating shafts through friction thereby transmitting torque from the input shaft, which acts as a power supply, to the output shaft which is the controlled member. In the dry powder magnetic clutch, a proportional torque between the shafts is provided by the magnetic particles when the magnetic field is applied to them. The cost of the basic clutch mechanism is less than $100 per unit and is generally in the same price range as step servomotors.

The chief requirements of an actuator in our application are: fast response, stability, repeatability, low cost, and the ability to operate reliably in the severe temperature, acceleration, and vibration environment of the fuel control. Torque and power output and gain are less important because the loading of the 3D cam on the actuator output shaft is expected to be low and gain can be provided in the electronic circuitry of the computer. An evaluation of the

several types of actuators discussed above supports the conclusion that the step servomotor type of actuator is best suited to meet our particular needs in this development.

If a proportional actuator (torque motor, proportional clutch, and so forth) is used, a digital-to-analog signal conversion is required between the computer and the actuator. This, in effect, results in a proportionally operating control system even though computing is performed digitally. Because the actuator must provide a torque under steady-state conditions to the 3D cam, a current proportional in amplitude to the required torque must be supplied continuously by the converter to the torque motor winding. If the digital-to-analog converter functions only as a code converter, that is, converting the digital control signal of the computer to a corresponding current amplitude level, then a steady-state error must exist between the engine speed and output shaft position in order to generate the counter balancing torque in the motor. This error can be minimized by providing high forward gain in the system but at the cost of reducing stability and increasing the tendency to limit cycle (due to the nonlinearities present in the system). A high gain system may also aggravate the problem of random noise disturbances. The steady-state error can be eliminated entirely by providing a floating control (integrator) as well as code conversion in the digital to analog converter. This results, however, in a more complex and costlier design with a reduction in response time. Because of the floating control, the system is more prone to hunt, thereby magnifying the problem of stability.

The problems inherent in a proportional actuator application are minimized or eliminated altogether by going to a digital device for actuation. Here, as in the proportional actuators, output shaft angular position is analog in character but the digital-to-analog conversion is produced by actuator operation rather than by signal processing at the output of the computer. Steady-state torque is supplied by fixed currents in the motor windings in the case of step servomotors, and by mechanical detent in stepping solenoids. Signal processing (translator circuit) may still be required between the actuator and computer to adapt the computer output signal to a form which is compatible with the requirements of the actuator.

Of the two types of digital actuators which were reviewed above, the step servomotor type is preferable even though the stepping solenoid type is significantly lower in price. The relatively

lower response speed, operating life, and reliability of stepping solenoids makes them less attractive than step servomotors in this application.

A commercially available step servomotor (IMC-model No. 015-802) appears to meet the performance and environmental requirements of the fuel controller and it is recommended on this basis. A detailed description of its operation in the proposed system is found in paragraph 4.2.12 of this report.

5.1.3 Compressor Inlet Temperature (CIT)

It is required to sense this temperature and provide an output, powered or otherwise, which will be insensitive to g loading. The overall accuracy of this device can possibly be of the order of $\pm$ 5°F depending upon the manner in which it is used.

No other device except a liquid-filled bellows has been considered for the sensing element as the output of this device in itself is effectively insensitive to g loading. The sensor operates to provide a stroke output with a relatively high force level as a function of temperature. The available spring rate, or output force to stroke, of a sensor of this type is of the order of 1500 lb/in. For low force level variations of the order of $\pm$ 4.0 pounds, the sensor alone would be adequate. The major limiting factor of this design would be the maximum force levels required with respect to the pressure rating of the bellows. The necessity of amplifying the sensor signals, therefore, will depend upon the output force required and the direction of the applied g loading. The g load could be applied either in a lateral or axial direction. The axial direction would cause an effect on the maximum usable output force of the sensor.

Amplification of the sensor output will most effectively be provided, if necessary, by a position follow-up servo system. No calibrated springs are necessary in this type system. The servo valve could be of the spool type with the g load applied through the axis of the valve. This type valve, although one of the more expensive type valves that could be used, would conserve the flow of servo fuel which may be a deciding factor during the initial cranking and starting range of engine operation. The linkages involved would have only to be balanced to the extent of the variation of load that the sensor could stand for the accuracy required. Considering the linkages which could be used for this design, the balancing will be no problem at all

and can be achieved within the standard limits of manufacturing tolerances. A three-way, half-ball servo valve could also be used with this amplifier design if there is sufficient servo flow available during the starting range of engine operation.

5.2 Mode of Computing

In order to compute the control signal to provide either the acceleration, steady-state, or deceleration fuel flow as a function of the engine input parameters, a multiplying device must be used. With reference to the block diagram, Figure 10, it is indicated that the basic control equation with respect to the control parameters will be as follows:

$$W_f = C_1 K P_{cd}, \text{ p.p.h.} \qquad (1)$$

where

C_1 = maximum control limit constant, p.p.h/p.s.i.
P_{cd} = compressor discharge pressure, p.s.i.a.
K = multiplying factor and is a function of engine speed, CIT, and governor set speed error, units are dimensionless.

As previously established, during acceleration the multiplying factor will be derived in accordance with a position taken from the surface of the 3D cam. Various methods of utilizing this position to provide a multiplying circuit are feasible. All of the methods considered in the following paragraphs would be capable of operating in the high-gravity field.

Engine speed governing is accomplished by overriding the position of the 3D cam with the governor mechanism as a function of set speed error in a manner such as to reduce the multiplying factor (K) and thus the flow of fuel until the steady-state speed is achieved. That is, the lowest multiplying factor will always be selected.

Deceleration is achieved by reducing the multiplying factor to a minimum value as a function of overspeed error and thereby providing a minimum flow of fuel to the engine.

5.2.1 Pneumatic

The method of multiplying pneumatically provides for the flow of compressor discharge pressure through two bleeds in series, the first of which is fixed in area, the second variable in area. The flow then exhausts to the ambient. The position taken from the 3D cam provides the means for varying the area of the second bleed. It is possible to vary this area with low force levels and therefore preclude the use of a servo amplifier for governing.

It can be shown that the ratio of intermediate pressure between the two bleeds to compressor discharge pressure is a function of the area ratio of the two bleeds. By making the area ratio a function of engine speed and CIT, it would be possible to schedule the required engine acceleration flows to the engine. The following equations would be combined to result in equation 1:

$$W_f = C_1 P_x, \text{ p.p.h.}$$

where

P_x = the intermediate pressure between bleeds, p.s.i.a.

also

$$\frac{P_x}{P_{cd}} = f(N, T_1) = K$$

Therefore,

$$W_f = C_1 K P_{cd}, \text{ p.p.h.} \qquad (1)$$

One problem with this system is that the pressure P_x can never be reduced below ambient pressure (P_o) and therefore the minimum value of K will be:

$$K \text{ (minimum)} = \frac{P_o}{P_{cd}}$$

The value of C_1 is established on the basis of the maximum required W_f/P_{cd}. The minimum permissible value of W_f/P_{cd} will be in accordance with the following equation:

$$W_f/P_{cd} = C_1 \frac{P_o}{P_{cd}}$$

There are cases at engine speeds of 50 percent and lower where the required W_f/P_{cd} ratio is less than that allowable and, therefore, the acceleration schedule would be too rich at these speeds. Other methods of scheduling the acceleration flow below 50-percent engine speed could be used at a compromise in engine performance. At engine speeds above 50 percent, certain performance compromises must be made to the nonlinear characteristics for this type of multiplying circuit as the pressure ratio across either orifice becomes less than 1.89 and unchoked flow occurs.

In conclusion, therefore, it may be stated that this mode of computing offers advantages of simplification, but at the expense of engine performance.

5.2.2 Mechanical

Various linear and nonlinear mechanical multipliers were investigated. A linear-type multiplier was finally selected as it was not possible to achieve the required results over the wide range of variables with a nonlinear multiplier. The resulting configuration is shown in Figure 26, and since this method of multiplying was selected for incorporation in the final control design, its description and operation was discussed in paragraph 4.2.10.

By using servoed input signals of P_{cd} the mechanical multiplier will be insensitive to the g field. Two additional servos, one for T_1 and one for governing, are required with this system as compared with the servos which would have been required in the pneumatic method of multiplying. However, these additional servos are not susceptible to the g field to the extent that the control accuracy would be affected. The orientation of the servos is not all-important although there is a preferred orientation as discussed in paragraphs 4.2.11 and 4.2.13.

The principle of operation associated with this method is entirely within the state of the art, and therefore the development effort should be kept to a minimum consistent with the design.

5.2.3 Hydraulic

The multiplication and governing functions may be performed hydraulically at low force levels in a similar manner as accomplished in the pneumatic method described in paragraph 5.2.1. In this case the multiplication will be truly linear and will not be affected by the pressure ratio across the bleeds in series. It will be possible to achieve all the acceleration schedules required at the specified engine speeds. The theoretical minimum value of the multiplying factor (K) is zero. The system converts the compressor discharge pressure to a hydraulic equivalent above the control boost pressure (P_B). All other computing components are referenced to the control boost pressure so that the boost pressure effect is eliminated. The equations representing the operation of this system would be as follows:

$$W_f = C_1 (P_{R3'} - P_B), \text{ p.p.h.}$$

where

$P_{R3'}$ = the intermediate pressure between bleeds, p.s.i.

$$P_{R3} - P_B = P_{cd}, \text{ p.s.i.a.}$$

where

P_{R3} = regulated pressure supplied upstream of the first orifice

$$\frac{P_{R3'} - P_B}{P_{R3} - P_B} = f(N_1 T_1) = K$$

Therefore, combining equations,

$$W_f = C_1 K P_{cd}$$

In converting the compressor discharge pressure to an equivalent hydraulic pressure, a throttling-type pressure regulator utilizing an evacuated bellows, a pressure-force-balancing diaphragm, and a calibrated spring will be necessary. The spring, throttling valve diaphragm, and bellows would require orientation to permit g loading in a lateral direction to these components. The orientation of these components is based on the design philosophy as presented in paragraph

5. 1. 1. 1 for the hydromechanical compressor discharge pressure servo amplifier.

Fuel flow in the order of 300 p. p. h. at the 100-percent speed condition would be required for the computing circuit, with a lesser flow required at engine starting conditions.

A disadvantage of this system is that any error in the pressure transducer will add directly to the error of the system. This computing system, therefore, will contain four components which must be insensitive to the high g field, whereas the other systems contain only three.

5. 2. 4 Hydropneumatic

A possible simplification of the hydromechanical method of paragraph 5. 2. 2 could be achieved by performing the governing function pneumatically as described in paragraph 5. 2. 1. The multiplying function to generate the acceleration schedules would still be done mechanically. Some sacrifice regarding the achievement of minimum flow upon deceleration would be experienced under certain conditions. However, the engine fuel flow would always be low enough to permit deceleration. The sacrifice in minimum flow with this system would be inherently less than with the all-pneumatic system, the reason for this being that the minimum ratio of W_f/P_{cd} would be as follows:

$$W_f/P_{cd} = KC_1 P_o/P_{cd}$$

where

K = the multiplying factor produced by the the mechanical multiplier

The value of K would generally be less than one. The entire equation for control fuel flow would be as follows:

$$W_f = C_1 K K_1 P_{cd}$$

where

K_1 = pneumatic multiplying factor and is a function only of set speed error.

This method would eliminate the necessity of the servo system for governing in the all-mechanical method, since the governor valve would be positioned by the 3D cam. It is assumed that adequate friction could be built into the throttle shaft to provide the opposing force in the linkage system for operating the pneumatic valve. The only forces required would be that to overcome a spring preload which would be necessary to overcome the g .oading effect on the unbalanced levers for operating the pneumatic valve.

Adequate filtration must be provided to protect against contamination in the compressor discharge air computing bleed circuit.

5.2.5 Electronic Computing

Multiplication and governing functions may be performed electrically either by analog or digital techniques. Analog computation is based on measuring the signal level (such as voltage) of an electronic device whose input-output function is analogous to a mathematical operation. Digital technique approaches electronic computing from the altogether different direction of counting discrete quantities (quantums) which, in the electronic computer, are usually voltage pulses. Utilizing this basic operation of counting, the digital computer is theoretically capable of performing all other mathematical operations such as multiplying, integrating, and so forth.

The basic computing device in the modern high-speed electronic analog is the d.c. operational amplifier. This device can provide all linear single variable mathematical operations by means of feedback circuits and summing networks to its input. It is designed to provide high gain, input impedance, and linearity in order to minimize the computing errors introduced by circuit loading effects, and nonlinearities.

The binary switching or "nor" circuit is the basic computing element in digital technique, Figure 34. It possesses only two states of operation. In its one state (transistor cutoff), it supplies full voltage signal level, whereas in its "zero" state (transistor saturated), its voltage level is near zero. The "nor" circuit and the several other basic digital circuits (flip-flop, multivibrator, and so forth) form the building blocks out of which all the required arithmetic and logic operations are formed. The digital computer consists of complex networks of "nor" and other basic circuit elements.

A comparison of these two basic approaches to computation shows that the accuracy of analog techniques in "on" line computers is limited, in most cases, to errors exceeding $\pm$ 1 percent of full scale. A resolution better than this would require exceptionally high component accuracies, environmental controls, high power supply regulation, and thermal compensation. Under the environmental conditions of the engine fuel control even $\pm$ 5 percent accuracy could be difficult to achieve with this technique. The primary sources of error in the analog computer are the presence of noise, drift, and nonlinearity in its fundamental computing device, the d.c. operational amplifier. Noise is introduced into the output signal level from external sources and internally from thermal activity in the amplifier circuit elements. The source of drift is largely power supply and thermal variations which unbalance the circuit, thereby producing null signal output. Nonlinearity is primarily a result of saturation and cutoff in the transistor when the signal level excursion gets too large. All of these produce error because they can add or subtract from the instantaneous signal amplitude whose measurement yields the information being processed.

The digital technique avoids or minimizes the effect of these sources because the information it is processing resides not in the amplitude of its signal but in the operating state of its fundamental computing device, the "nor" circuit. Variations in signal amplitude produced by noise, drift, and nonlinearity will not produce an error in its computations as long as it does not prevent the "nor" circuit from switching when a command signal is present at its input or produces inadvertent switching.

The error produced by a digital computer is the magnitude of the quantum or discrete quantity which can be provided by the designer to meet the accuracy requirements of the computation. The size of the quantum can be reduced by increasing the number of switching elements in the counter. The quantum error in a binary register is divided in half by each additional flip-flop. The number of elements therefore increases with increased accuracy; the time required to "switch" each element remains the same, however, and therefore greater accuracy will require a longer computation time. Higher accuracy, therefore, requires faster switching circuits if the computation period is limited to a maximum allowable time. Without considering cost and size, switching speed limits digital computer accuracy. Additional circuitry is required by a practical digital computer besides the basic binary counter. These are: logic circuitry

for determining on the basis of the sum registered in the counter the command required of the actuator, a clock oscillator for providing a time reference (since engine speed is proportional to pulse repetition rate) and for synchronization, and translating circuitry for converting the command signal into a form which is compatible with actuator operating requirements. In general, a computer's size and complexity increases with the number and complexity of the arithmetic and logical operations it is required to perform and with the accuracy requirement .

Since the error toleration of the speed computer servo is in the order of $\pm$ 0.1 percent of full-scale signal under an extreme operating environment, analog techniques are not recommended for application in the proposed fuel control system.

Digital computing techniques, though requiring more complex circuitry, can provide the accuracy required of the speed computer servo well within their inherent limitations.

A fully electronic fuel control would compute the fuel schedule equations to the required accuracy and within the allowed time. Its inputs are signals from the P_{cd} engine speed and temperature transducers of the system. Its output is a command signal to the fuel metering valve which sets fuel flow rate.

Figure 10 is a signal flow block diagram describing the specific functional operations required of the computer and their interrelationships. The equation that is being computed is shown graphically in Figure 10.

Figure 44 is a system block diagram of an electronic fuel controller synthesized to perform the requirement of the signal flow block diagram depicted in Figure 10. For acceleration scheduling, the value of W_f/P_{cd} is read off the 3D cam by a technique utilizing a read-write magnetic memory disk in a digital control circuit. The surface height of the 3D cam, which represents W_f/P_{cd}, proportionally positions the readout head relative to the write head of a magnetic memory disk about the disk perimeter. The operation of the magnetic memory disk is based on the operating principles of a magnetic recording disk speed sensor described in paragraph 5.1.2.2. However, here only the feedback measurement is required. It is assumed that the 3D cam is positioned electronically by a digital computing model also described in paragraph 5.1.2.2. The readout pulse

is fed back to the recording head to produce transport delay oscillations whose period is directly proportional to read head angular position and inversely proportional to engine speed. These pulses are supplied to a single flip-flop whose output is a square wave with a period equal to twice that of the memory disk oscillations. The square wave half period is therefore directly proportional to the computed acceleration schedule.

The governor proportional cut-in schedule is generated in the form of a square wave whose pulse width is directly proportional to the difference between the engine speed (N) and the reference speed (N*) and inversely proportional to engine speed. The output signals from both the acceleration and governor schedule computers are supplied to the input of a comparator circuit where the signal with the shortest pulse width is gated to the input of the multiplier. The multiplier consists of a gate which receives both the gated schedule square wave and a signal which has been frequency modulated by the compressor discharge pressure. The F.M. P_{cd} signal is transmitted to a binary register during the period that the schedule signal is "on," producing a count of the number of pulses of the P_{cd} signal occurring during the schedule "on" period. This pulse count is taken for a fixed period of time as determined by the clock oscillator signal (c.p.). The total count registered during this period is of course the computed fuel rate in binary form. The sum registered in the binary counter is transmitted to the translator through the output gate which is "on" when the synchronous signal is generated. The translator is provided to convert the information to a form compatible with the fuel meter actuator input requirements. It should be noted that engine speed synchronizes all the computer operations in this system. Acceleration and governor schedules are functions of engine speed and therefore are inherently synchronized with this parameter. While in the multiplier the binary counter is "cleared" at the end of the counting period in some appropriate phase of the engine speed cycle.

The primary problem in designing a computer such as described is providing a P_{cd} F.M. signal with the required accuracy (less than 1 percent of full scale, see paragraph 5.1.1.2). Also, a substantial program could be involved in the development of a magnetic memory drum as previously discussed in paragraph 5.1.2.2

5.3 Metering System

The information provided in the computing circuit has all been directed toward the delivering of an output to which fuel flow can be

metered in a proportional manner. Conventionally, this is accomplished by maintaining a constant pressure drop across a metering valve whose area is proportionally positioned in accordance with the computer output signal.

The positioning of the metering valve will be integrated with the mechanisms selected for engine signal amplification and computing to the extent that no additional mechanisms will be necessary which are required to be insensitive to the g field. The metering valve could be of the sleeve type with the applied g load in any direction.

The metering head regulator design must be patterned after the design approach as presented in paragraph 5.1.1.1 insofar as the orientation of components is concerned, that is, the g load must be lateral to the axis of the components. The regulator could be of the flow bypassing or throttling type, both of which would utilize a differential sensing diaphragm, a spring, and a valve. The valve would be supported on a ball bushing to essentially eliminate the effect of the laterally directed g load insofar as friction is concerned.

5.4 Pumping System

Since fuel will be provided to the engine fuel control from the aircraft through the whirling rotor blade, the first thought that comes to mind is to let the rotor blade do the pumping. However, there are operating conditions wherein the rotor blades will not be whirling and, therefore no pumping action is exhibited. This suggests that a pump of one form or another is required. The question is: should the pump be engine-mounted and therefore operate in the g field, or should the pump be airframe-mounted ?

An airframe-mounted pump would be required to provide sufficient pressure and flow to satisfy all the engine operating conditions when the rotor is not whirling and, in addition, provide adequate flow capacity at reduced pressures when the rotor is whirling. Also, a system of this type would require a throttling regulator at the control inlet or outlet to reduce the fuel pressure for admittance to the engine. At 267g and a 65-foot radius rotor the fuel pressure will be approximately 2820 p.s.i.

$$P = \frac{\rho r}{2} g, \text{ p.s.i.}$$

where

ρ = fuel density, lb/in.^{3}
r = rotor radius, in.
g = number of times gravity

With no pump at the engine to provide a sump for return of servo flow, any servos which are operated on fuel must use only metered flow. This servo flow must be obtained by a parallel path around the throttle regulator. This would place severe operating requirements on the throttle regulator which already has a difficult job to perform. In addition, this would critically restrict the dynamic performance and number of servo valves which could be used if operated on engine fuel. At times engine flow is very low, less than that required to operate one servo system having a response of the order of 10 milliseconds.

Since throttling of the high-pressure fuel is necessary anyway, an engine-mounted pump located downstream of the throttling regulator could be supplied with normally encountered boost pressures of the order of 50 p. s. i. g. With this arrangement the pump would be operated in a normal manner, and a low-pressure sump at the pump inlet would be provided for bypassing adequate quantities of servo fuel. Also, this system would permit the operation of the fuel pump and control at normal control pressure levels, thereby permitting the use of standard lightweight aluminum castings. Steel housings would be required only for the high-pressure throttling regulator if adequate safety features were provided to ensure fuel shutoff in the event of a throttle regulator failure.

The operation of an engine-mounted fuel pump in the g field appears feasible, especially for the CAE model 357-1 engine. The pump discharge pressure level for the engine configuration being used is relatively low compared with other configuration engines, and therefore additional bearing loads can be tolerated without having to oversize the pump bearings.

It is preferred to orient the pump so that the axis of the gears is perpendicular to the direction of g loading. Although an orientation in which the gear axis is parallel with the rotor axis would eliminate gyroscopic coupling effects on the bearings, this couple is so low that it is of no consequence in considering the orientation. In the application being considered the level of pump pressure rise is so low that if

it were directed on the gears so as to oppose the g load force, the gears would at some time during the operation change the direction of bearing loading in the housing. This load direction change would be detrimental to the pump operation in more ways than one. It is therefore necessary to orient the pump inlet on the outboard side, and the discharge port on the inboard side of the pump. With this orientation, the bearing load due to the g field adds to that produced by the pressure load.

In conventional installations an engine-mounted boost pump of the impeller-type design is used to provide added pressures for charging the gear pump for operation at high altitudes. Also, the gear pump is required to operate in the event of a tank-mounted boost pump failure; the impeller pump permits this due to its favorable lift characteristics. With the proposed aircraft configuration, it is considered that, in the event of a boost pump failure, an impeller pump mounted at the engine would not be capable of lifting the fuel from the tanks and through the rotor hub up into the rotor to continue the supply of fuel to the gear pump. Also, it is possible under all other conditions to have adequate fuel pressure at the pump inlet. There appears to be no useful purpose to an engine-mounted impeller boost pump.

Unless an all-electronic control is used so that no fuel is required for the operation of servo valves, it is recommended that an engine-mounted pump be used. In any case, an engine-mounted, impeller-type boost pump is considered to be unnecessary.

6. DYNAMIC STUDIES

Engine Dynamics

From References 1 and 2, and assuming a 20-percent reduction in the engine time constant per CAE, the estimated engine transfer function from fuel flow to speed at 100-percent speed, sea level, standard day, is given by:

$$\frac{\Delta N}{\Delta W_f} = \frac{3.6e^{-0.18s}}{0.24s + 1} \qquad (1)$$

Figure 45 shows a frequency response plot of the engine transfer function. The allowable control gain as a function of phase margin is tabulated below:

Phase Margin degrees	Control Gain p.p.h/r.p.m.
15	0.85
25	0.66
35	0.60
45	0.56

Control Dynamics

Dynamic performance of the proposed fuel control is described in terms of linearized transfer functions for acceleration and governor operation. The analysis is based on differential equations that express: (1) conservation of mass, and (2) transient force balance between applied pressure forces and spring loads. A more rigorous analysis would require the determination of the effects of inertia loads, including fluid inertia, and damping loads due to viscous and sliding friction.

Response During Acceleration

With reference to the fuel control schematic, the components contributing to the transient response during acceleration include the CDP amplifier and electronic stepping motor. The estimated response of both components is equivalent to a first-order lag whose time constant is 0.007 second. The transfer function from P_{cd} to W_f is

$$\frac{\Delta W_f}{\Delta P_{cd}} = \frac{W_f/P_{cd}}{0.007s + 1}$$

and the transfer function from N to W_f is

$$\frac{\Delta W_f}{\Delta N} = \frac{0.280}{0.007s + 1}$$

Response During Governor Operation

The components contributing to the response of the fuel control during governor operation include the electronic stepping motor and the

speed governor amplifier. The estimated response of the speed governor is also 0.007 second. The transfer function of the fuel control during governor operation is therefore

$$\frac{\Delta W_f}{\Delta N} = \frac{0.675}{(0.007s + 1)(0.007s + 1)}$$

The control gain (0.675 p.p.h./r.p.m.) was required to meet the governor speed accuracy specified. Comparing this gain with the phase margin-control gain table on page 73 indicates a phase margin of approximately 15°. However, further studies are required to establish the required control mode, governor gain, and closed-loop response required for stable flight control. Cyclic variations in compressor inlet temperature and pressure which result during forward flight might introduce speed and thrust variations which are considered excessive. A linearized analysis was conducted to determine the effects of these cyclic variations; however, the errors introduced as a result of linearizing were too large and therefore the results were inconclusive. It is apparent from engine performance data shown on Figure 1 of Amendment 1, Reference 3, that the net thrust variations of a constant speed control will be approximately 20 pounds or 1.7 percent of normal power rating. However, if the thrust variations which result with a conventional control system are found to be excessive, modifications to the proposed control to provide constant speed control could result in hardware equivalent to the present computer section of the proposed control.

The problems associated with a constant speed control are manifest in the engine transportation and inertia lags. The speed control system of the fuel control is quick enough to modulate fuel flow almost at the instant a speed error is sensed. However, at the cyclic frequencies* associated with the helicopter rotor speed the fuel flow delivered by the control is not seen at the engine for a time equivalent to the rotor moving approximately 100°. This phase lag is caused by the engine transportation lag. Coupling this lag with the inertia lag of the engine rotor results in a phase lag between a change in fuel flow from the control to a change in engine speed which approaches 180°. It is therefore apparent that a constant speed control system will have to incorporate lead and adaptive networks. A more rigorous study is therefore warranted. This study would include nonlinear electronic simulation of the complete power control system and would serve to define the various ramifications of a stable flight control system. * (65-ft. radius, 10.8 rad/sec. rotational speed.)

7. PACKAGING

Figures 13 and 46 are layout drawings for a typical fuel pump and fuel control system designed in accordance with the details as presented early in this report. For these typical layout drawings no effort was made to integrate the pump and control package. Therefore, two packages are presently defined. Upon consideration of a definitive envelope requirement, the integration of the two would be a desirable goal.

The upstream shutoff valve, throttle regulator, and safety shutoff valve permit segregation of the control housing with regard to proof pressure levels. These components protect the pump and fuel control from exposure to the high fuel pressure levels developed by the whirling rotor. As depicted in Figure 46, one housing contains both the high- and low-pressure components. This is desirable because of the interconnecting throttle shaft. The entire housing will be cast of aluminum with the high-pressure section design upgraded to withstand the increased pressure levels. The low-pressure level section will be designed for the normal operating pressure levels. Upon redesign of the control to a specific layout requirement, a study will be necessary to determine the weight tradeoff between using aluminum or steel for the high-pressure section of the control.

An estimated dry weight of the design as illustrated by Figure 46 is 19 pounds; the net weight is estimated at 20.5 pounds. It is considered that every effort will be made in detailing the components to lighten the structures where strength is not of major importance. Shafts will be hollow where possible. This effort will not only lighten the control but will also aid in reducing the sensitivity to the g field.

The electronic components are packaged using printed circuit boards with solder hook terminals. Transistors are used throughout the design with heat sinks provided as necessary. The entire circuitry is encapsulated in an epoxy having a high coefficient of thermal conductivity. The epoxy also serves as a binder for supporting the circuit boards in the g field. The boards will be oriented such that the g field will be directed perpendicular to the boards, thus loading the components against the boards. Heat transfer calculations have been made, assuming lumped parameters, which reveal a maximum temperature rise of 25°C above the component

ambient. The component ambient is assumed to be fuel temperature, since the package will be inserted into a cavity in the fuel housing. At a 250°F fuel temperature, therefore, the maximum component temperature of the electronic elements will be about 300°F. The electronic elements are capable of operation to 350°F.

Some weight-saving advantages may be gained through the efforts of parallel development programs in certain areas of design which were not selected. For instance, it is conceivable that the flyweight type speed sensing and amplifying system described in paragraph 5.1.2.1 can be made to work with good accuracy and reliability. It is anticipated that a savings in weight and space could be achieved with this system. Also, the method of governing which combines the pneumatic governor with the mechanical multiplier described in paragraph 5.2.4, although not affecting weight and size, would most likely be less costly.

8. FAILURE ANALYSIS

The table on the following pages outlines the results of a preliminary failure analysis. The table lists each component in the fuel control system, the possible failure, and the effect of this failure on the performance of the fuel control. The components referred to are depicted in Figure 7.

The results indicate that with the exception of failure 10, all failures will result in a lean fuel flow or a complete shutdown of the control and therefore fail safe. Failure 10 can be made fail safe by incorporating a check valve in the P_{cd} line. This would ensure that fuel could not enter the combustion chamber through the P_{cd} sensing line and therefore failure 10 was not considered in more detail.

The possibility of links, shafts, or springs breaking is remote and therefore was not considered. Also, a failure analysis of the electronic circuits would require a detailed study which is not warranted in this part of the program. Moreover, should the need arise, the electronic control can be designed to incorporate a fail-safe circuit.

The analysis presented herein is preliminary in that it considers only the effects of the more salient modes of failure. It was conducted to ensure that components were designed and oriented so

that if a subcomponent failure occurred, it would result in a safe failure. During the course of a detailed design of the proposed fuel control, a rigorous failure analysis will be conducted.

TABLE I
PRELIMINARY FAILURE ANALYSIS

COMPONENT	FAILURE	FUEL CONTROL PERFORMANCE
Fuel shutoff valve upstream	1. Seal in main flow path	1. High-pressure throttling regulator diaphragm will break. Safety shutoff valve closes. Control is protected from high pressure, but will not function.
	2. Seal between P_R and throttle shaft	2. As above
High-pressure throttling regulator	3. Diaphragm	3. Safety vent valve closes. Safety shutoff valve closes. Control is protected from high pressure and will not function.
Safety shutoff valve	4. Seal	4. As a single failure, will have no effect on fuel control. As double failure, coupled with failure 1, 2, or 3, will allow high pressure into fuel control.
Metering head regulator	5. Diaphragm breaks	5. Metering head regulator valve will open and bypass pump output thereby reducing fuel flow to engine.
Main metering valve	6. Valve seizure	6. The valve is powered in the closing direction and therefore this failure will cause a lean fuel flow when the control calls for increasing fuel flow.

TABLE (Cont'd)

COMPONENT	FAILURE	FUEL CONTROL PERFORMANCE
Fuel shutoff valve downstream	7. Seal in main flow path	7. Fuel allowed to enter engine before light-off resulting in hot start. However, the amount of flow leaking by the seal will be small and effect will be negligible.
	8. Seal between P_N and P_B	8. The amount of leakage by this seal will be loss of metered flow.
Compressor discharge pressure amplifier	9. Vacuum bellows breaks	9. Shift in output from P_{cd} absolute to $P_{cd}-P_B$ therefore fuel schedule will be lean.
	10. P_{cd} bellows breaks	10. Fuel can enter engine combustion chamber through P_{cd} sensing line.
	11. Upstream bleed clogs	11. P_{cd} output signal goes to zero thereby reducing fuel flow.
T_1 Sensor	12. Bellows breaks	12. Loss of T_1 signal. Schedule shifts to -75°F. Therefore, fuel schedules run lean.
T_1 Power amplifier	13. Upstream bleed clogs	13. As above.
Governor power amplifier	14. Servo valve seizure	14. Force levels available to move servo valve are high enough to break servo valve free should it seize due to contamination.

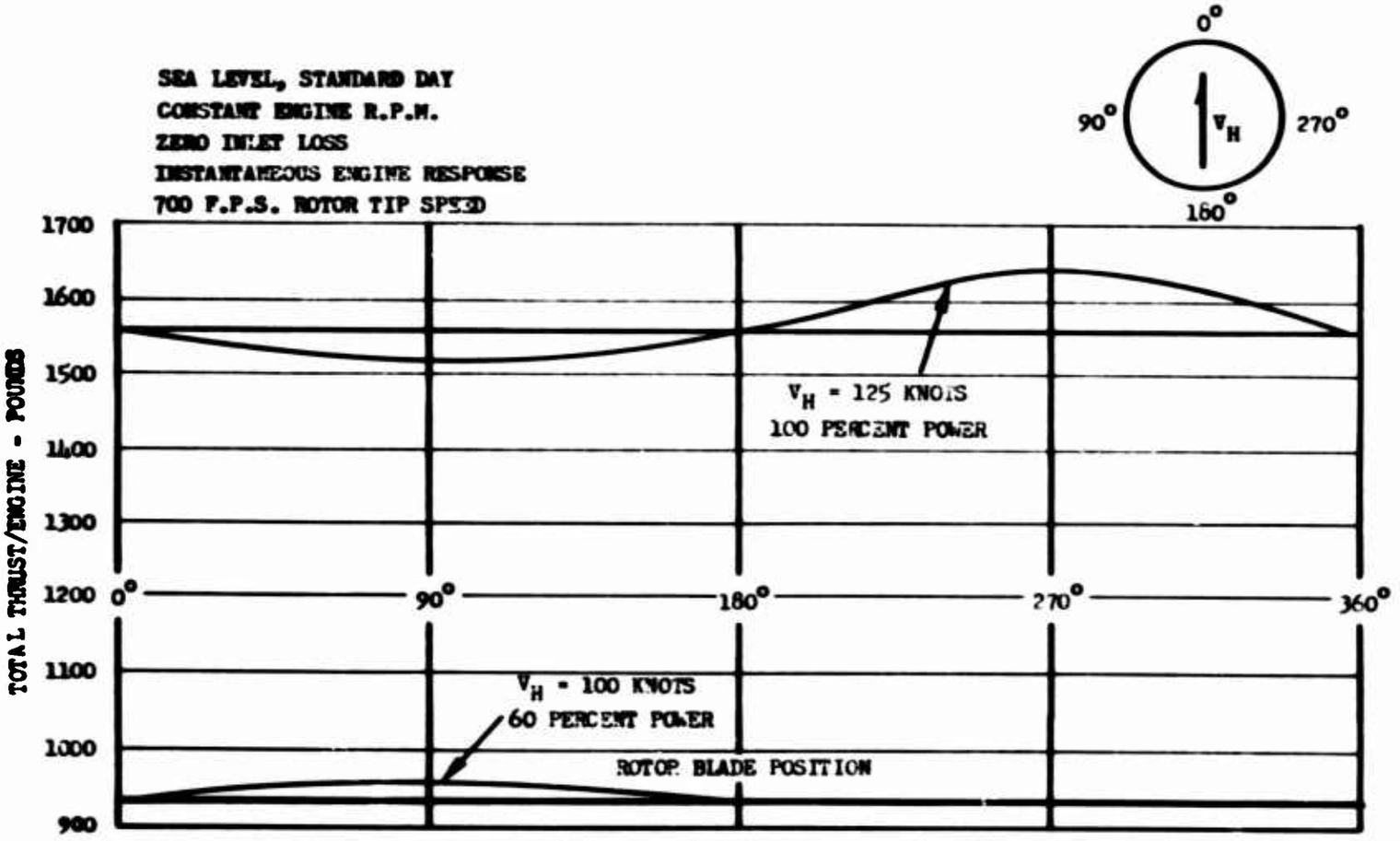

Fig. 1. Thrust Versus Rotor Blade Position - Model 357-1 Tip Turbojet Engine.

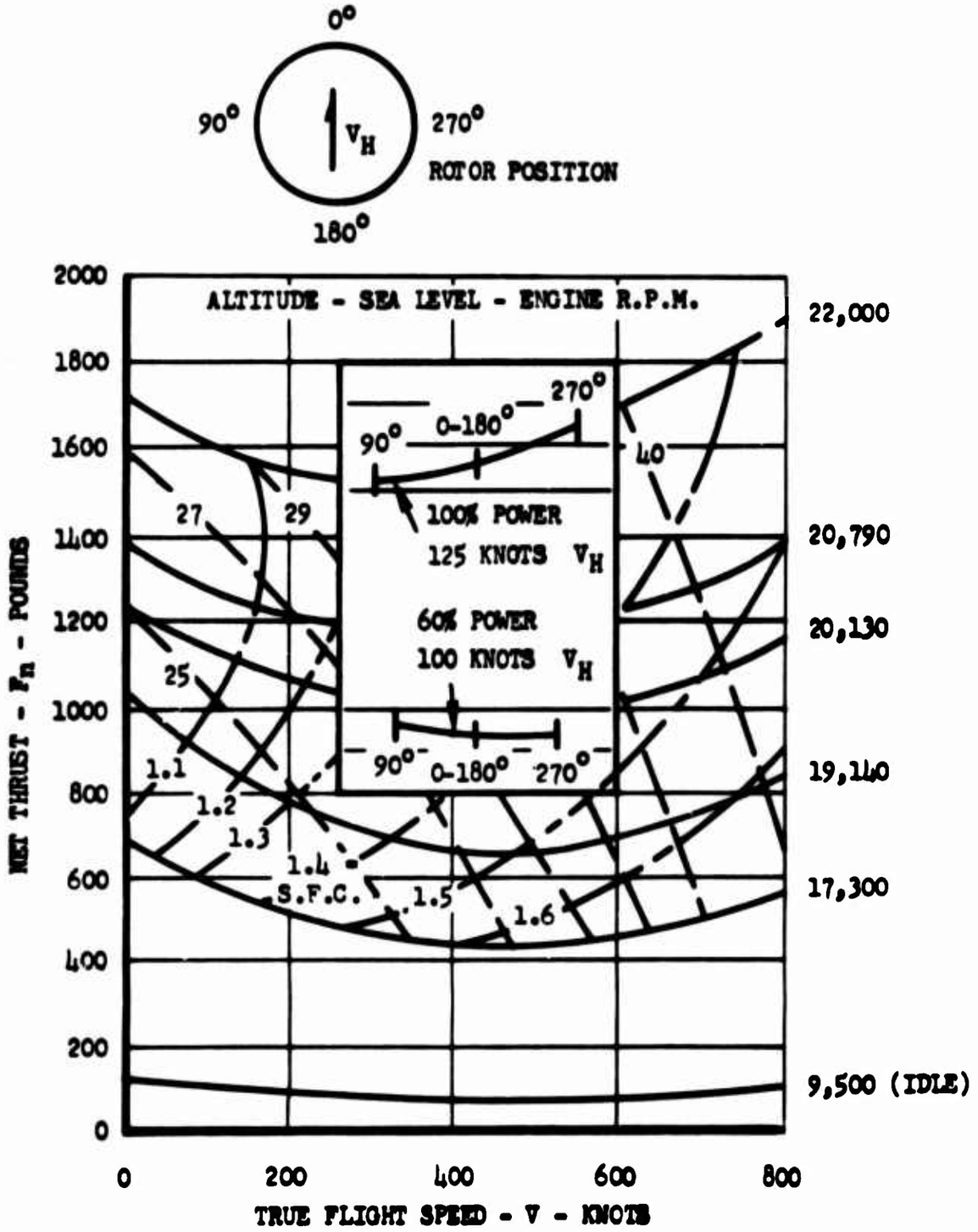

Fig. 2. Performance Characteristics - Model 357-1 Tip Turbojet Engine.

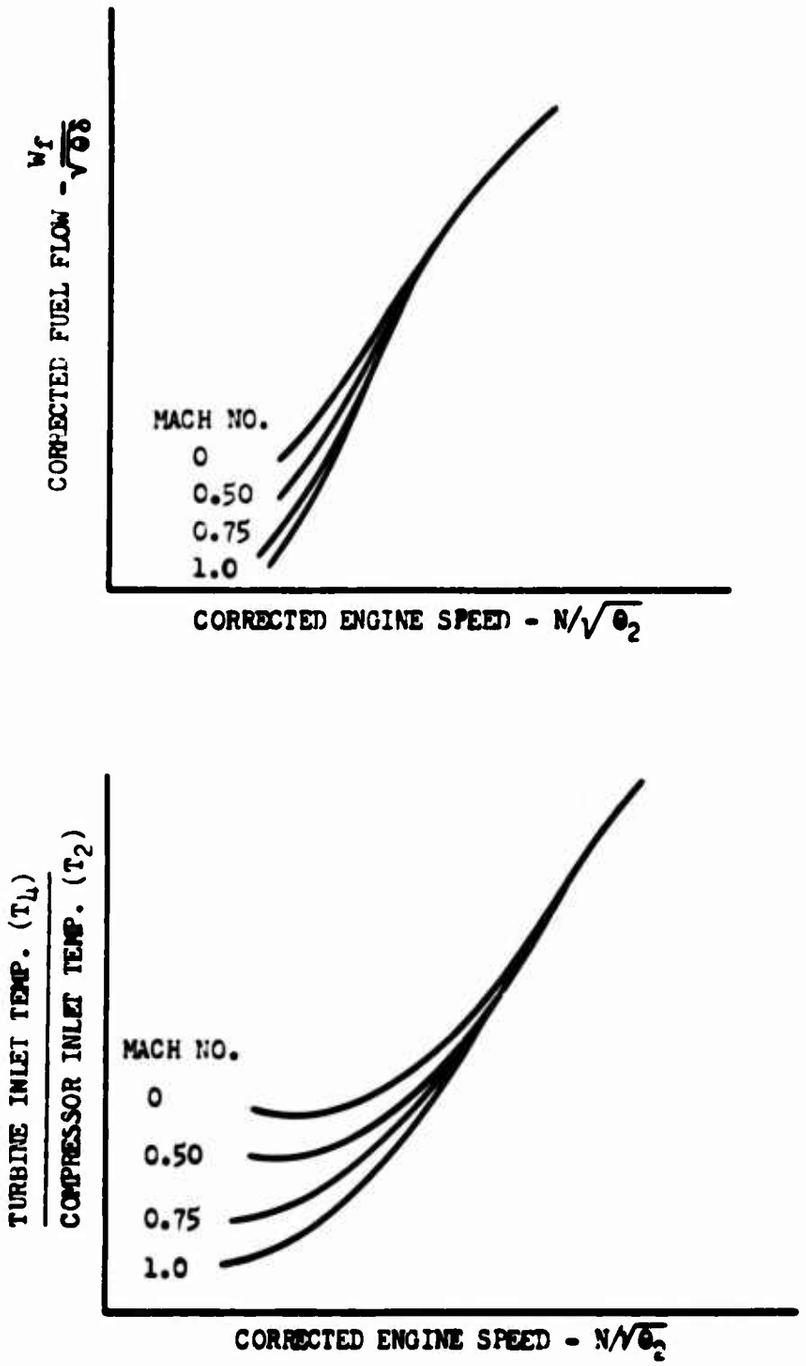

Fig. 3. Example of Generalized Performance Curves Used in Estimating Condition Parameters Under Rotor Environment - Model 357-1 Tip Turbojet Engine.

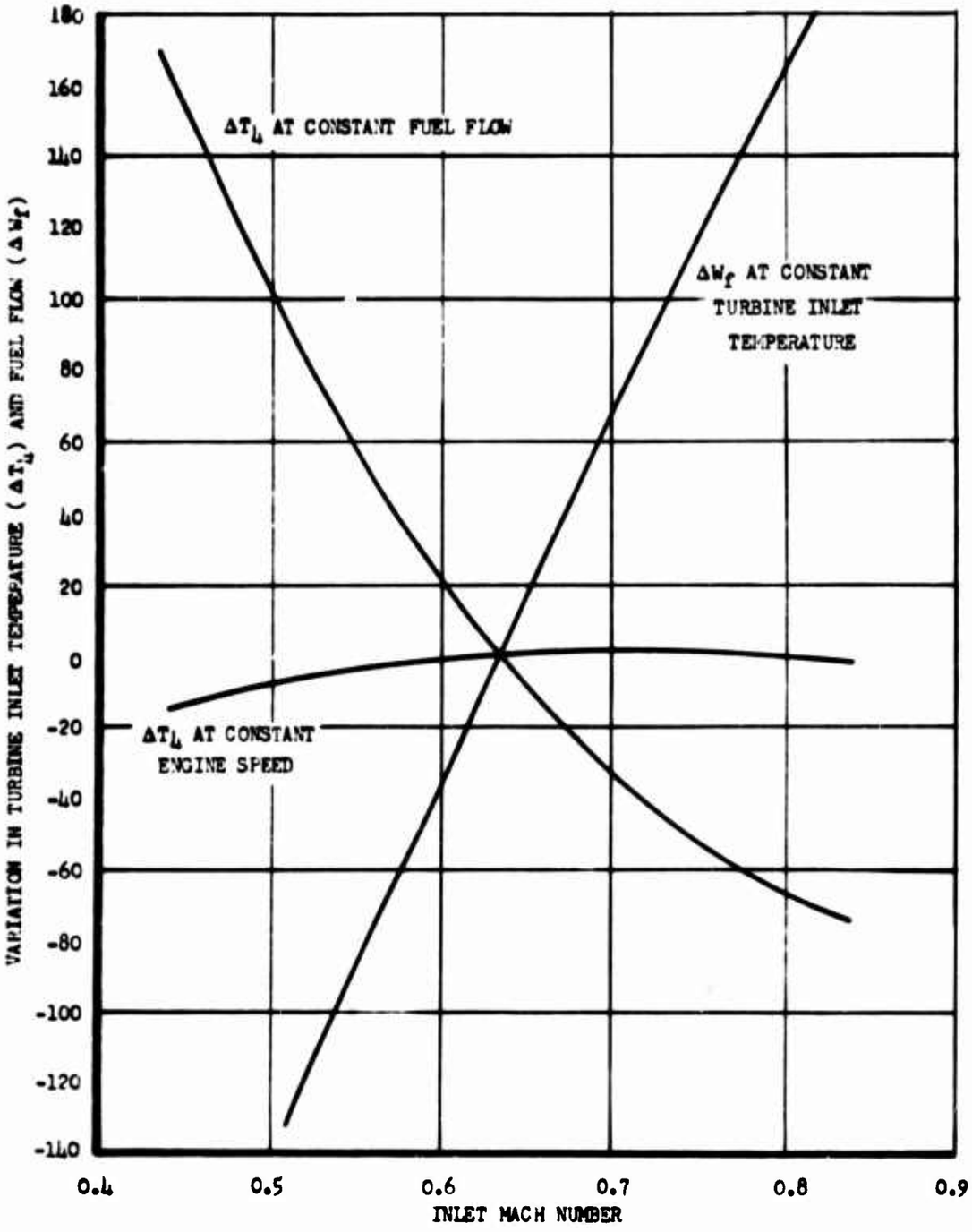

Fig. 4. Estimated Performance Characteristics Under Rotor Conditions - 100 Percent Power, 125 Knots - Model 357-1 Tip Turbojet Engine.

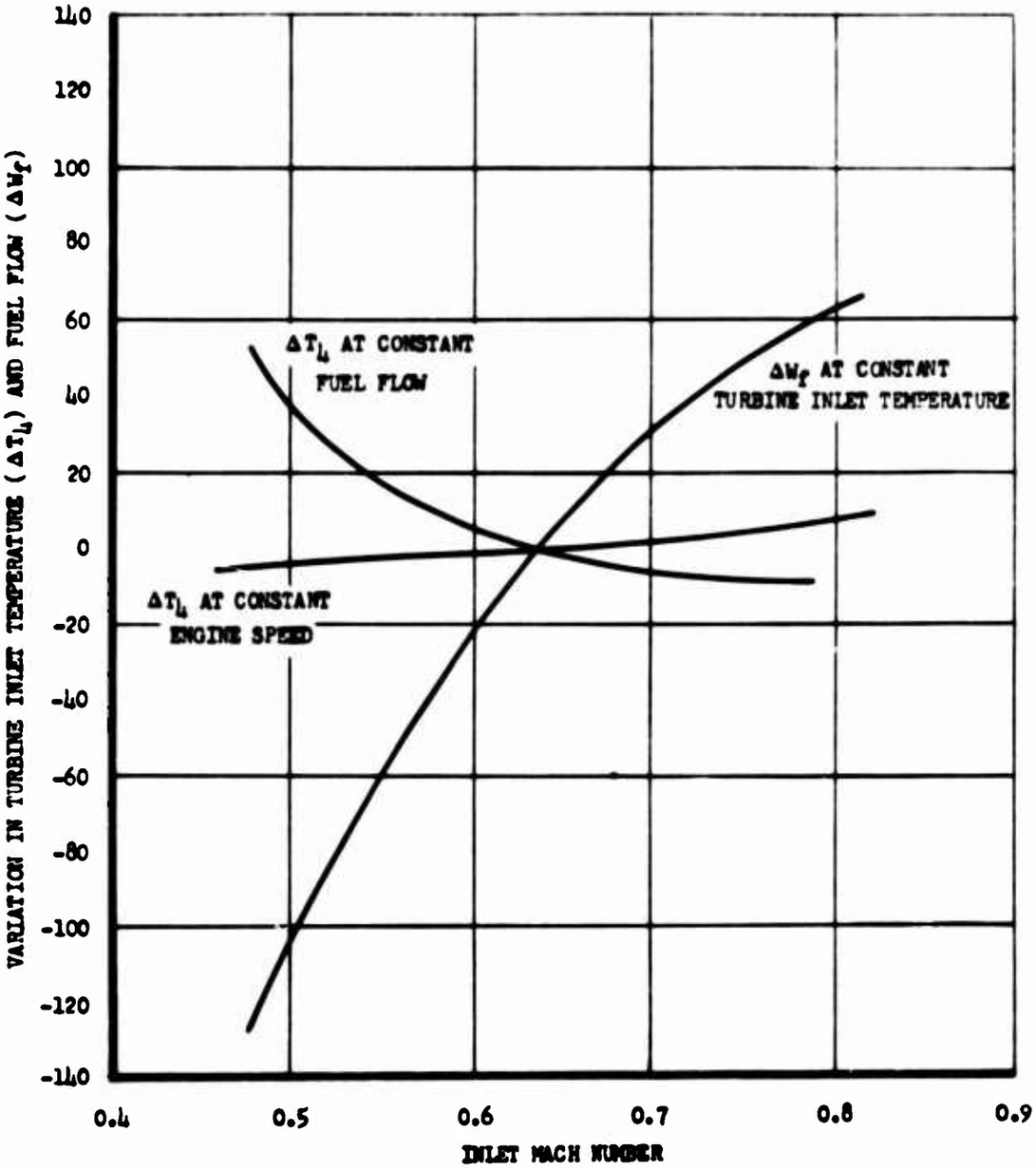

Fig. 5. Estimated Performance Characteristics Under Rotor Conditions - 60 Percent Power, 100 Knots - Model 357-1 Tip Turbojet Engine.

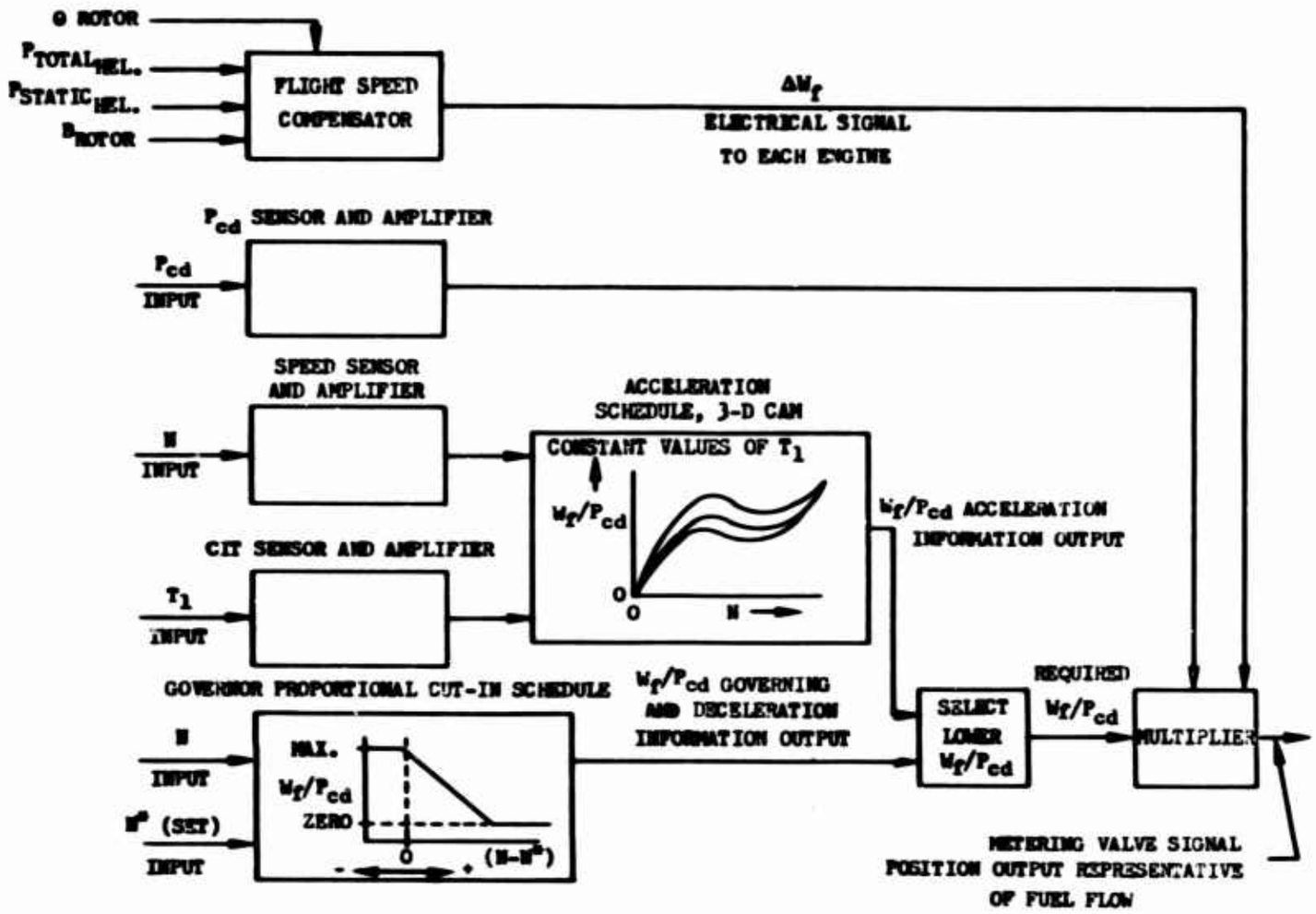

Fig. 6. Rotor Tip Fuel Control System.

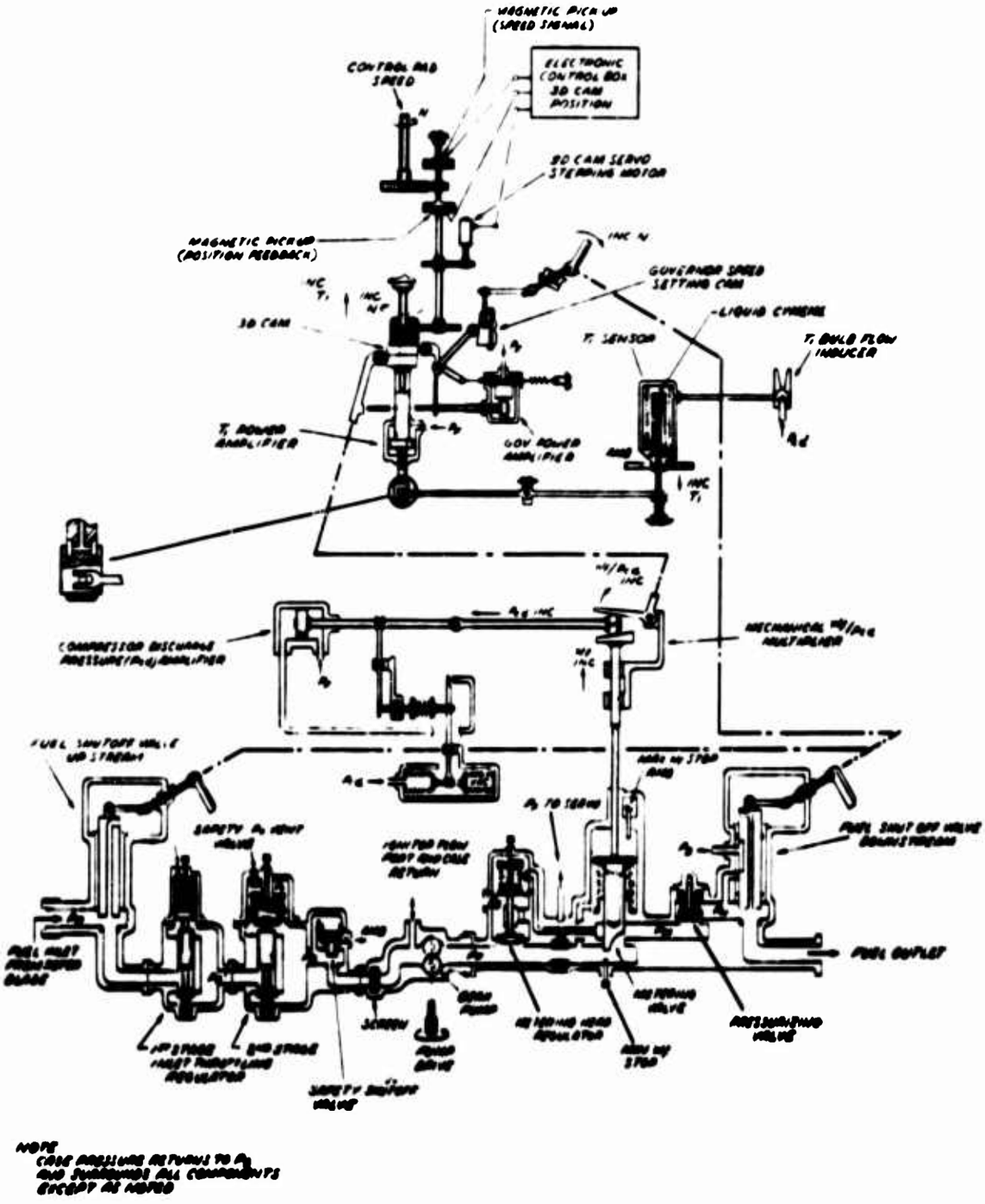

Fig. 7. Model 357-1 Tip Turbojet Engine Main Fuel Control.

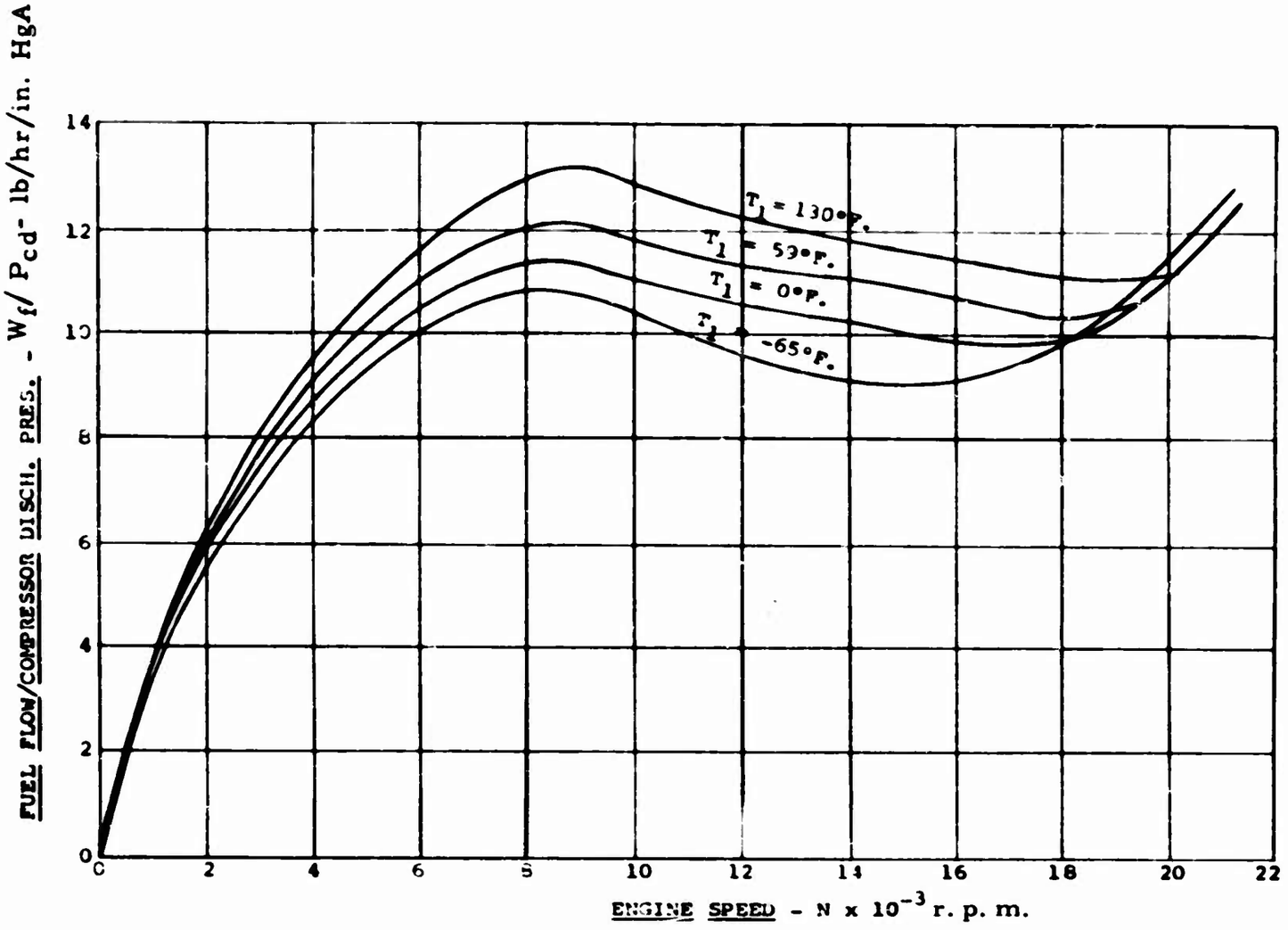

Fig. 8. Rotor Tip Fuel Control - Engine Required Acceleration Fuel Schedule.

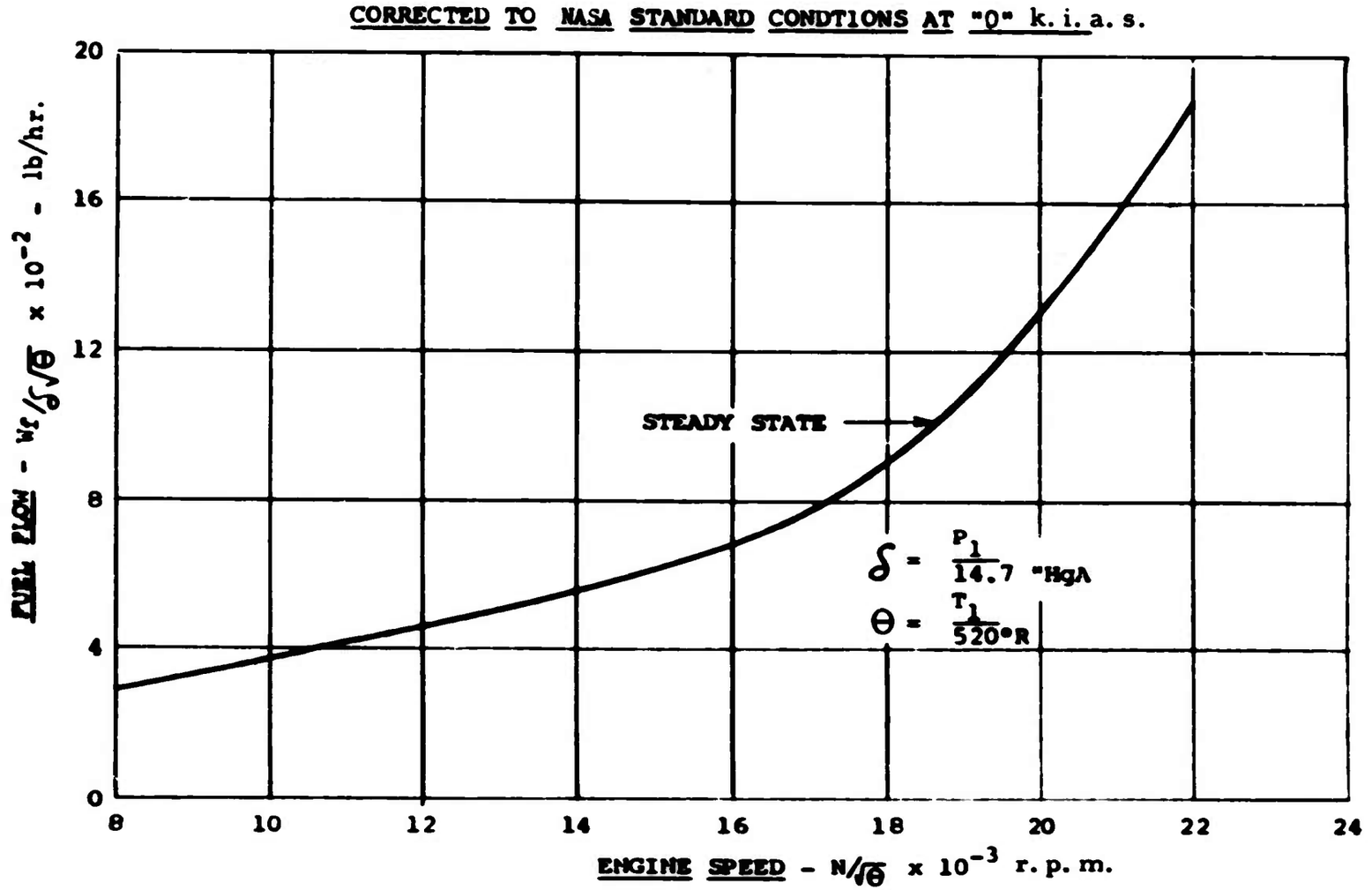

Fig. 9. Rotor Tip Fuel Control - Engine Fuel Flow Requirements, Altitude - Sea Level.

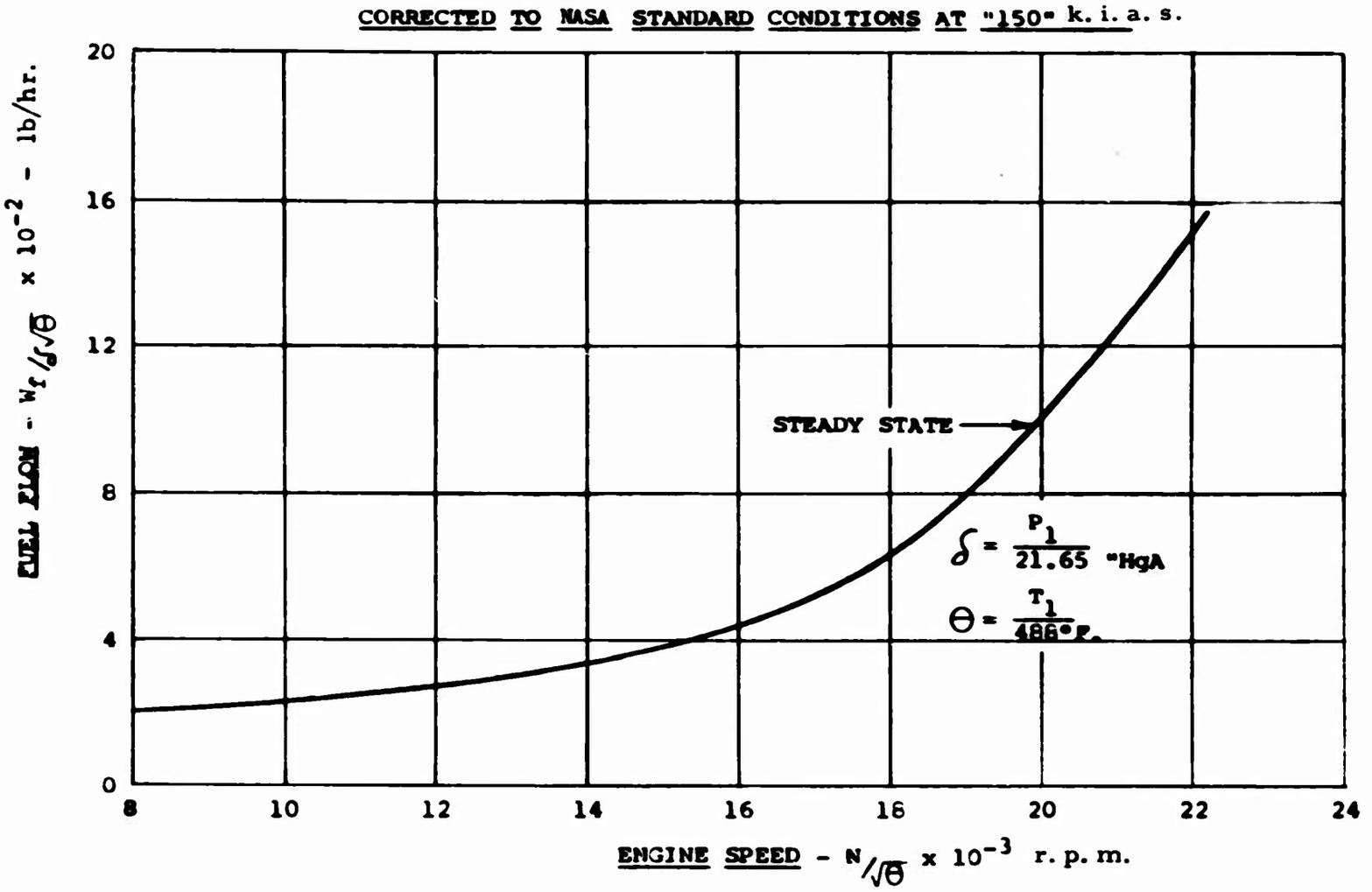

Fig. 9a. Altitude - 10,000 Feet

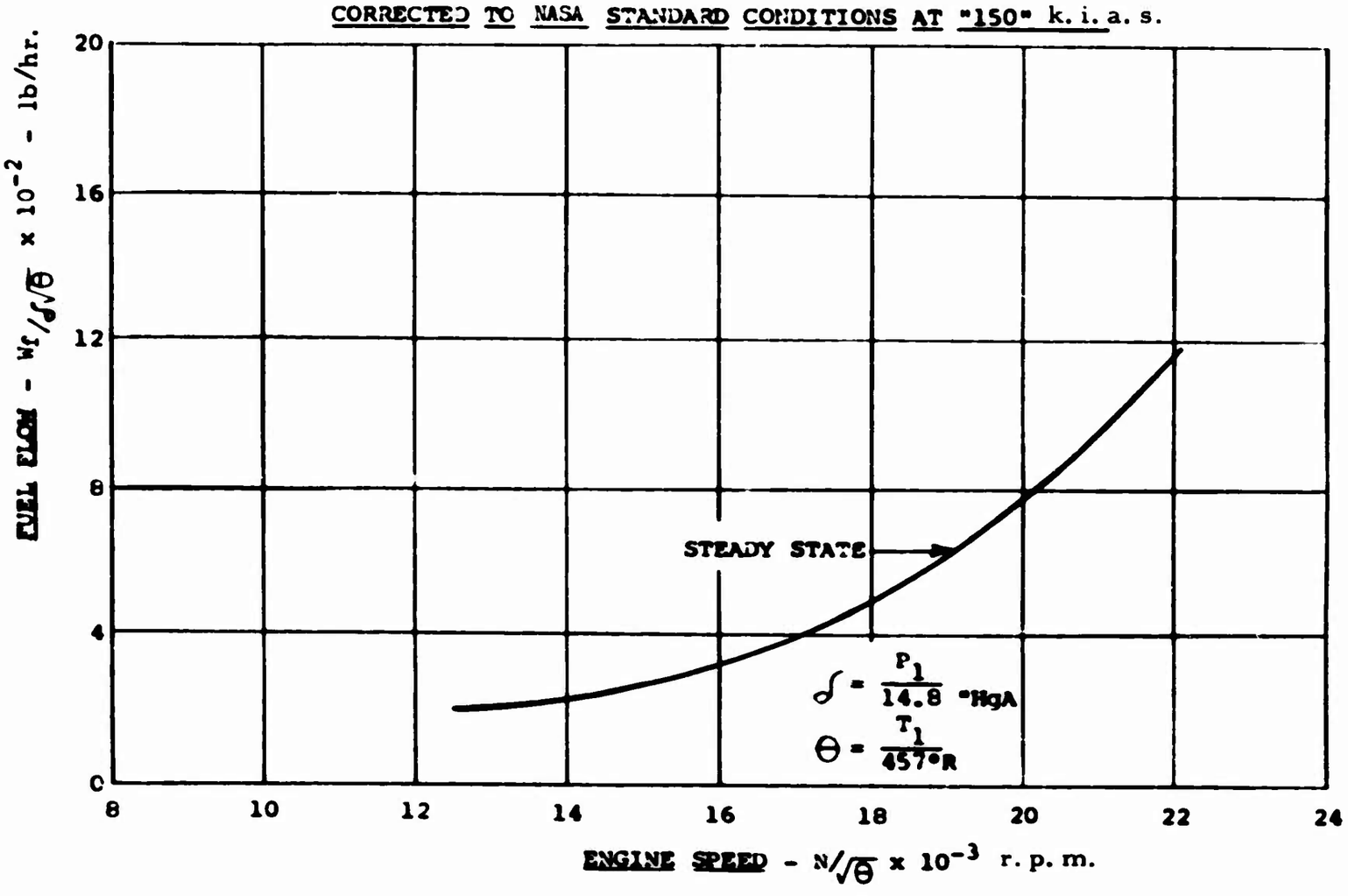

Fig. 9b. Altitude - 20,000 Feet.

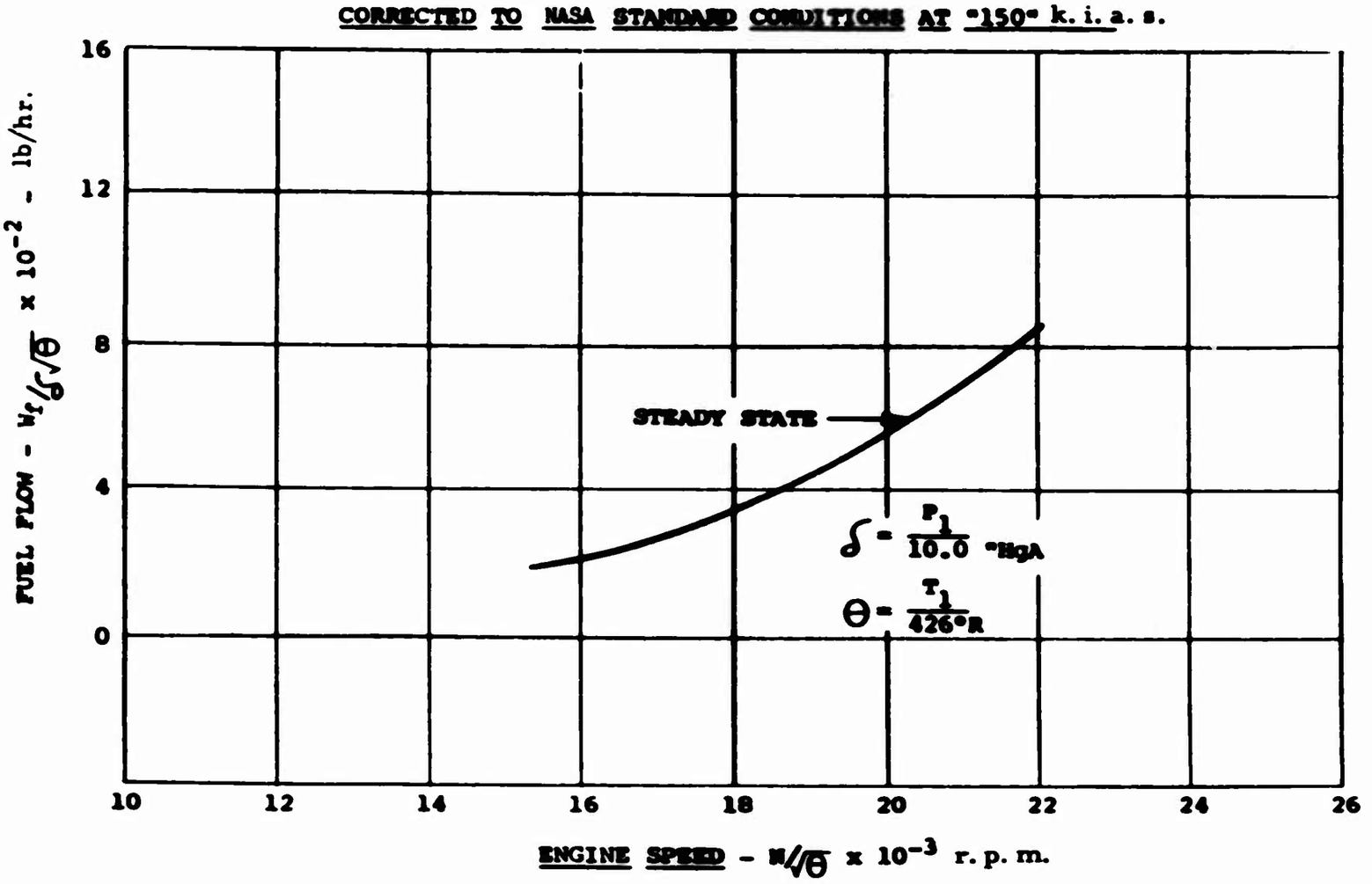

Fig. 9c. Altitude - 30, 000 Feet

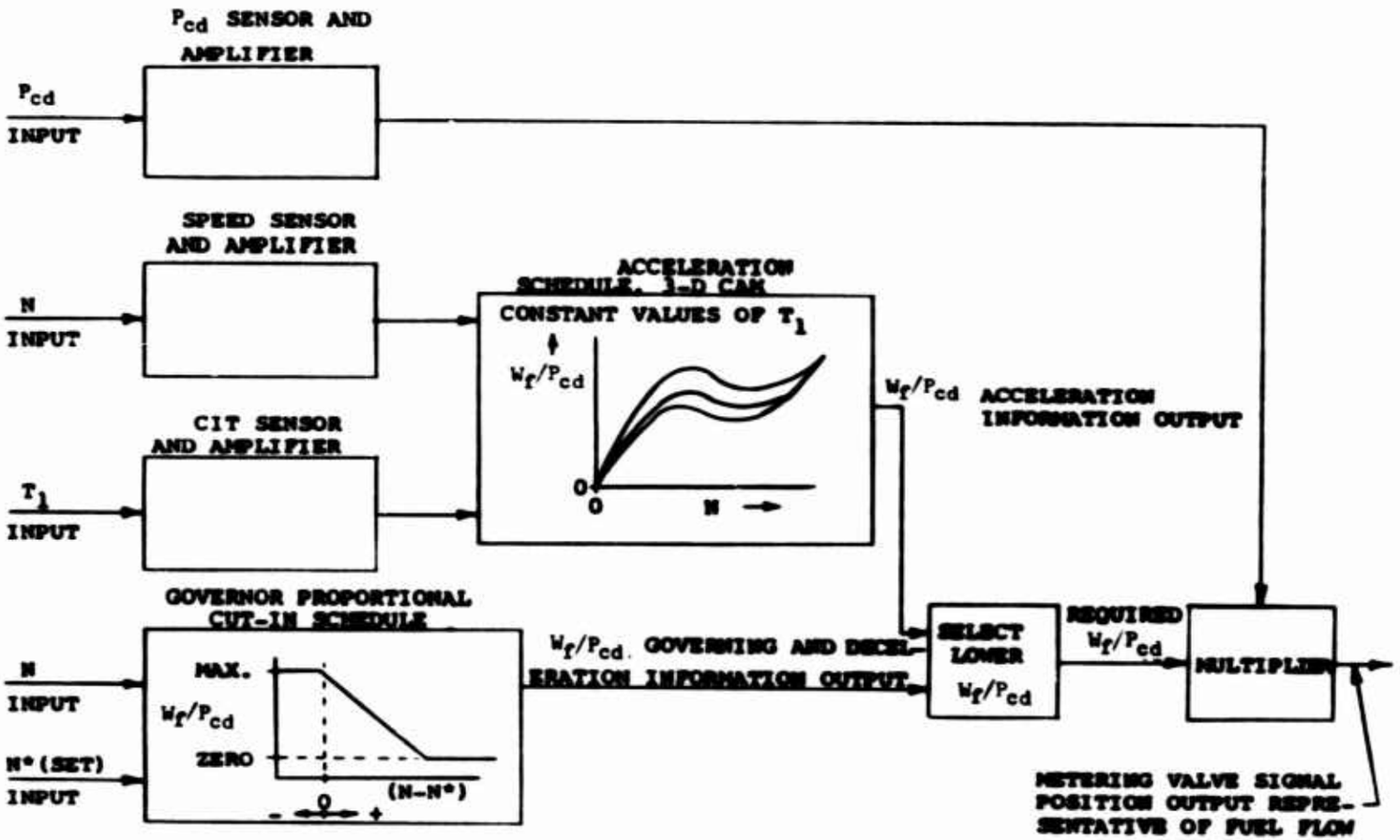

Fig. 10. Rotor Tip Fuel Control - Fuel Control System.

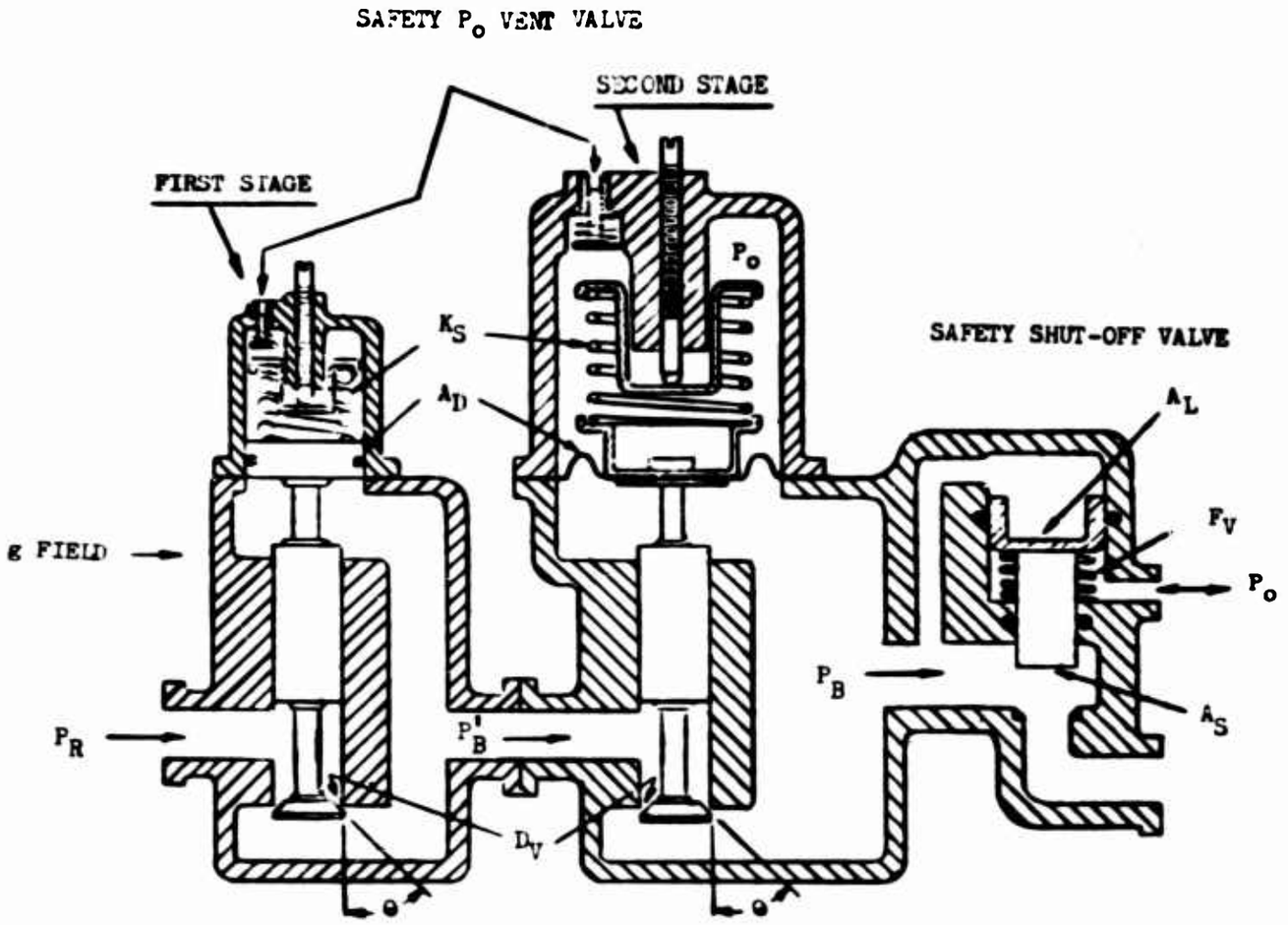

Fig. 11. Rotor Tip Fuel Control - Inlet Throttling Regulator.

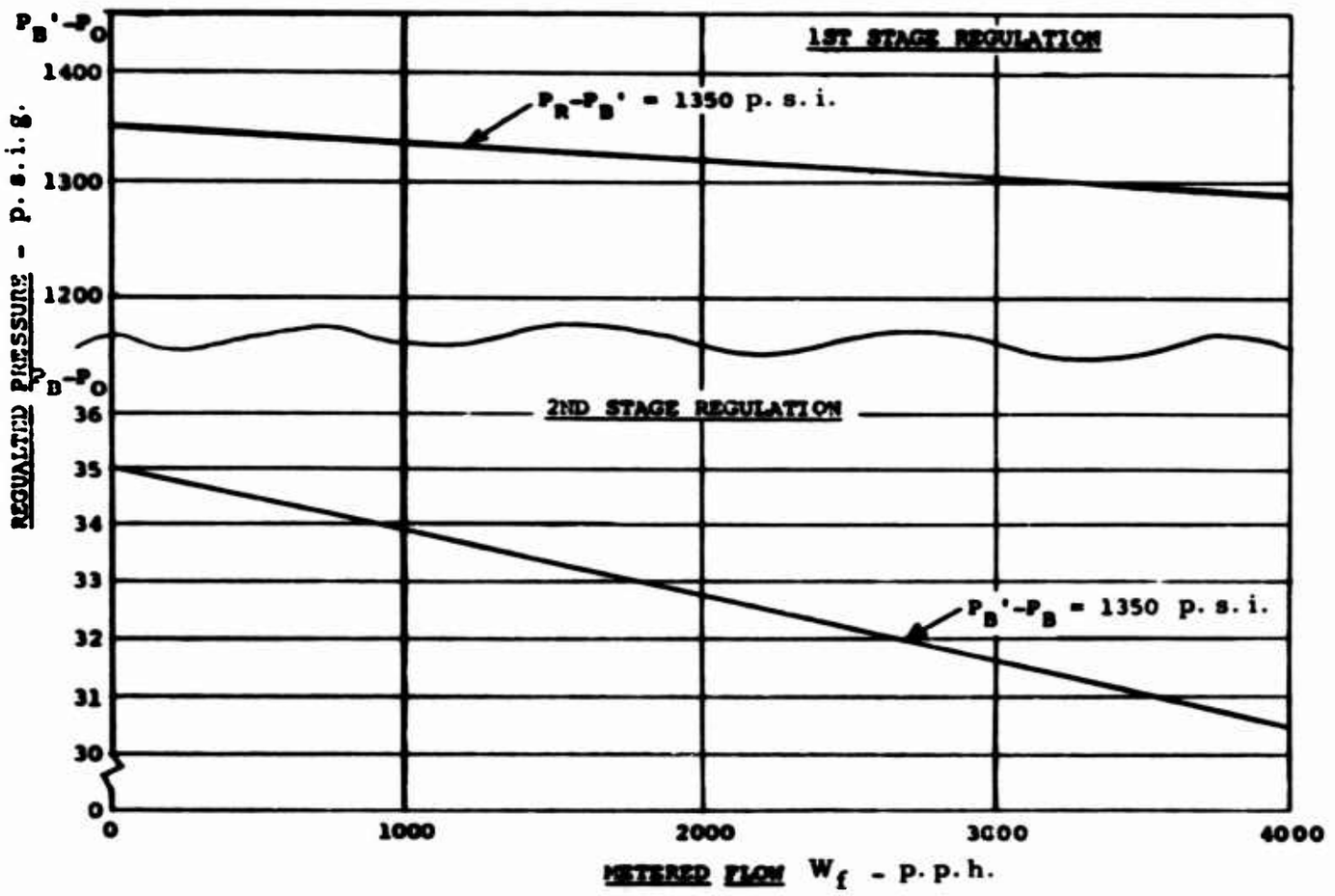

Fig. 12. Rotor Tip Fuel Control - Inlet Throttling Regulator Performance, Boost Pressure Versus Metered Flow.

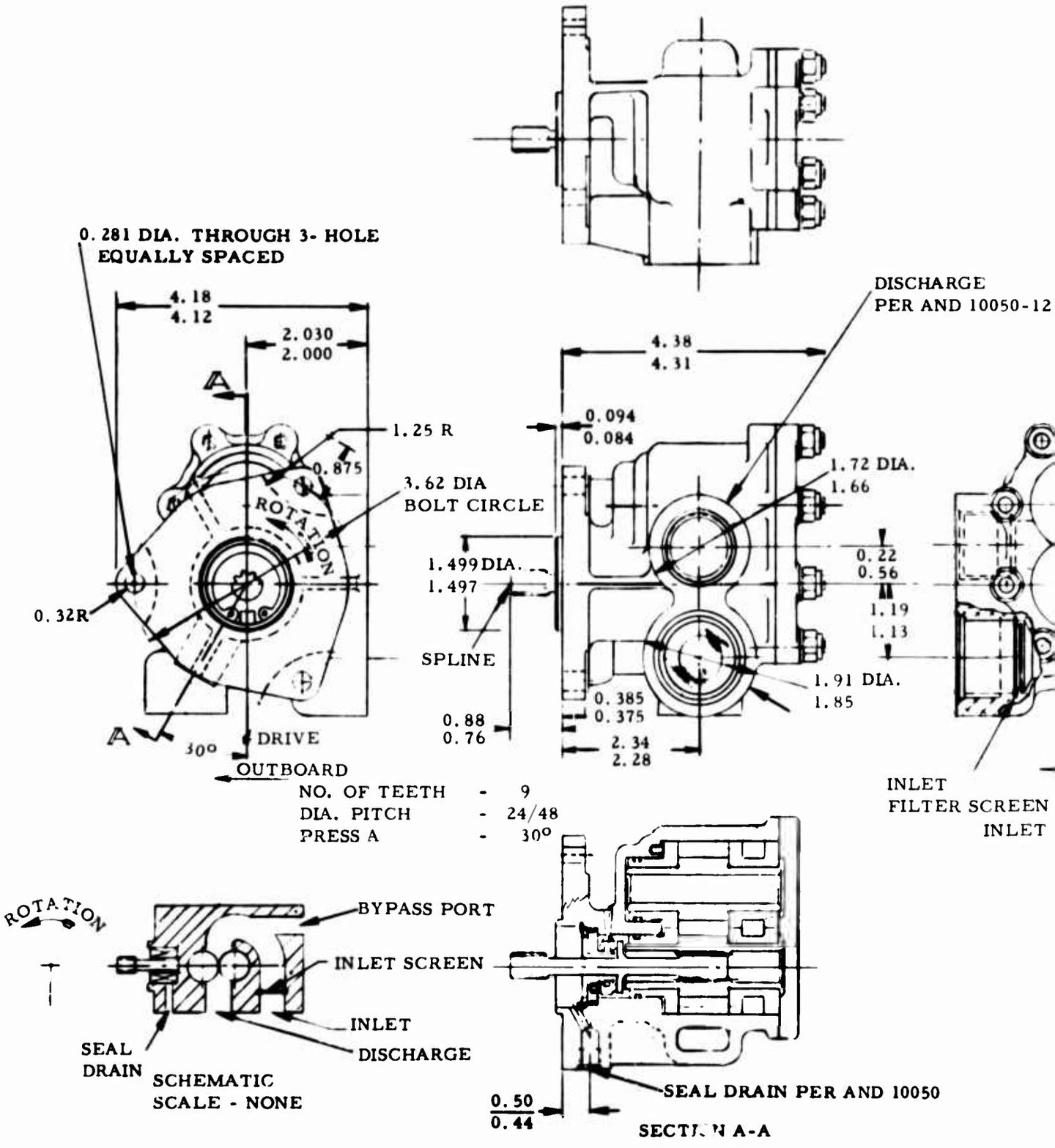

Fig. 13. Pump Single Element.

A

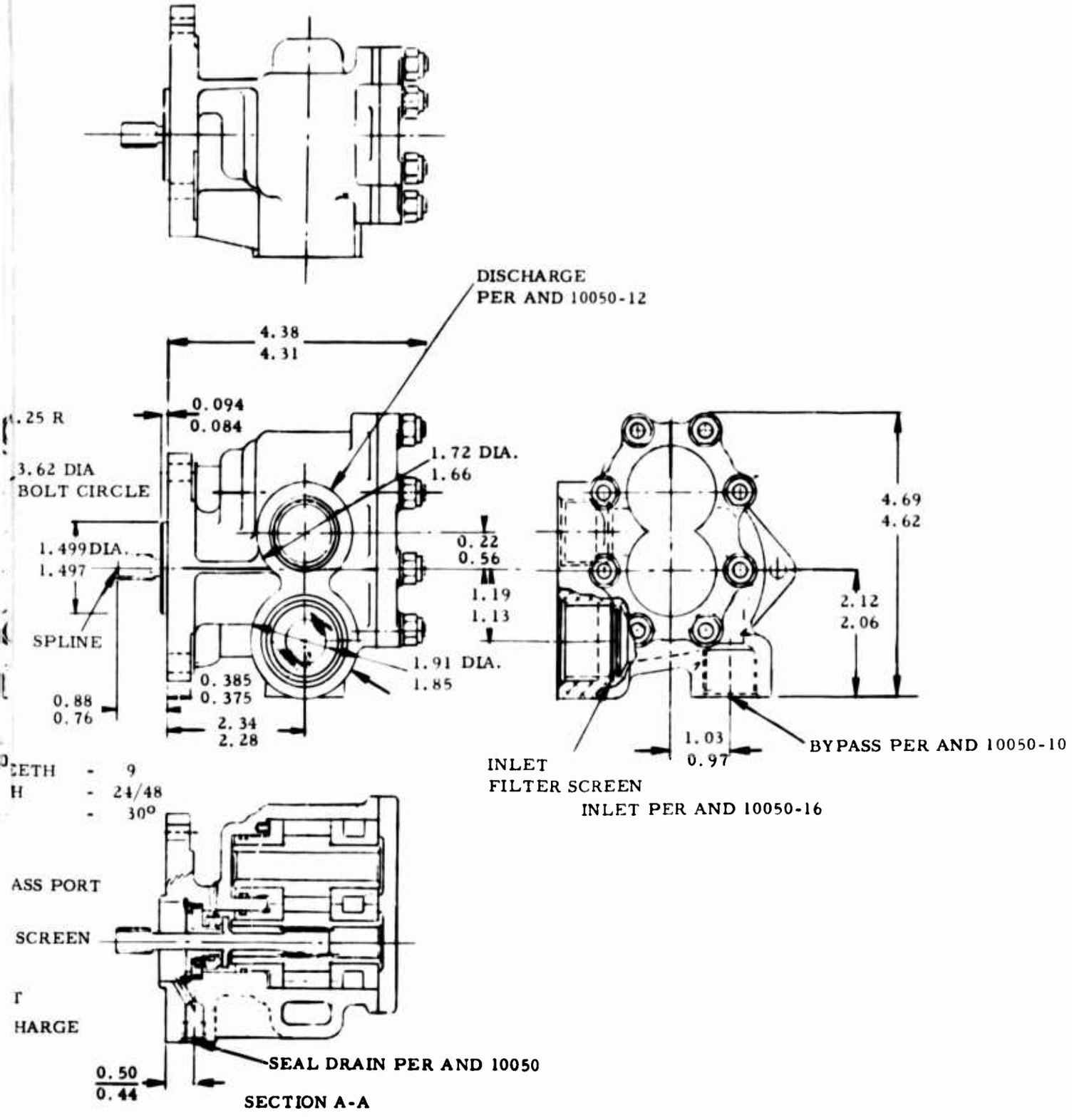

ıp Single Element.

8

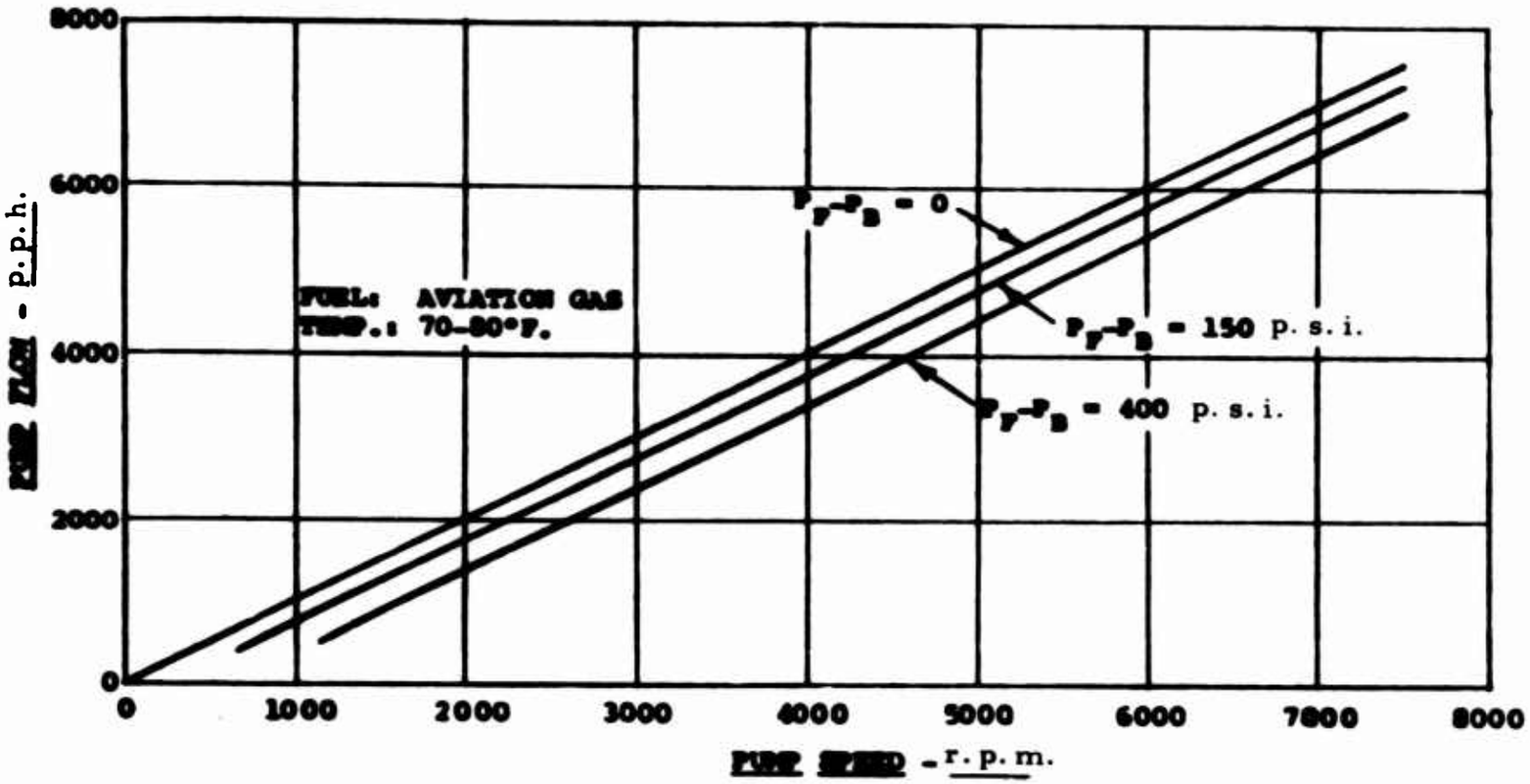

Fig. 14. Rotor Tip Fuel Control - Estimated Fuel Pump Performance.

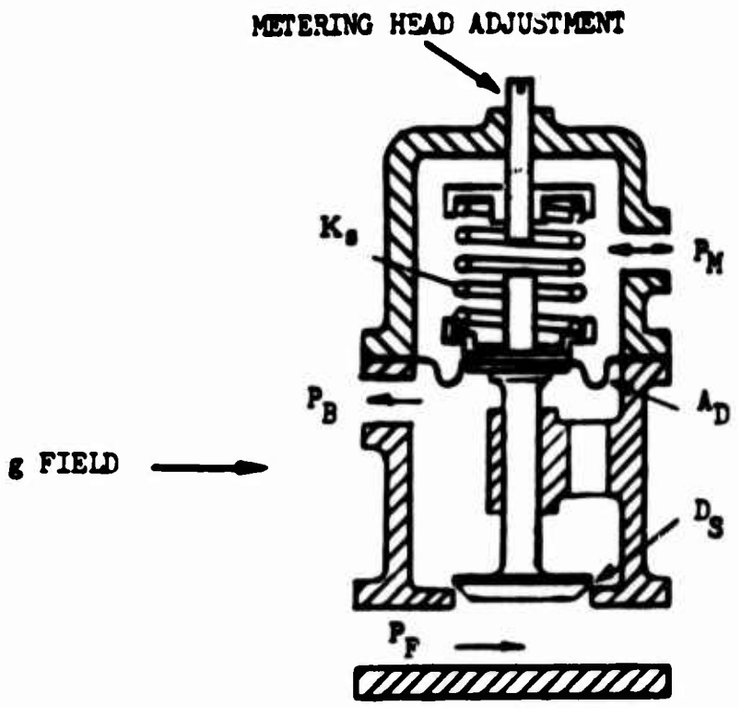

Fig. 15. Rotor Tip Fuel Control - Metering Head Regulator.

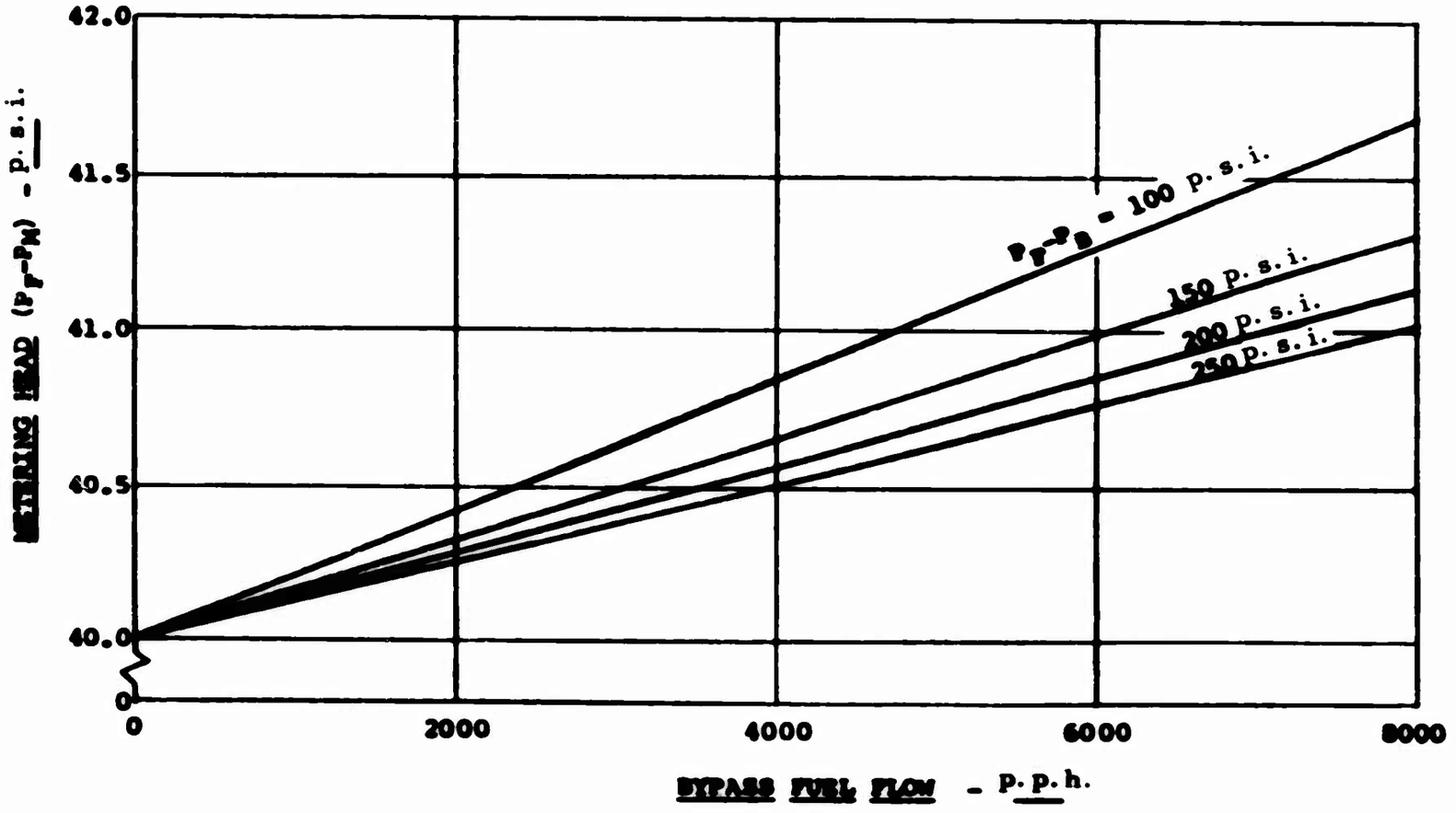

Fig. 16. Rotor Tip Fuel Control - Metering Head Regulator Performance, Metering Head Versus Bypass Fuel Flow.

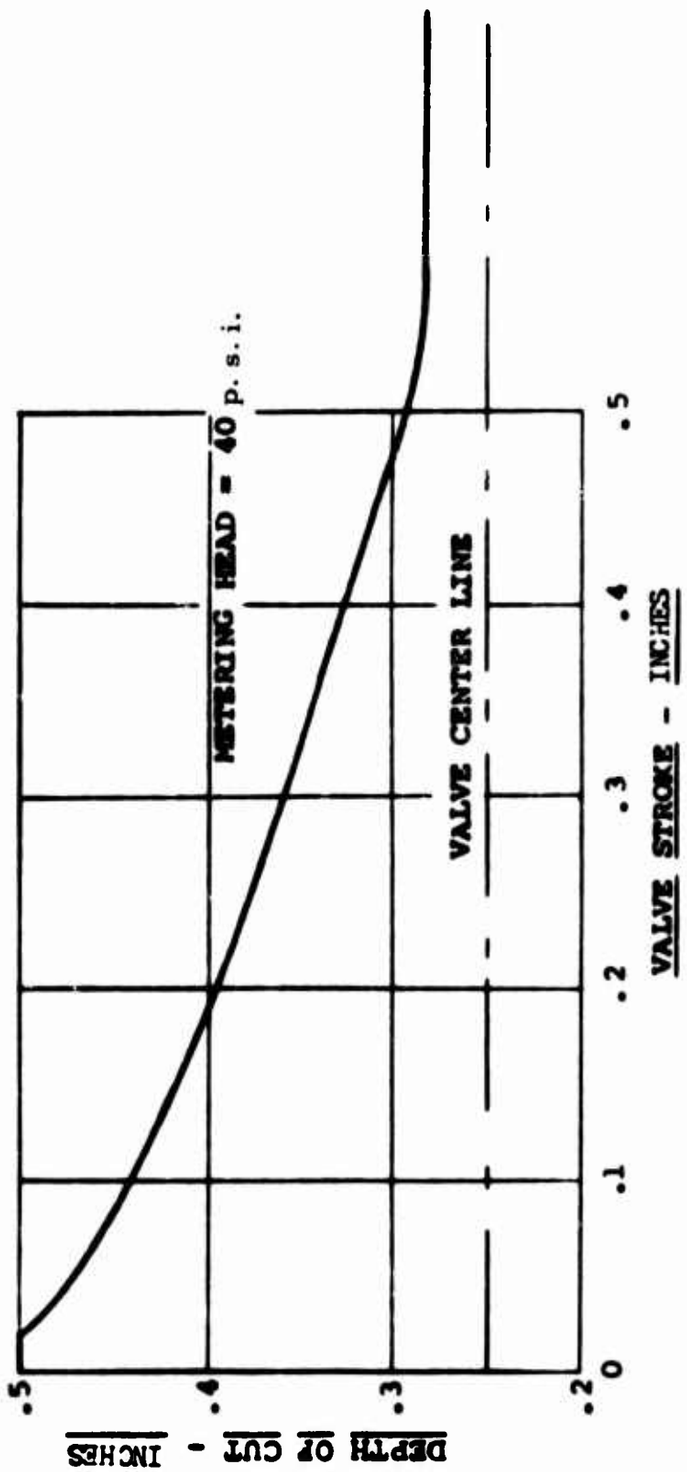

Fig. 17. Rotor Tip Fuel Control - Metering Valve Area Profile, Depth of Cut Versus Stroke.

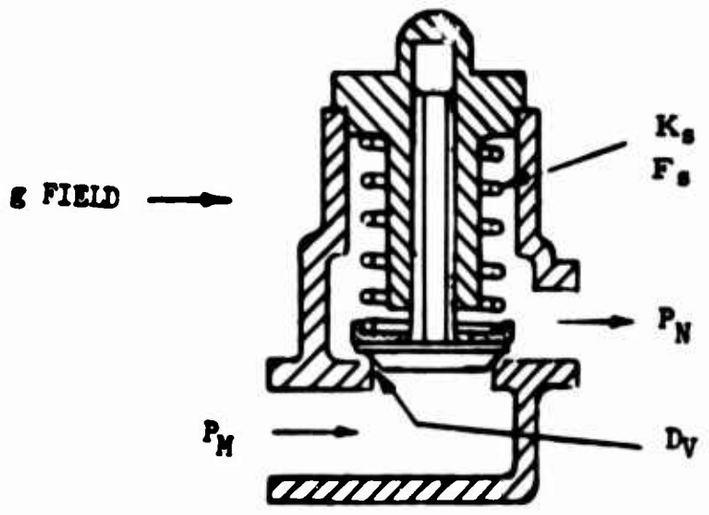

Fig. 18. Rotor Tip Fuel Control - Pressurizing Valve.

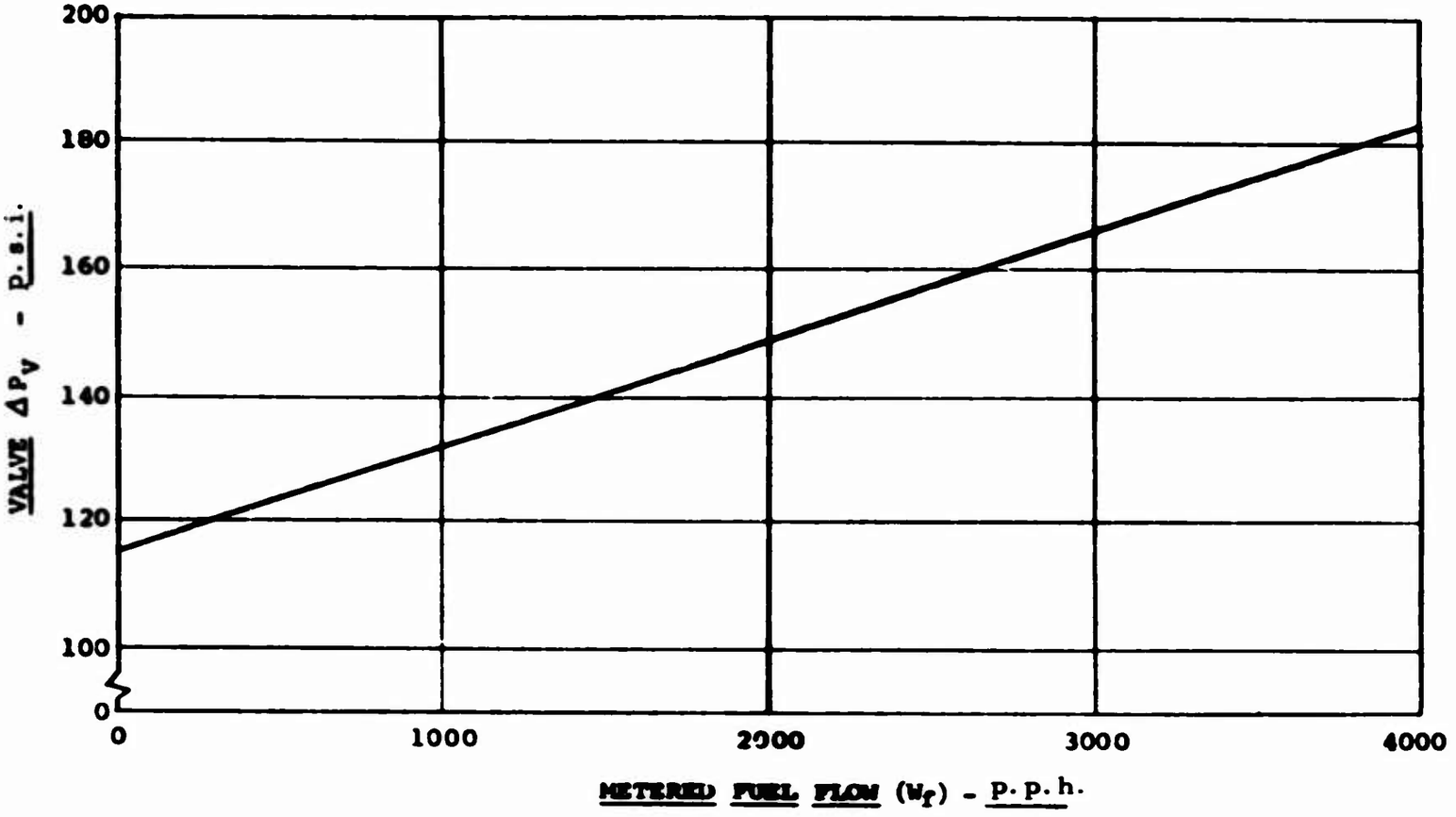

Fig. 19. Rotor Tip Fuel Control - Pressurizing Valve Performance, PM-PN Versus Metered Flow.

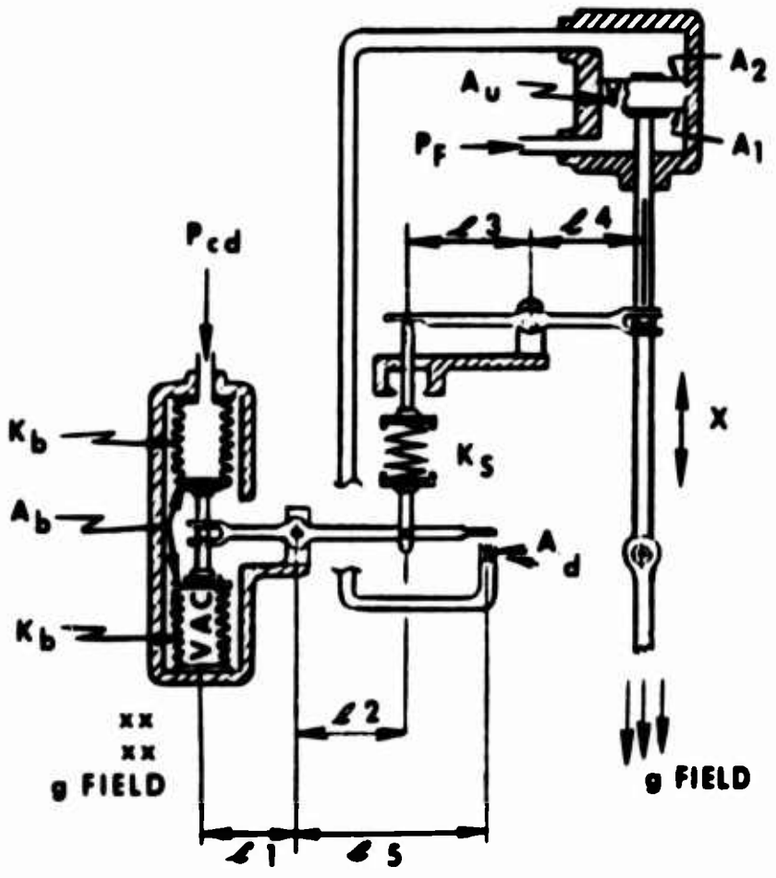

Fig. 20. Rotor Tip Fuel Control - P_{cd} Amplifier.

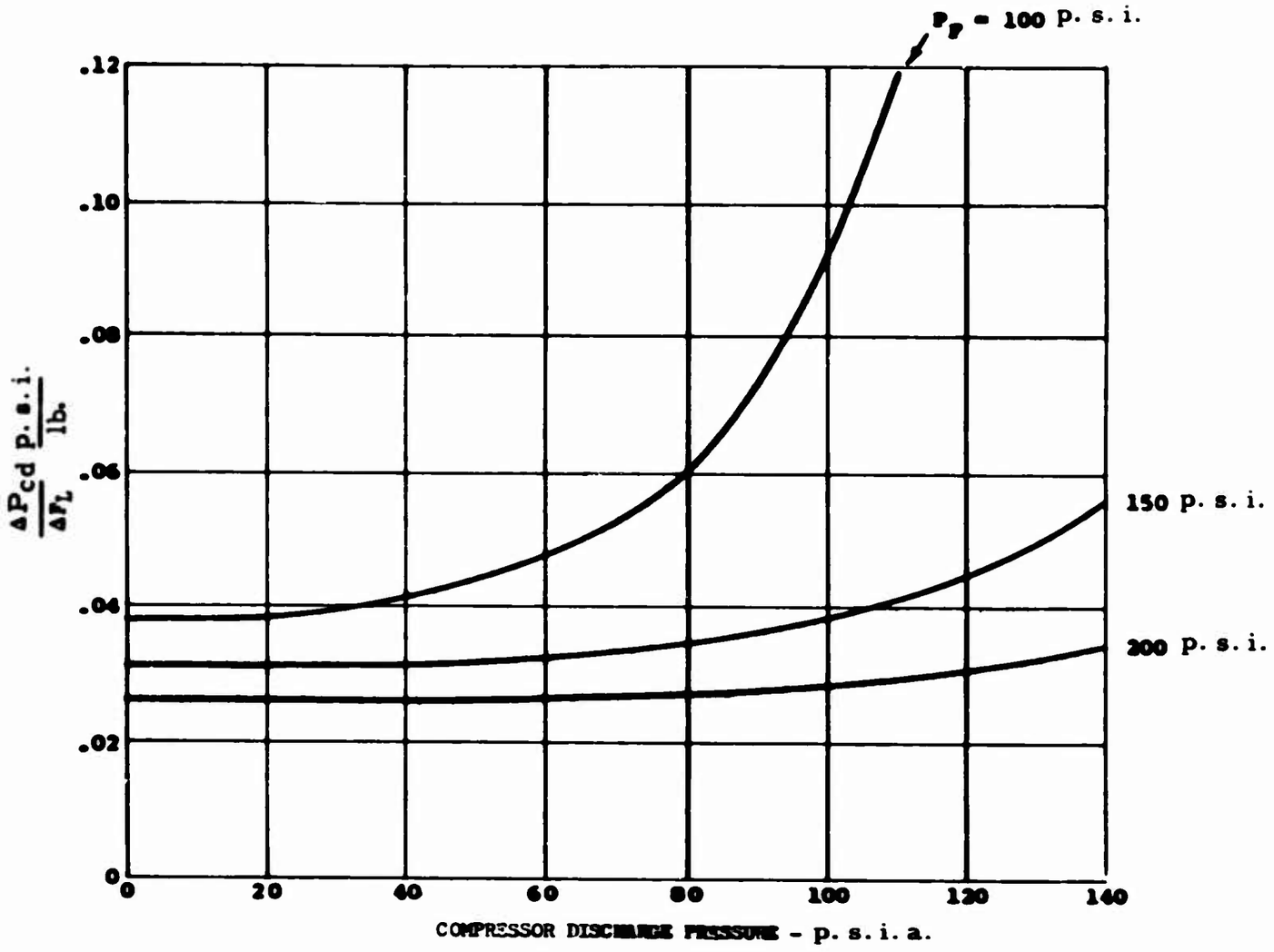

Fig. 21. Rotor Tip Fuel Control - P_{cd} Error/Change in Actuator Load Versus P_{cd}.

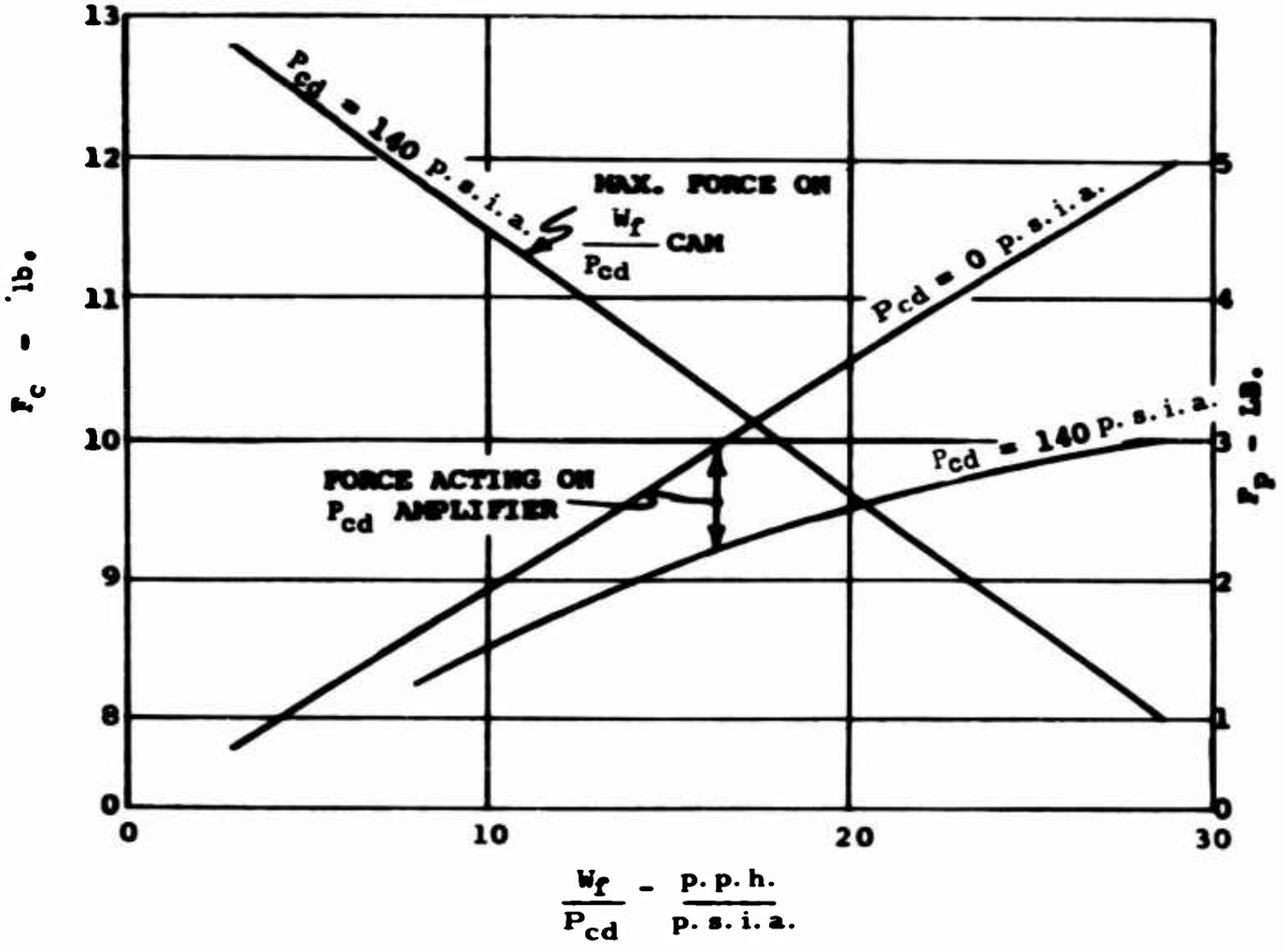

Fig. 22. Rotor Tip Fuel Control - W_f/P_{cd} Multiplier Force Level Requirements.

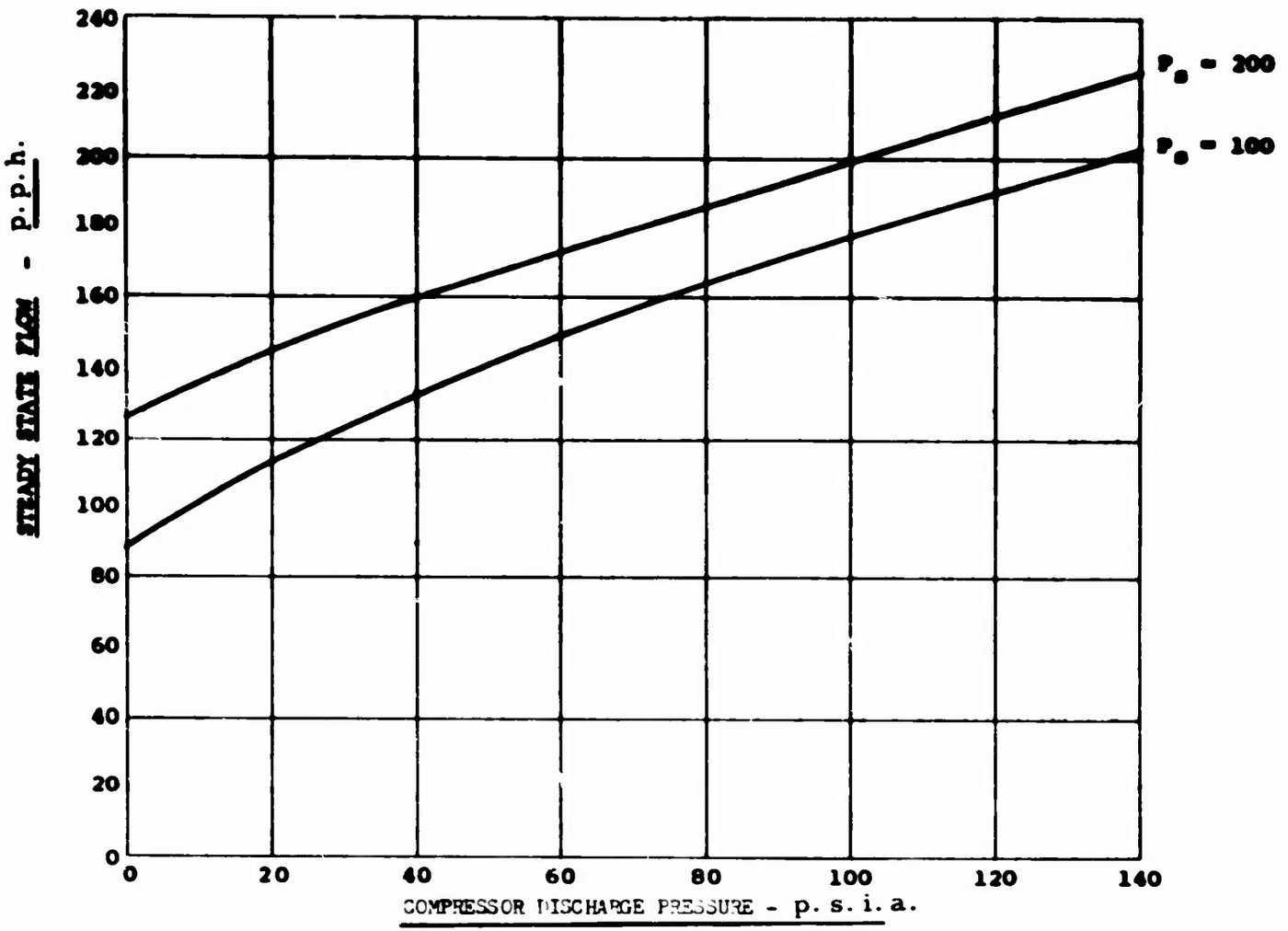

Fig. 23. Rotor Tip Fuel Control - P_{cd} Amplifier, Steady Versus P_{cd}.

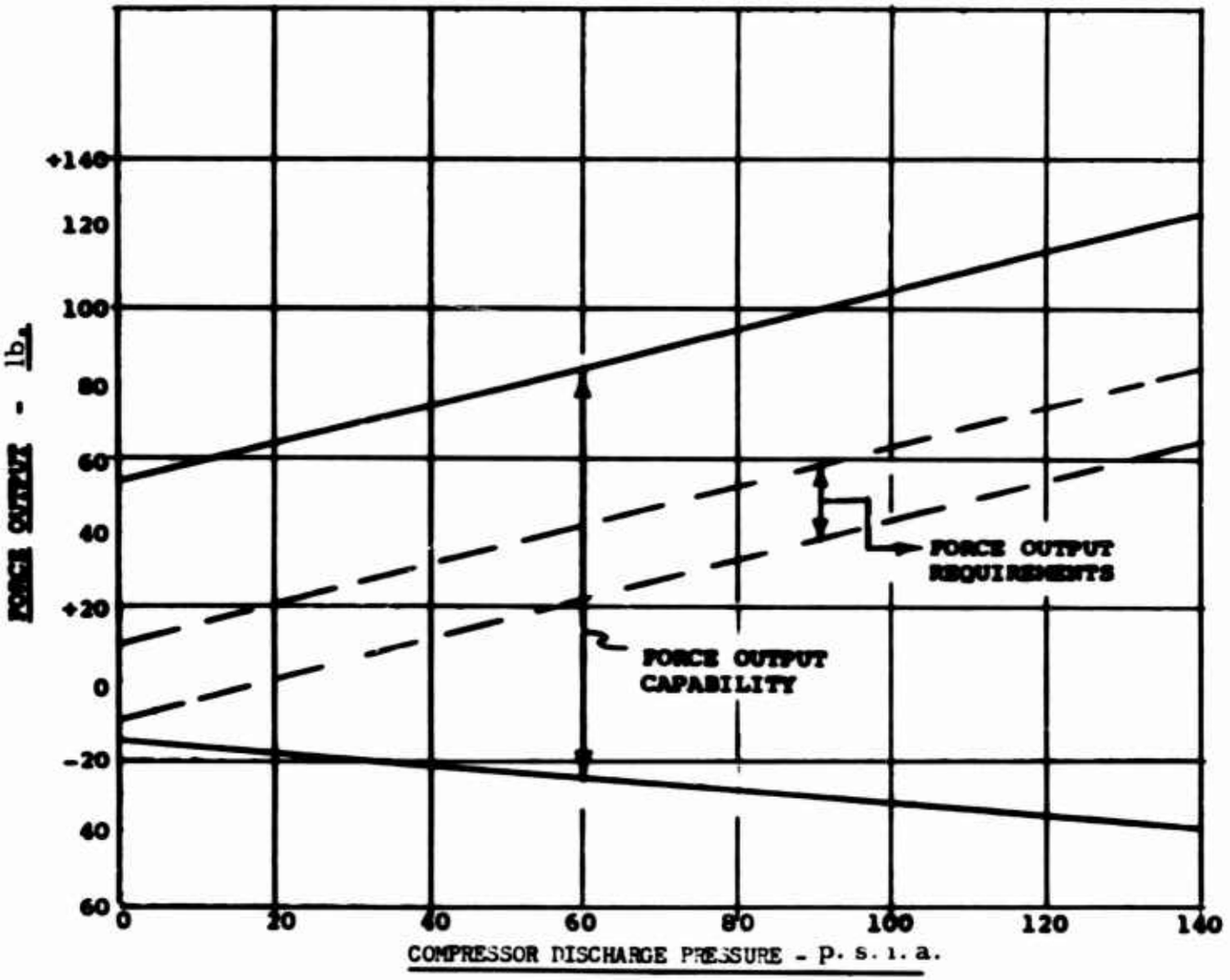

Fig. 24. Rotor Tip Fuel Control - P_{cd} Amplifier, Force Output Capability Versus P_{cd}.

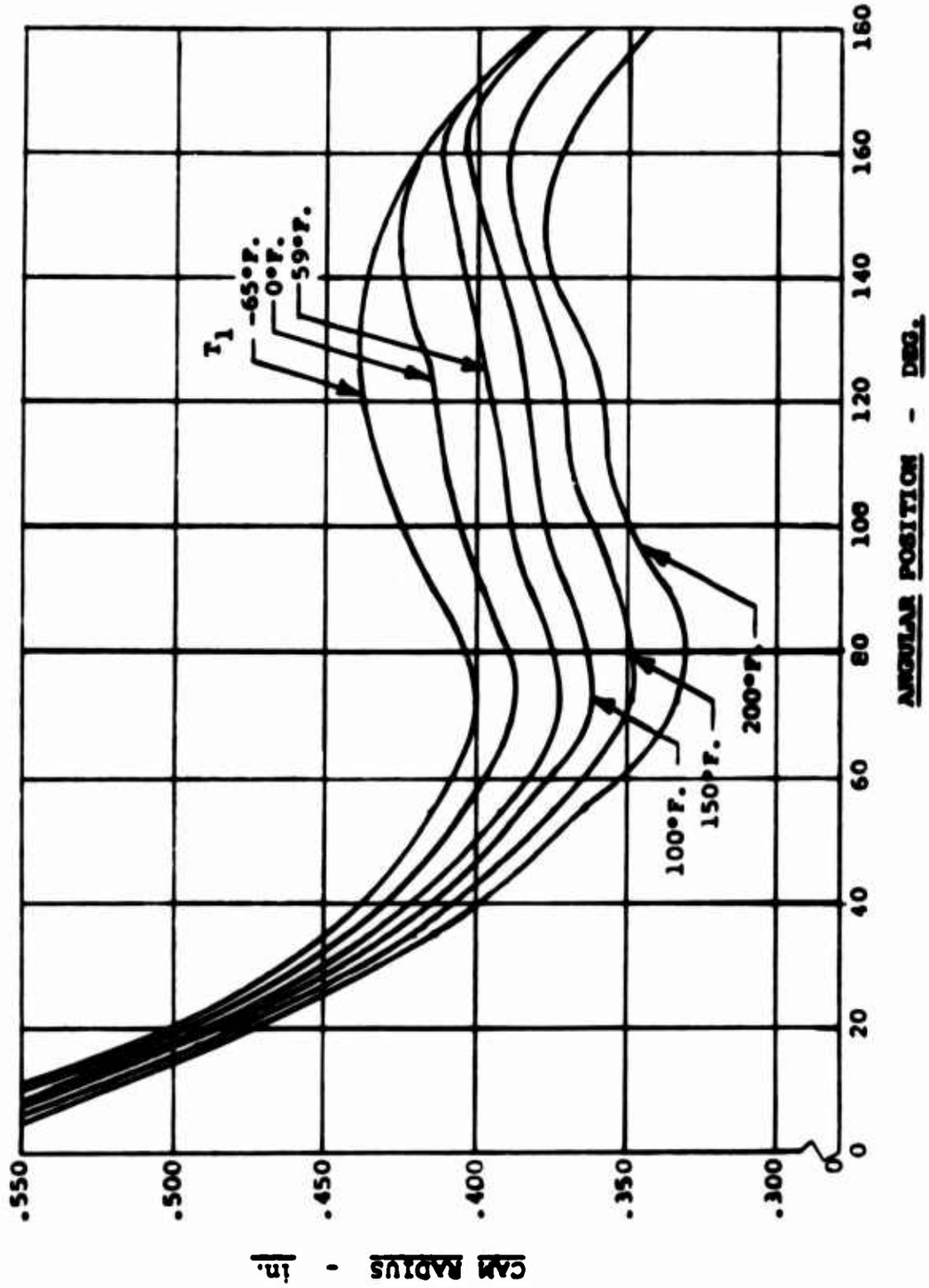

Fig. 25. Rotor Tip Fuel Control - 3D Cam Acceleration Schedule, Cam Radius Versus Angular Position and Compressor Inlet Temperature.

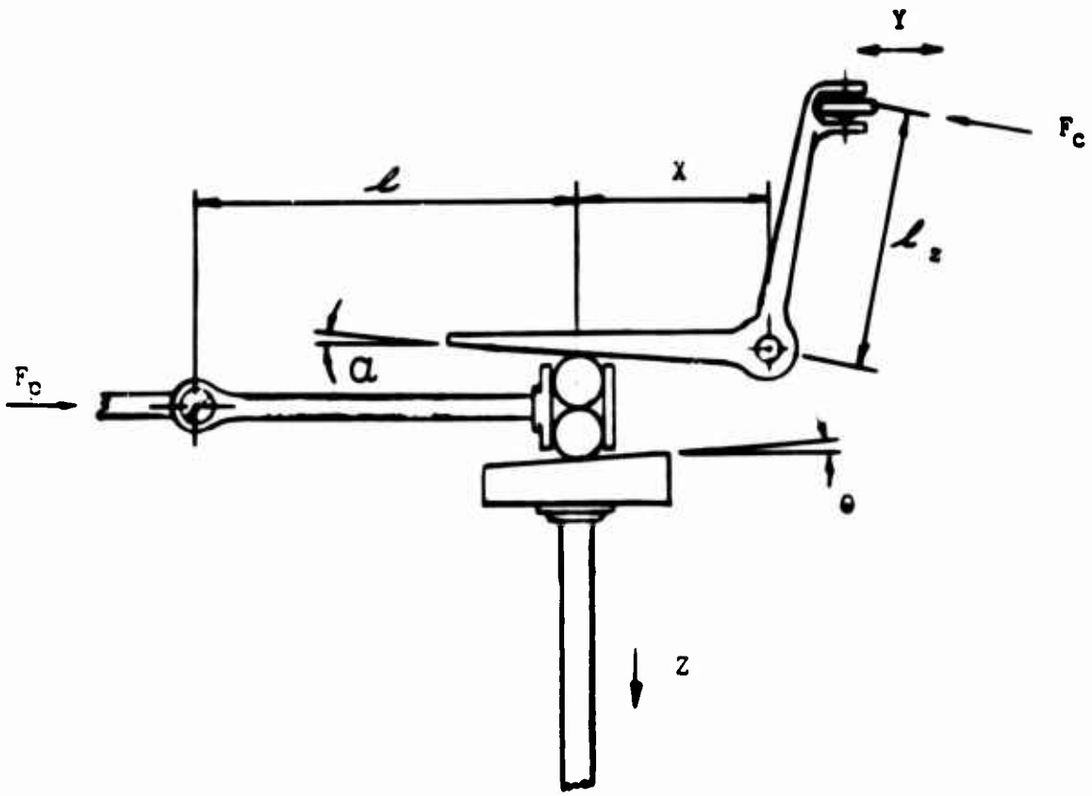

Fig. 26. Rotor Tip Fuel Control - W_f/P_{cd} Multiplier.

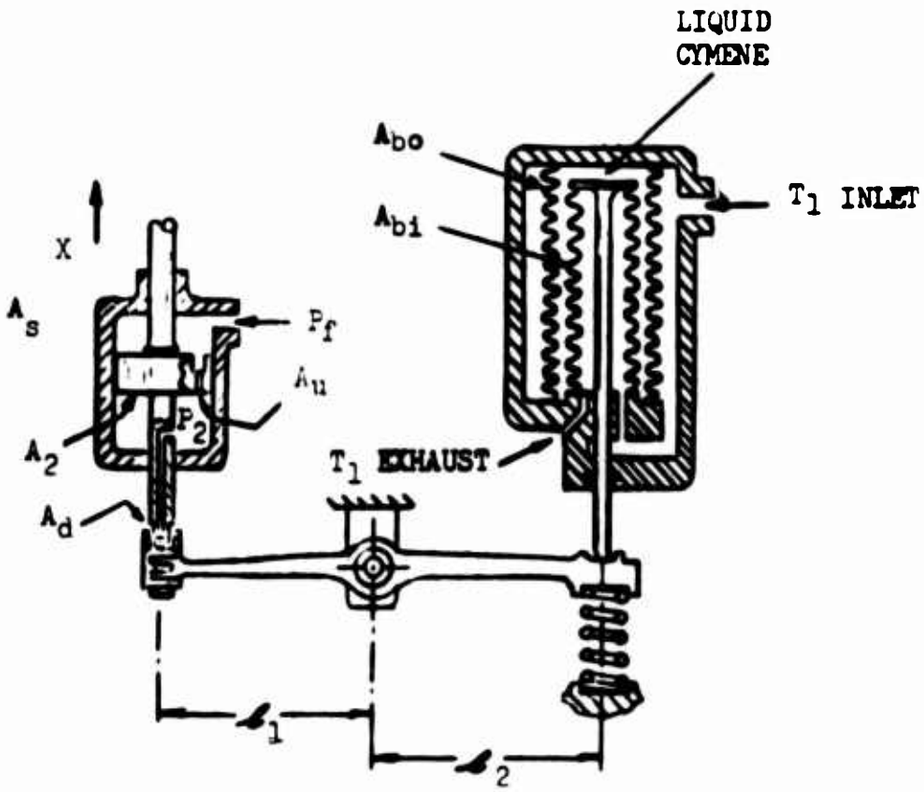

Fig. 27. Rotor Tip Fuel Control - Compressor Inlet Temperature Sensor and Amplifier.

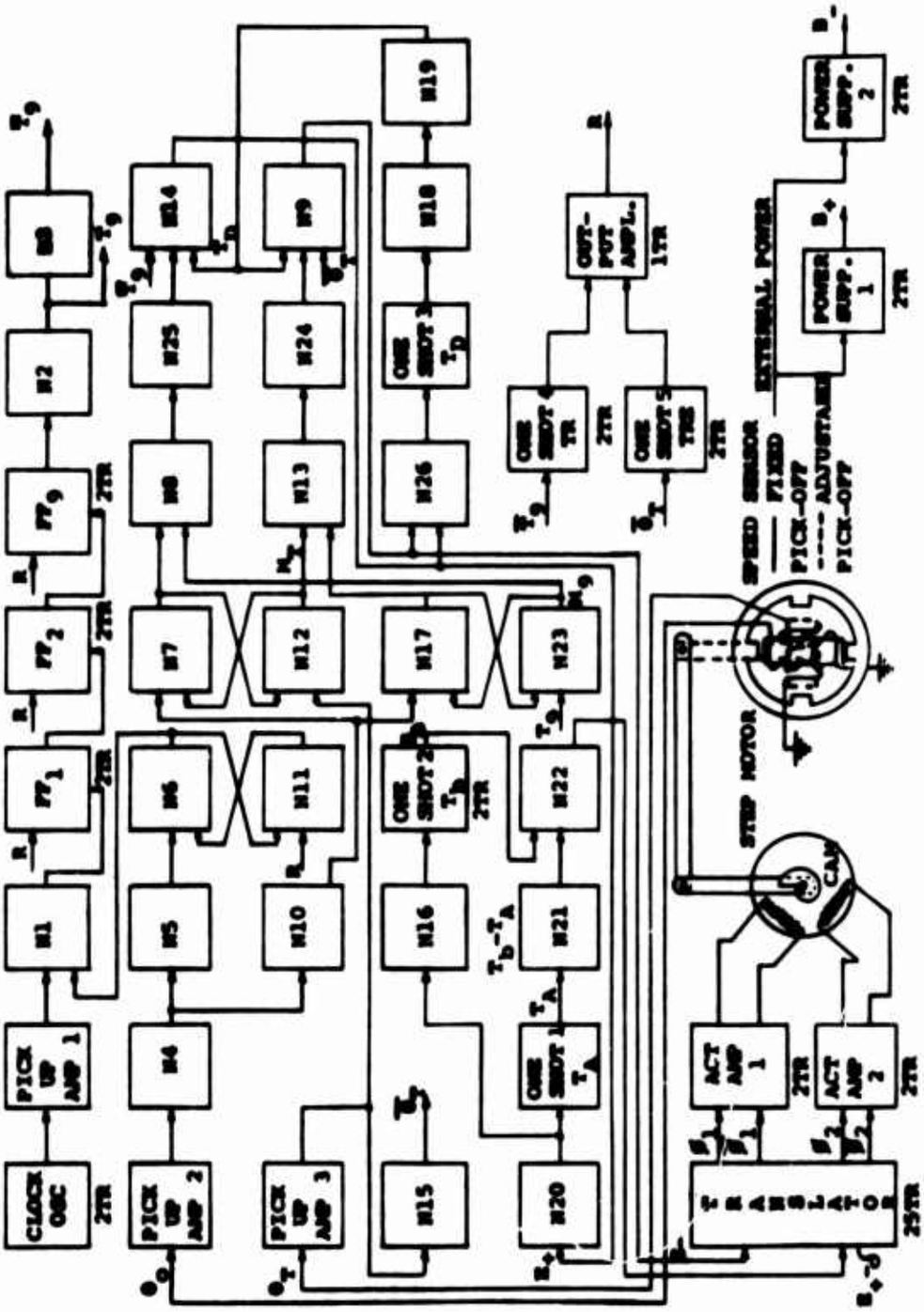

Fig. 28. Rotor Tip Fuel Control - Engine Speed Sensor and Amplifier.

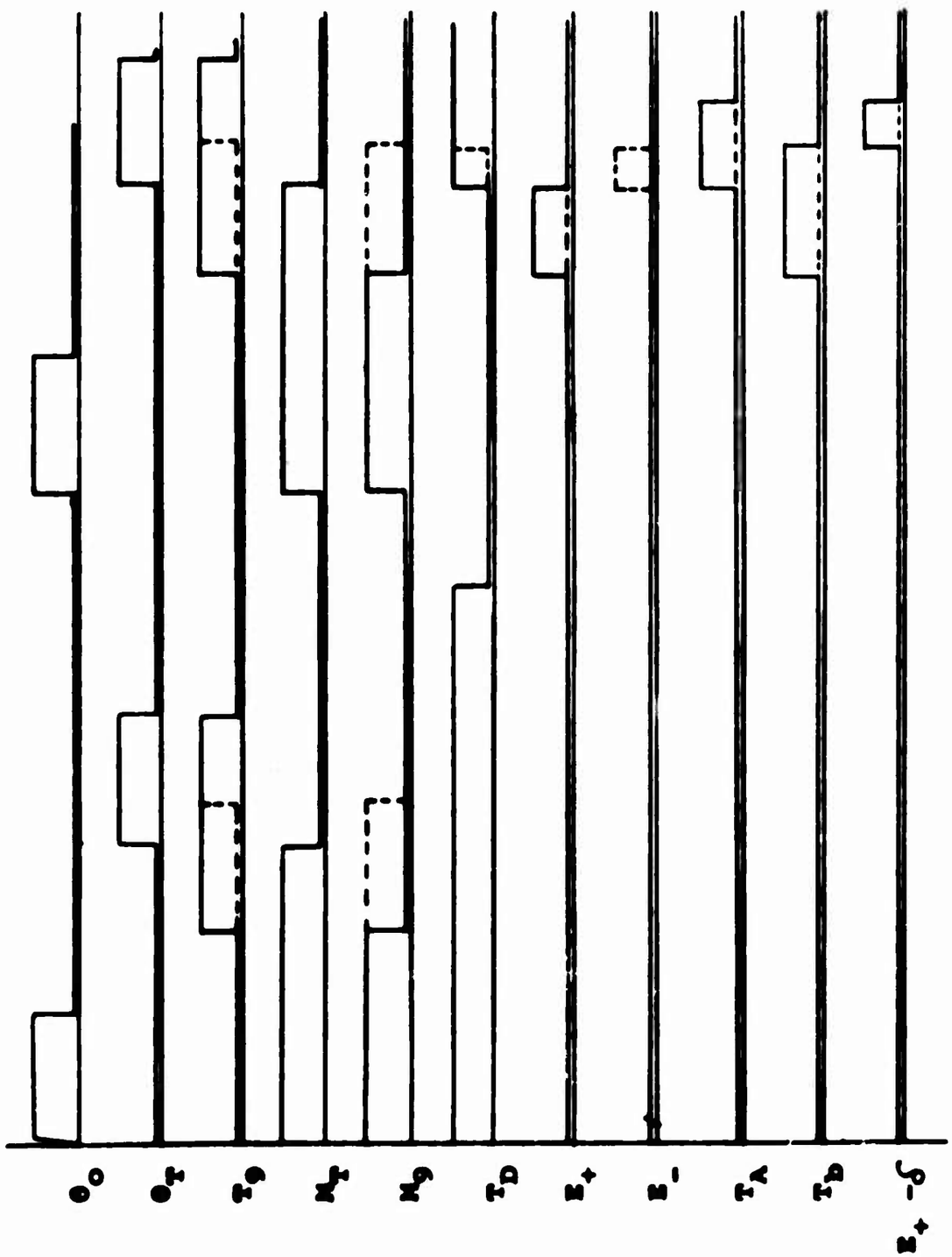

Fig. 29. Rotor Tip Fuel Control - Timing Diagram.

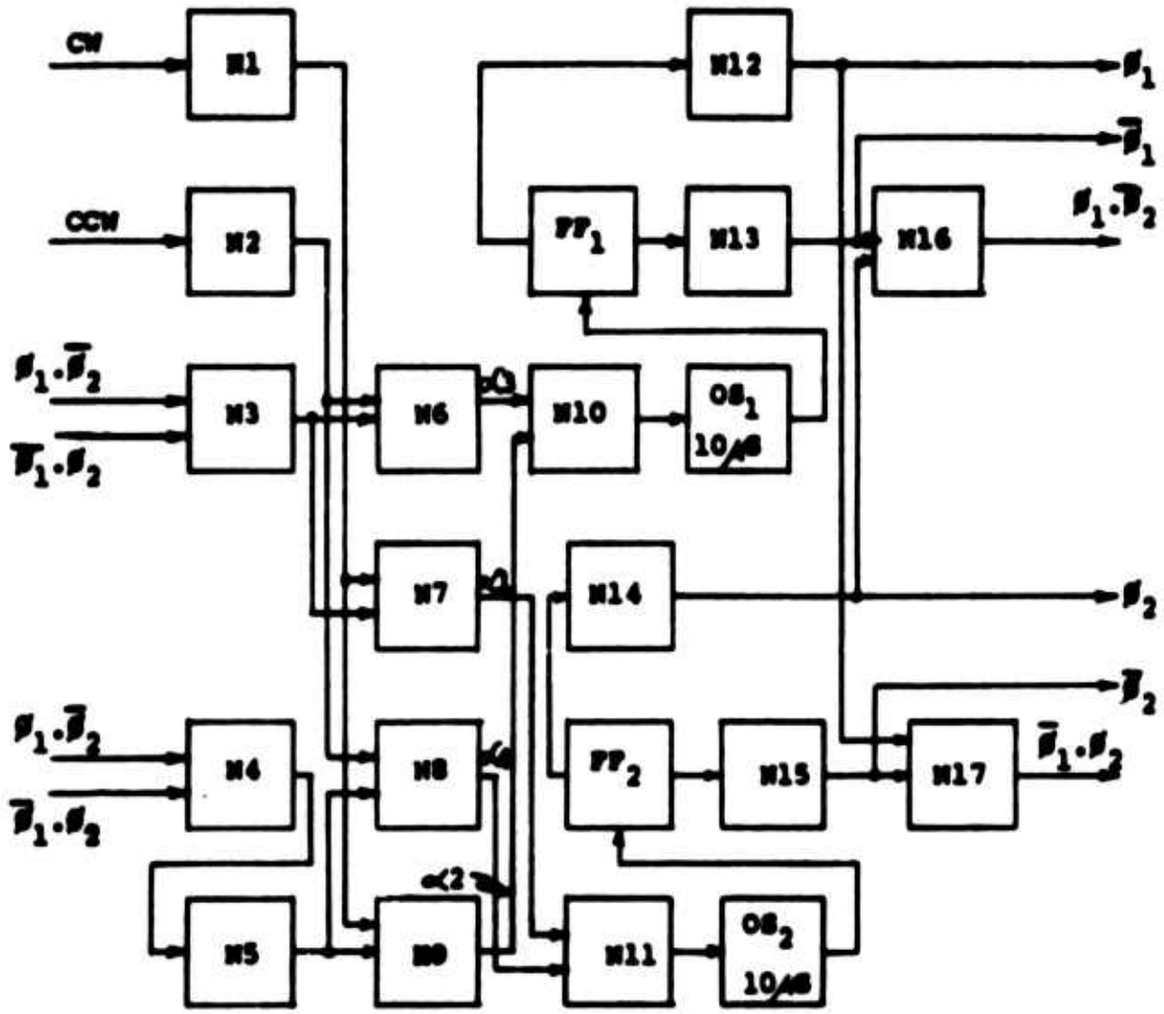

$$\alpha_1 = CW\ (\bar{\beta}_1 \cdot \beta_2 + \beta_1 \cdot \bar{\beta}_2)$$

$$\alpha_2 = CW\ (\beta_1 \cdot \beta_2 + \bar{\beta}_1 \cdot \bar{\beta}_2)$$

$$\alpha_3 = CCW\ (\bar{\beta}_1 \cdot \beta_2 + \beta_1 \cdot \bar{\beta}_2)$$

$$\alpha_4 = CCW\ (\beta_1 \cdot \beta_2 + \bar{\beta}_1 \cdot \bar{\beta}_2)$$

$$P_1 = \alpha_2 + \alpha_3$$

$$P_2 = \alpha_1 + \alpha_4$$

Fig. 30. Rotor Tip Fuel Control - Step Motor Translator.

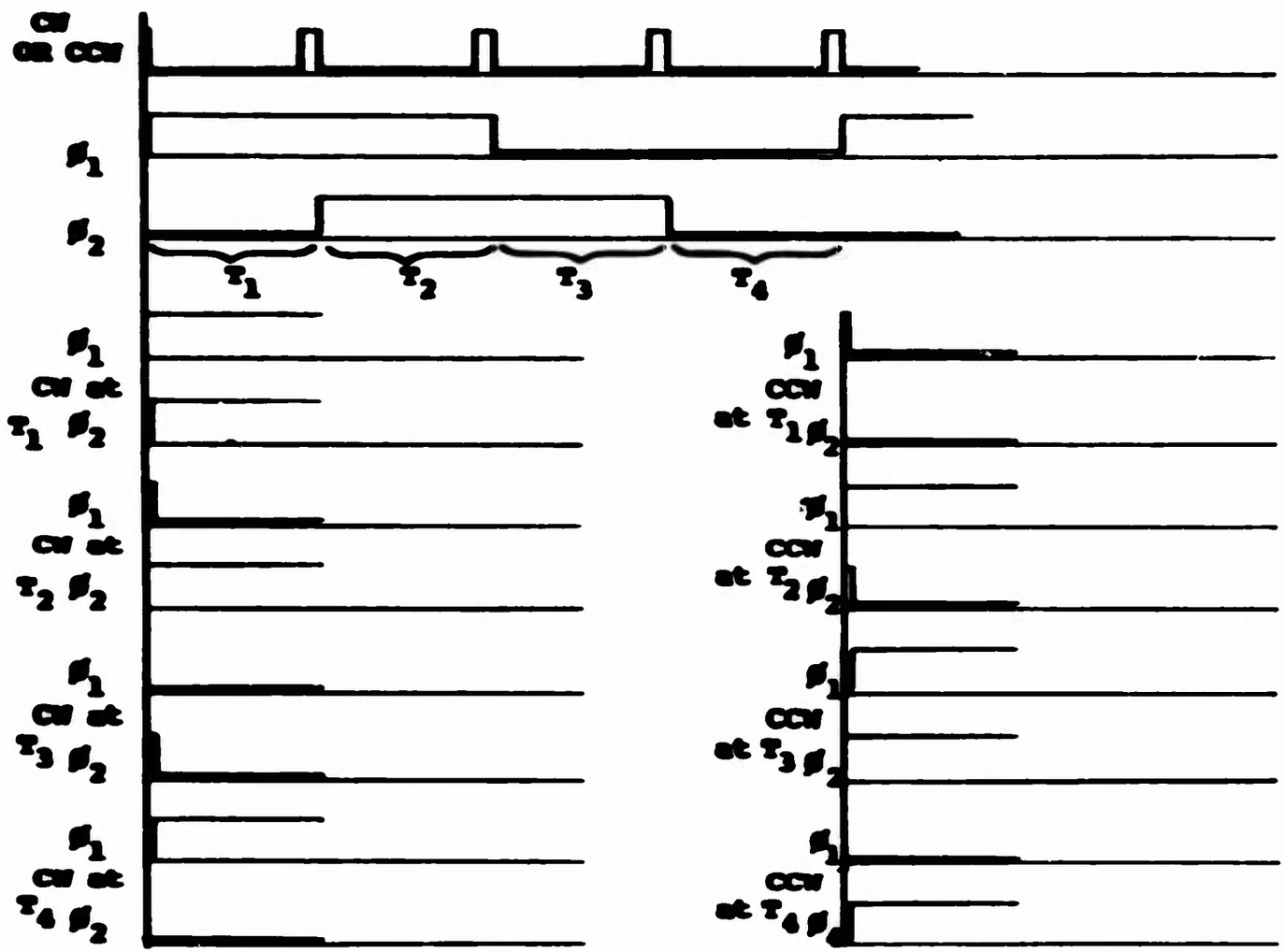

Fig. 31. Rotor Tip Fuel Control - Step Motor Translator Timing Diagram.

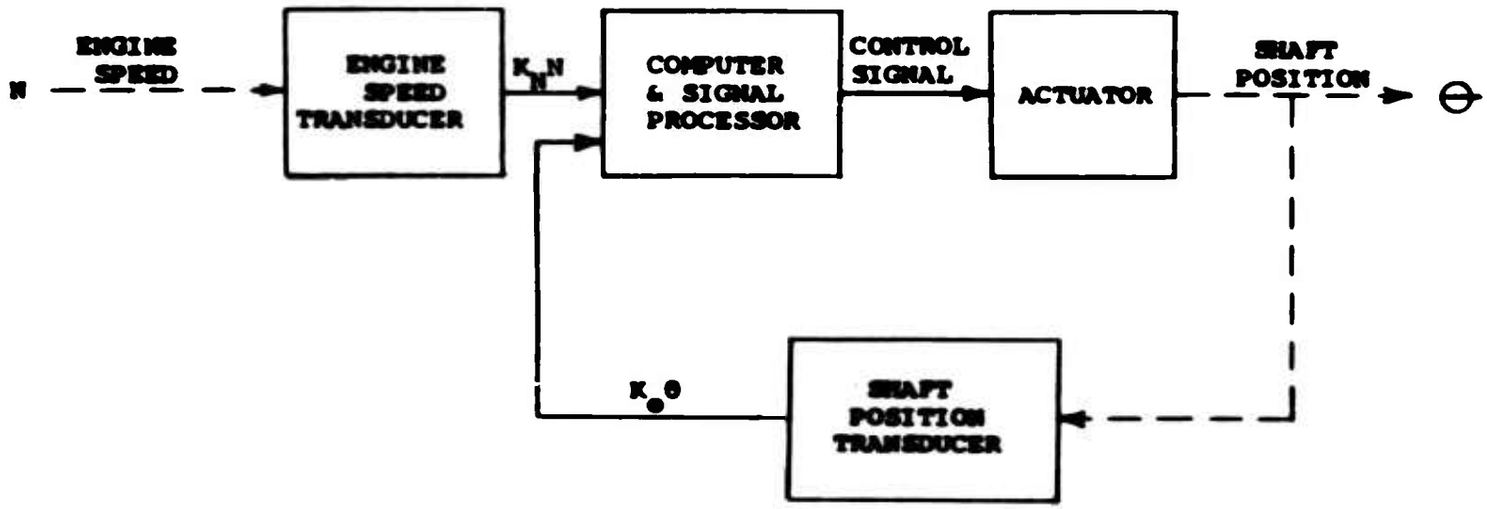

NOTE: BROKEN LINES REPRESENT MECHANICAL COUPLING.
SOLID LINES REPRESENT ELECTRICAL COUPLING.

Fig. 32. Rotor Tip Fuel Control - Engine Speed Sensor and Amplifier Block Diagram Electronic Design.

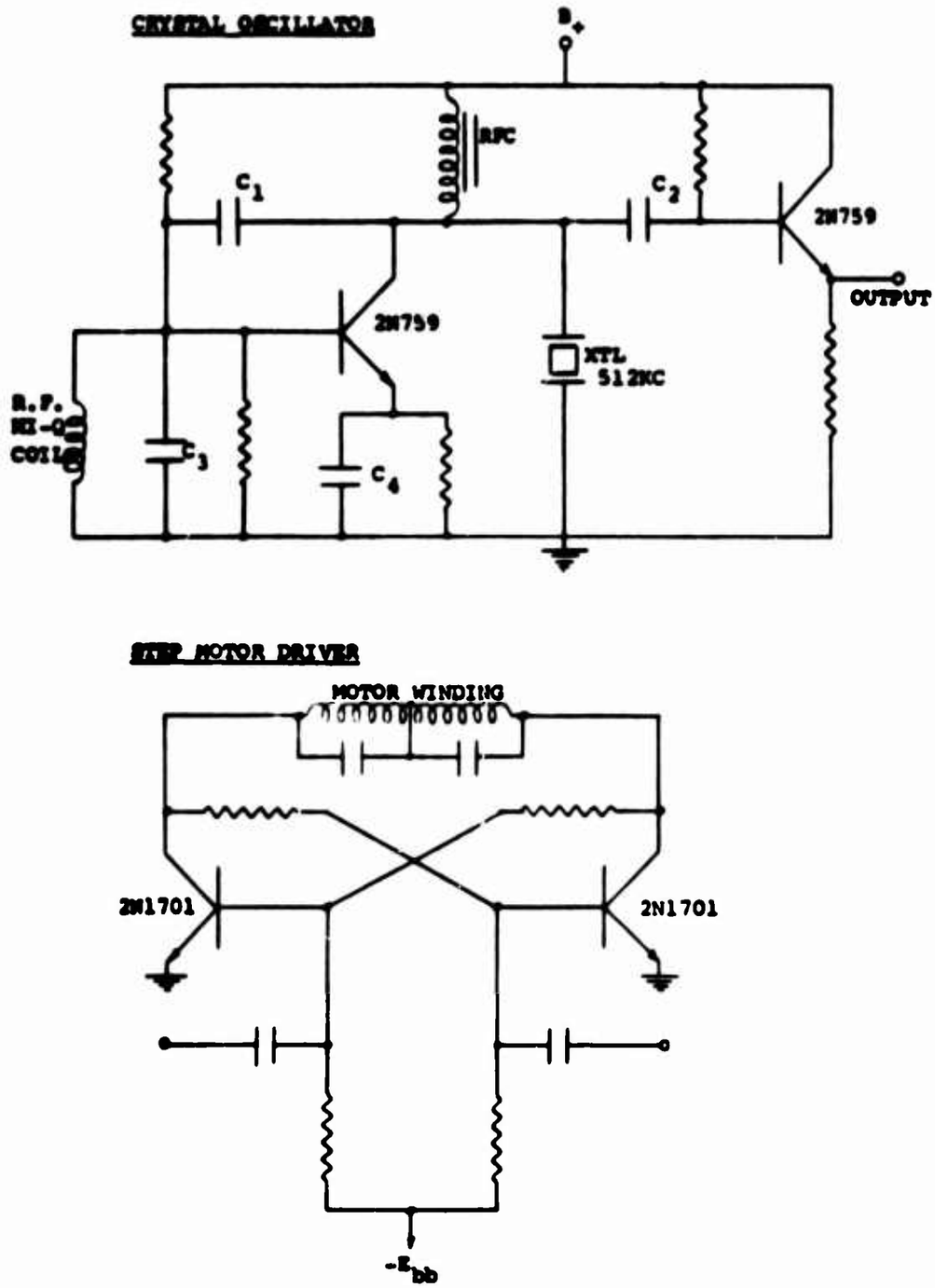

Fig. 33. Rotor Tip Fuel Control - Crystal Oscillator and Step Motor Driver.

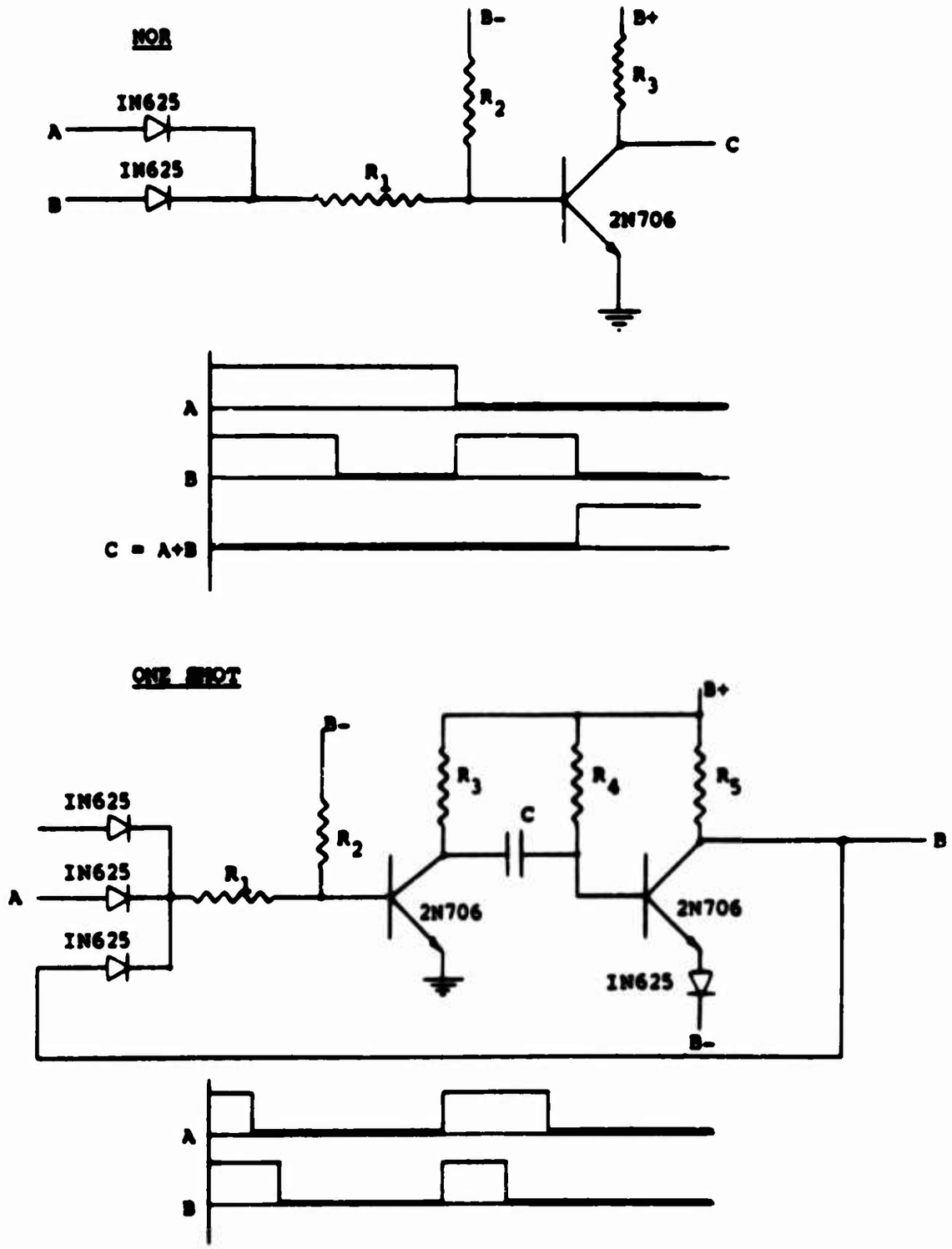

Fig. 34. Rotor Tip Fuel Control - Logic Circuits.

PICKUP AMPLIFIER

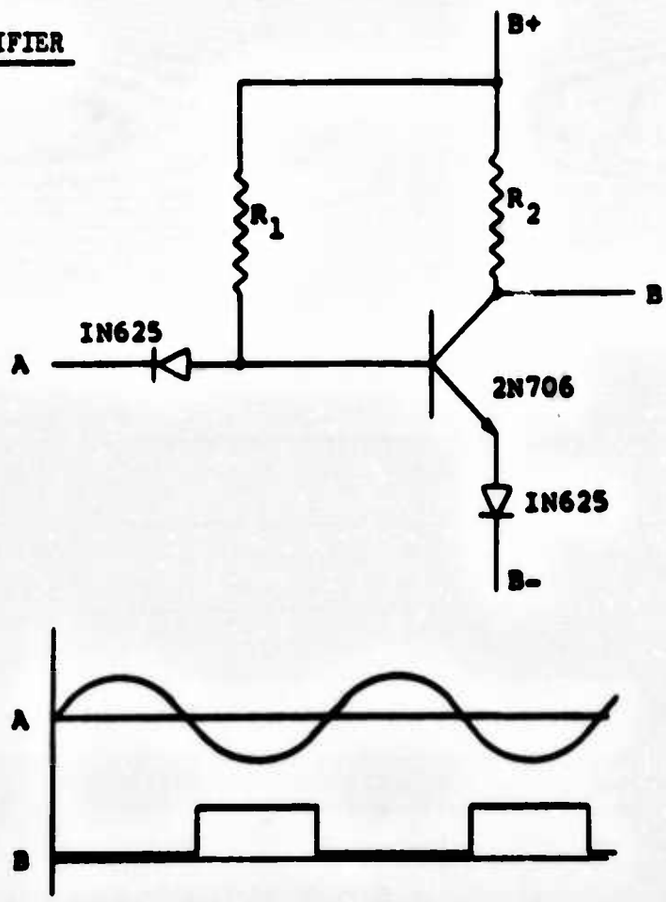

OUTPUT AMPLIFIER

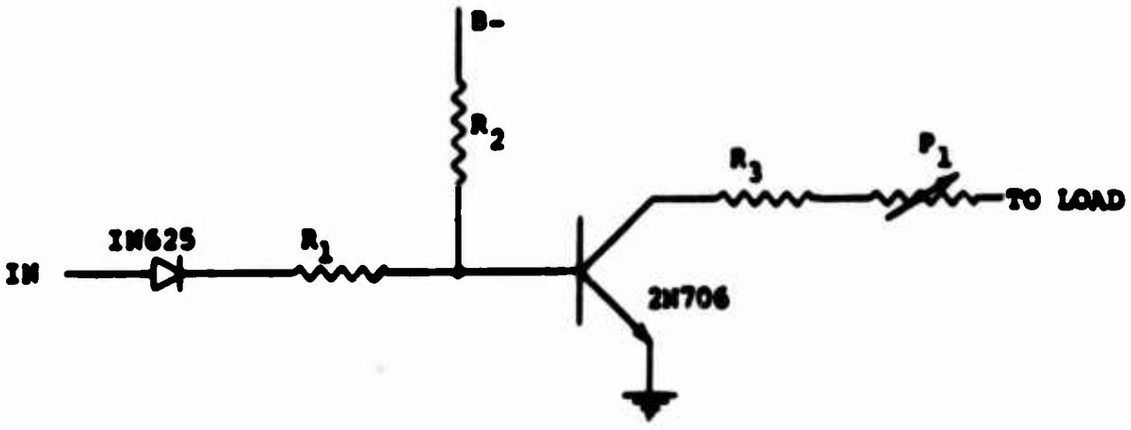

Fig. 34. (Cont'd)

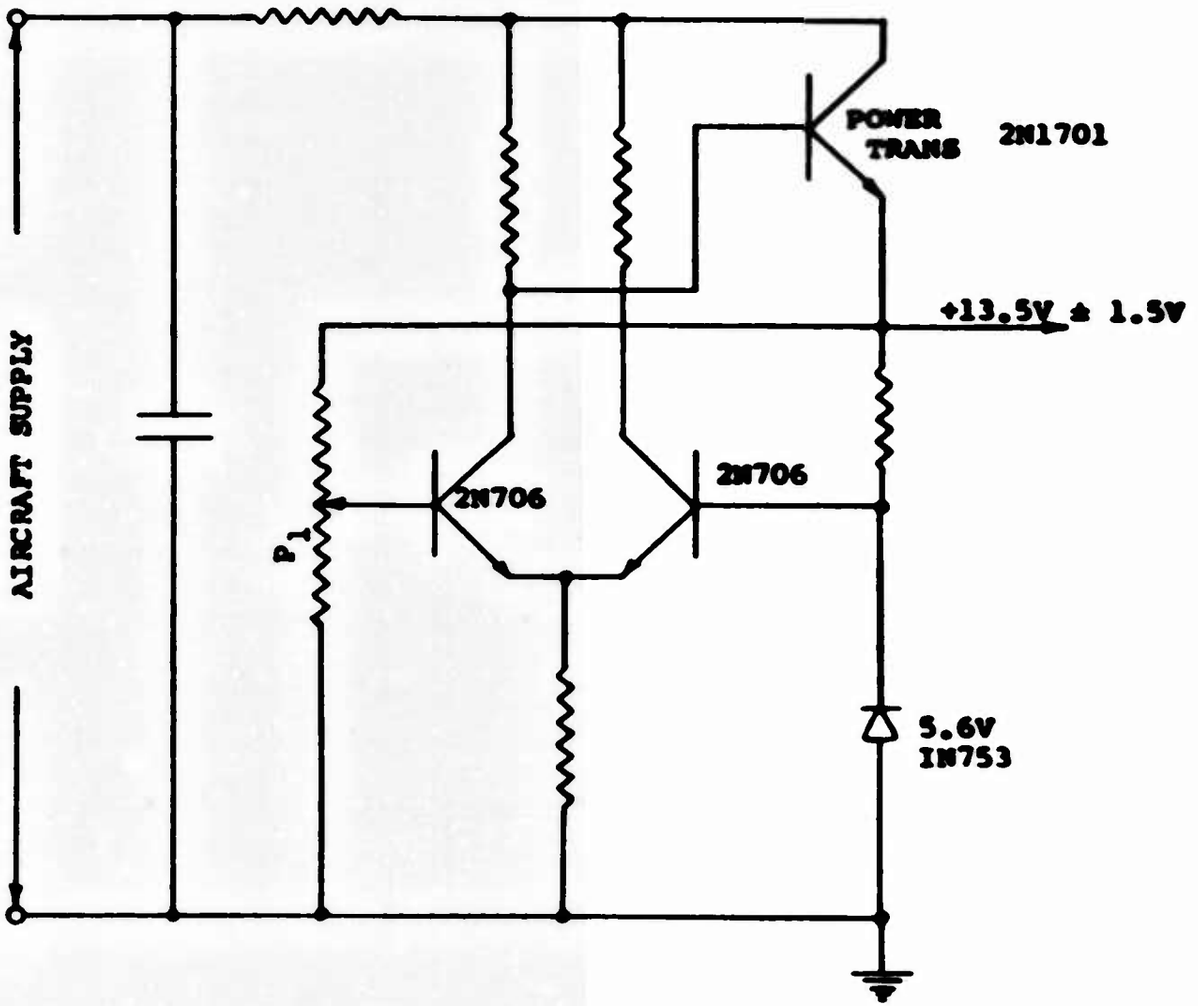

Fig. 35. Rotor Tip Fuel Control - B + Regulated Power Supply.

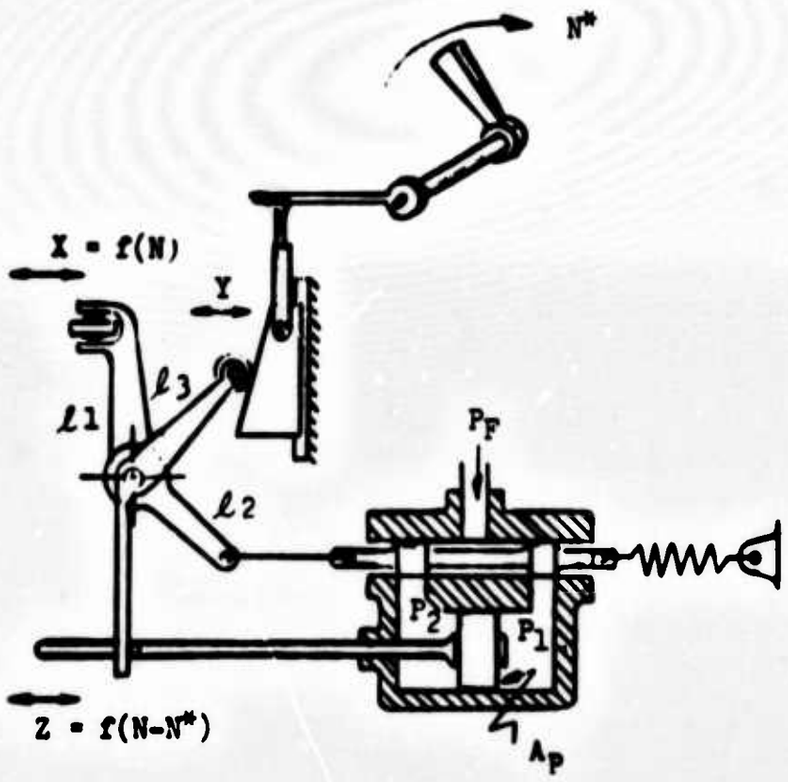

Fig. 36. Rotor Tip Fuel Control - Speed Governor Amplifier.

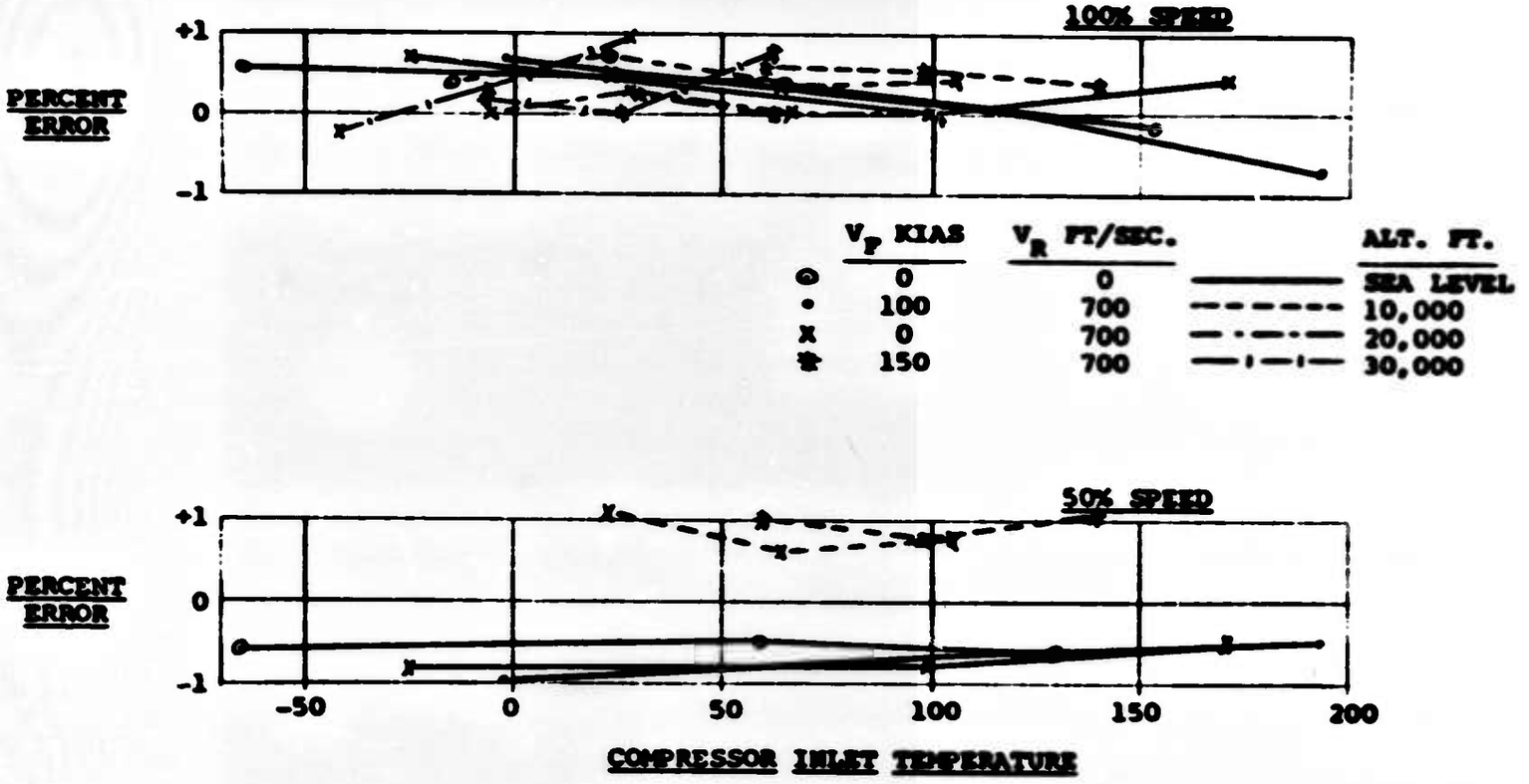

Fig. 37. Rotor Tip Fuel Control - Governor Speed Error Versus Compressor Inlet Temperature.

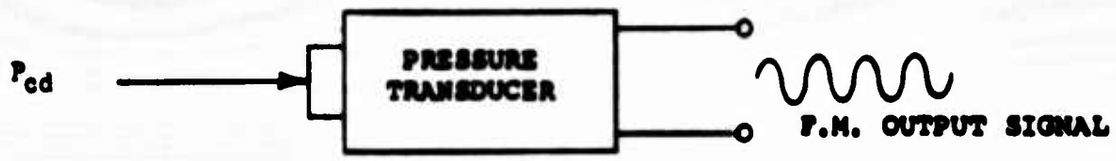

REQUIRED ACCURACY	≤1% RMS ERROR	ENVIRONMENT
TEMP. RANGE:	-65°F. to 250°F.	
ACCEL. RANGE:	367g MAX.	
SHOCK:	30g ▶ 10 MS	
VIBRATION:	20g 0-2KC	

Fig. 38. Rotor Tip Fuel Control - Basic Transducer Function.

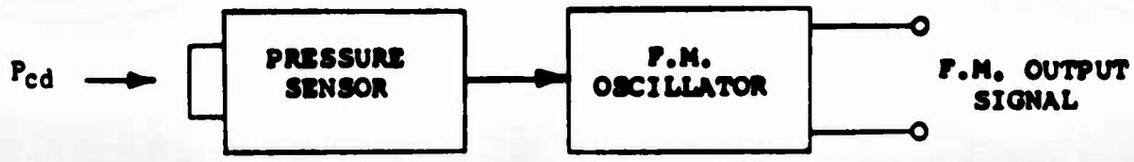

ACCURACY: 3 PERCENT OR GREATER RMS ERROR

Fig. 39. Rotor Tip Fuel Control - Analog Pressure Sensor With F. M. Signal Transducer.

Type	Frequency Transducer	Manufacturer	Price	Range p.s.i.a.	Max. r.m.s. Error	Elect. Input	Elect. Output
Silicon Semicond. Strain Gage (35-G Silicon)	Included in Package	Fairchild Controls Model No. 990571		0-140	4.7%	28 v.d.c. ± 10% 40 ma. Nominal 50 ma. Max.	2v r.m.s. Nominal at Center Freq. & No Load
Silicon Semicond. Strain	VCO	Fairchild Controls Model No. 990560 (Includes Amplif.)	$700 1-9 (Includes Amplif.)	0-140	≈3.2%	28 v.d.c. ± 10% 35 ma. Max.	Nominal 5 v.d.c. Full Scale
Semi-Conductor Strain Gage	VCO	Micro Systems Inc. Subs. Electro Optical Systems Inc. PT3C-B1 (with Driver)	$395 Unit 1-9 Price (No Amplif.)	0-140	≈2.5%	28 v.d.c. ± 4 v.d.c. at 30 ma.	0.5v Max. (No Amplif.) 10v Max. (Amplif.) 0% to Full Scale at 78°F Open Circuit
Piezo Electric Crystal	DOFL Valve	Endevco Corp. Model No. 2501 -500	$190 Unit	0-500 p.s.i.a. 2-9 kc.	<10% Amplif. Only	None	See Press. Sensitivity
Piezo Electric Crystal (Ceramic)	DOFL Valve	Model P-450M-1 Gulton Industr.	$175 Unit for 600	0.001-500 25-20 kc.		None	See Press. Sensitivity
Variable Reluctance Inductor	Hartly or Colpitts Osc:	Pace Engineering Company Model No. OP 33		0-140	6.5%	None	With Osc. ± 7.5% Freq. Deviation About Center Freq.
Variable Reluctance Transducer	VCO	Internat. Resist. Corp. Model No. 70.6206		0-140 p.s.i.a.		40 ∮06v 400 c.p.s.	0-0.5v Min. into 50k Load (400 c.p.s.)

NOTE: ALL PERCENTAGES REFER TO FULL SCALE

Fig. 40. Pressure Transducer Evaluation.

	Sensitivity				Extreme Operable Environment			
Type	Pressure	Temperature	Accel.	Vibration	Temperature	Accel.	Shock	Vibration
Silicon Semicond. Strain Gage (35-G Silicon)	0.1% p.s.i.e. Non-Linear ≤ 1% Repeatable ≤ 0.1% Long Term Stability ≤ 1%	Null Shift ≤ 0.02%/°F Sensitivity Change ≤ 0.02%/°F			-65° to 200°F Operable 0° to 150° Compensated	200g Max.	200g Max.	200g Max. to 2 kc.
Silicon Semicond. Strain	0.036v/ p.s.i.e. Nominal Tol. ≤ 2% Zero <Bal. 3% Linearity ≤ 0.25% Repeatable 0.05%	Null Shift ≤ 0.01%/°F Sensitivity Shift ≤ 0.01%/°F (Centered at 75° F)	0.007% g All Axis	≤0.007% g	-65°F to ≤250°F Operable 0 to ≤150°F Compensated	1000g Max.	1000g No Damage	35g 0-2 kc. Sine Wave
Semi-Conductor Strain Gage	0.0715v p.s.i.e. Accuracy ≤ 1% Zero Bal. 5%	Null Shift < 2% Full Scale Sensitivity <1% Full Scale	0.002% g Max.	0.002% g Peak	-65°F to 300°F Operable	2300g	2300g	35g 0-10 kc.
Piezo Electric Crystal	50-pk-mv. pk.-p.s.i. Nominal 2-9 kc. Dynamic Response 2% Linear	≤ 10% Max.		0.5pk-mg. pk.-g	-22°F to ≤ 230°F			
Piezo Electric Crystal (Ceramic)	0.25v p.s.i.	≤ 10%			-65°F to ≤ 250°F	300g		
Variable Reluctance Inductor	0.1% p.s.i.e. ≤ 2% Linearity (Inductance) Hyster. 0.5%	Zero Shift 0.04% /°F Sensitivity 0.03% /°F	0.004% g		-65°F to ≤ 250°F			
Variable Reluctance Transducer	0.36% p.s.i.e. Hyst. ≤ 0.1% Linearity ≤ 1% Repeat ≤ 0.1%				-320°F to 500°F	10og Any Axis	50og Any Axis	50g at 28-9kc

NOTE: ALL PERCENTAGES REFER TO FULL SCALE

Fig. 40. (Cont'd)

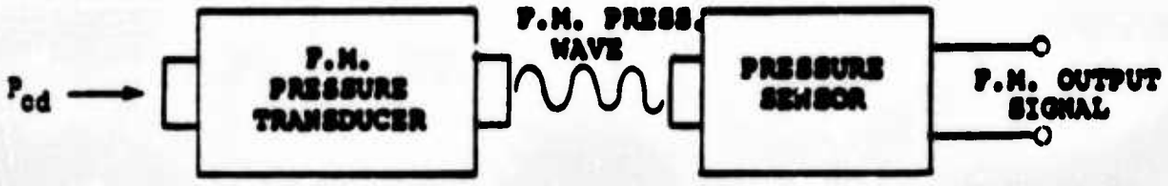

Fig. 41. Rotor Tip Fuel Control - F.M. Pressure Transducer With Sensor Pickup.

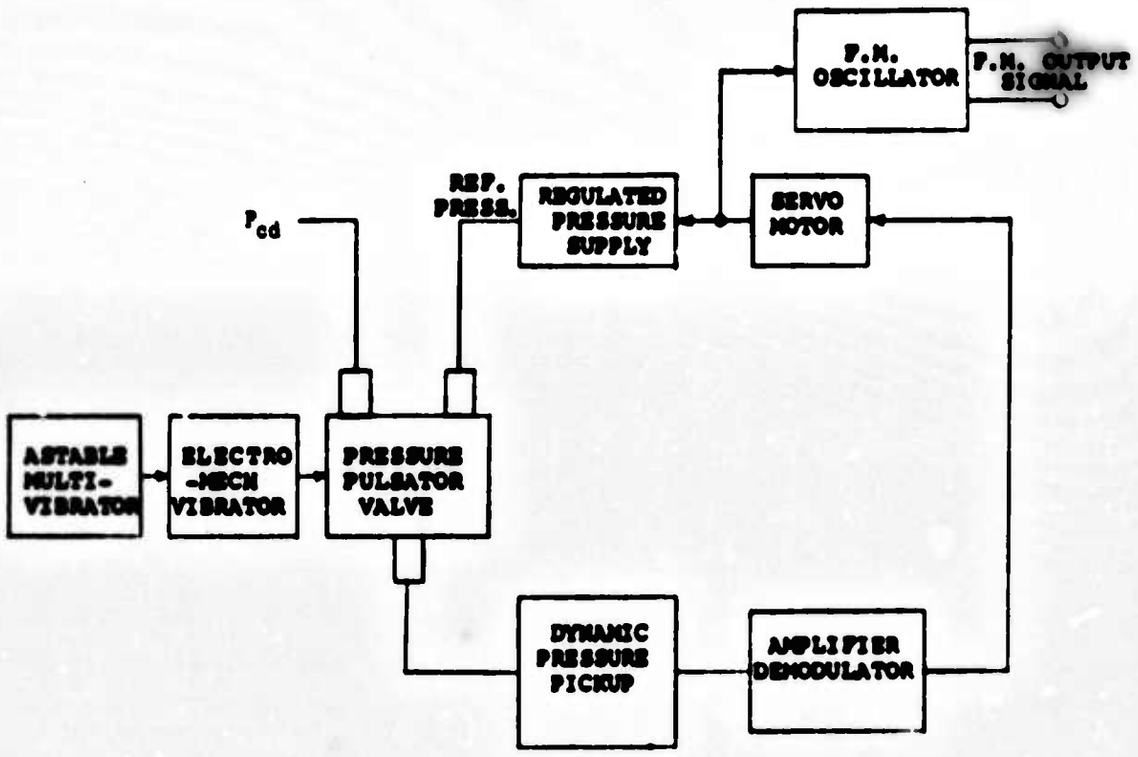

Fig. 42. Rotor Tip Fuel Control - Servo Pressure Sensor With F. M. Signal Transducer.

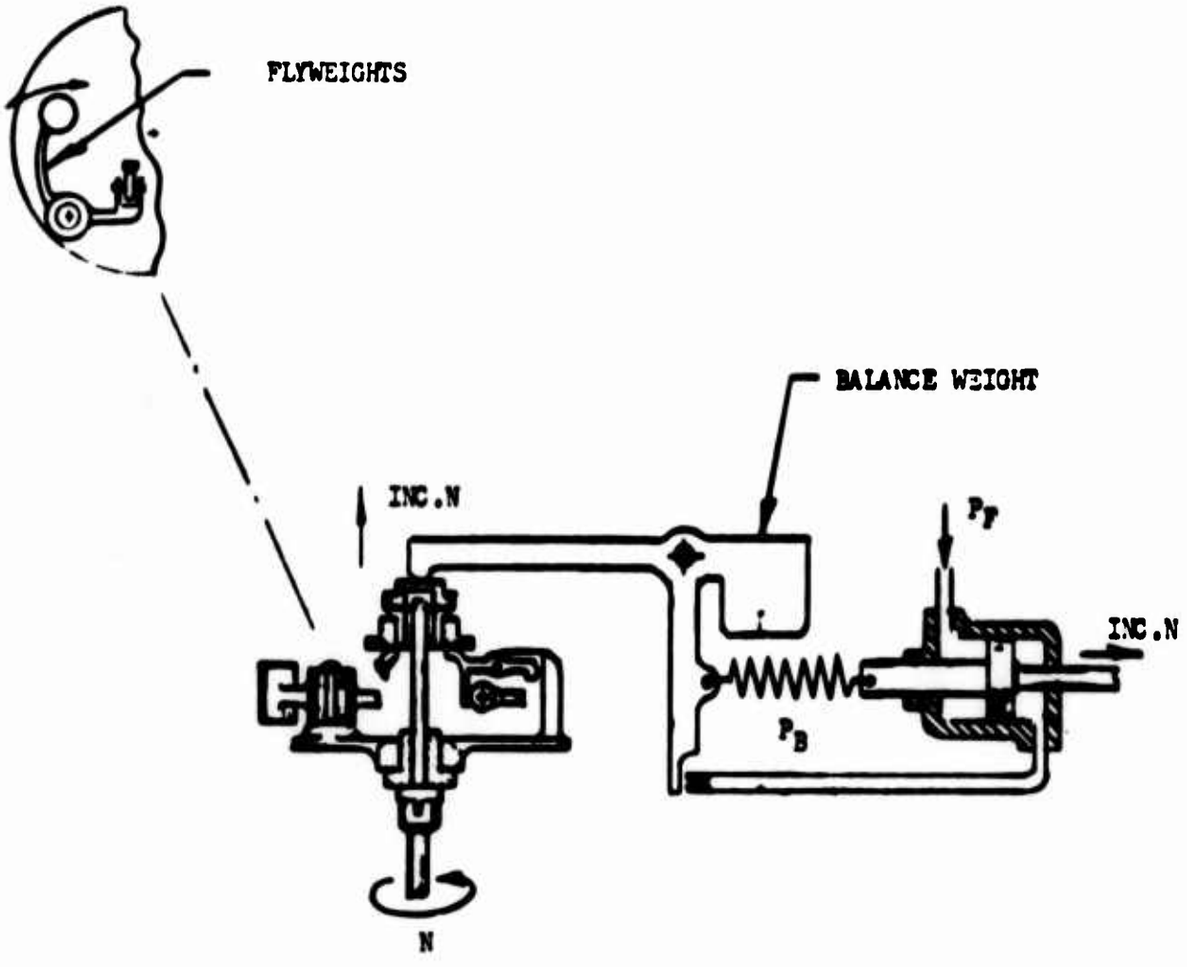

Fig. 43. Rotor Tip Fuel Control - Engine Speed Sensor and Amplifier Hydromechanical Design Schematic.

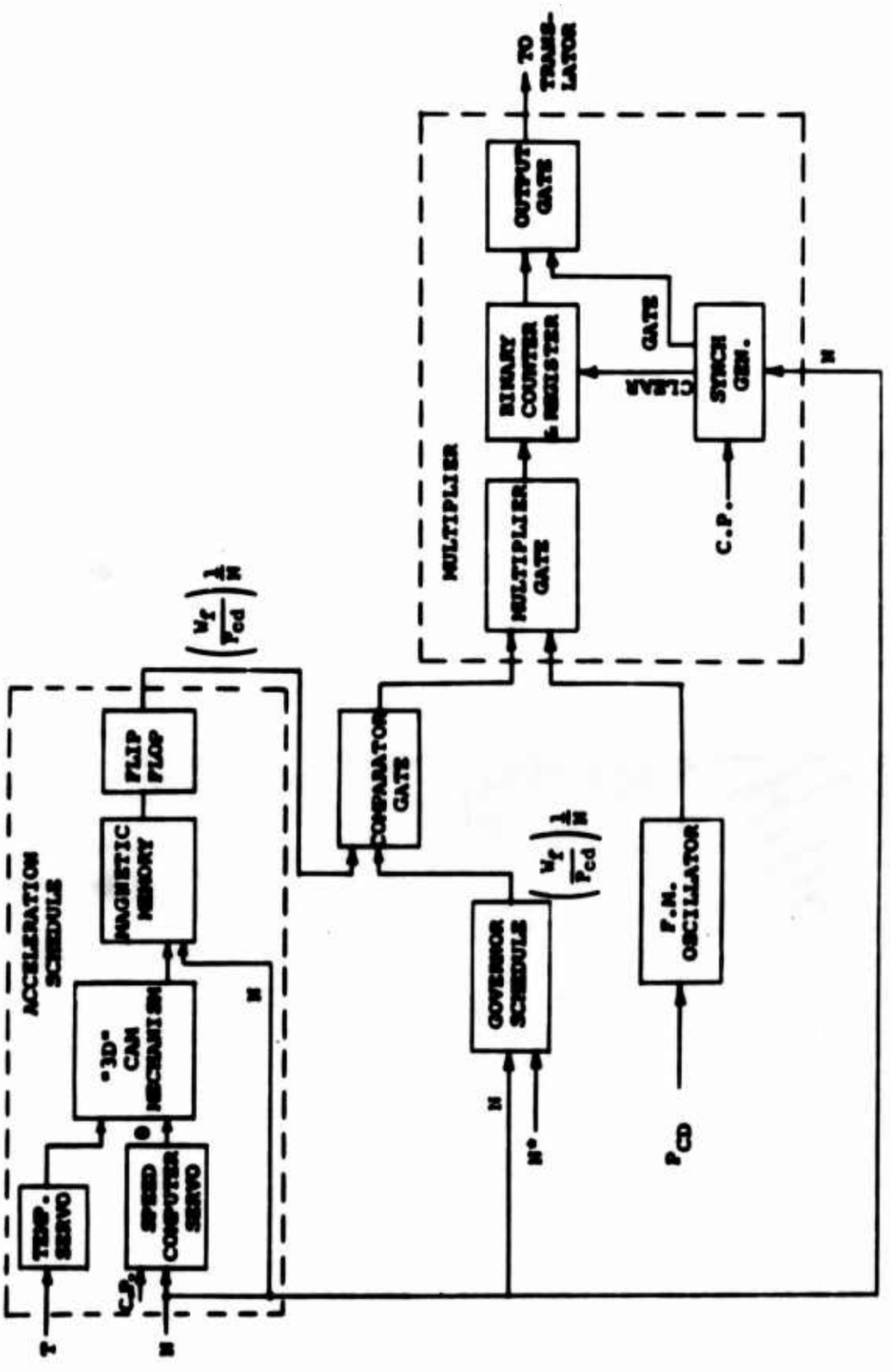

Fig. 44. Rotor Tip Fuel Control - System Block Diagram, Electronic Computer.

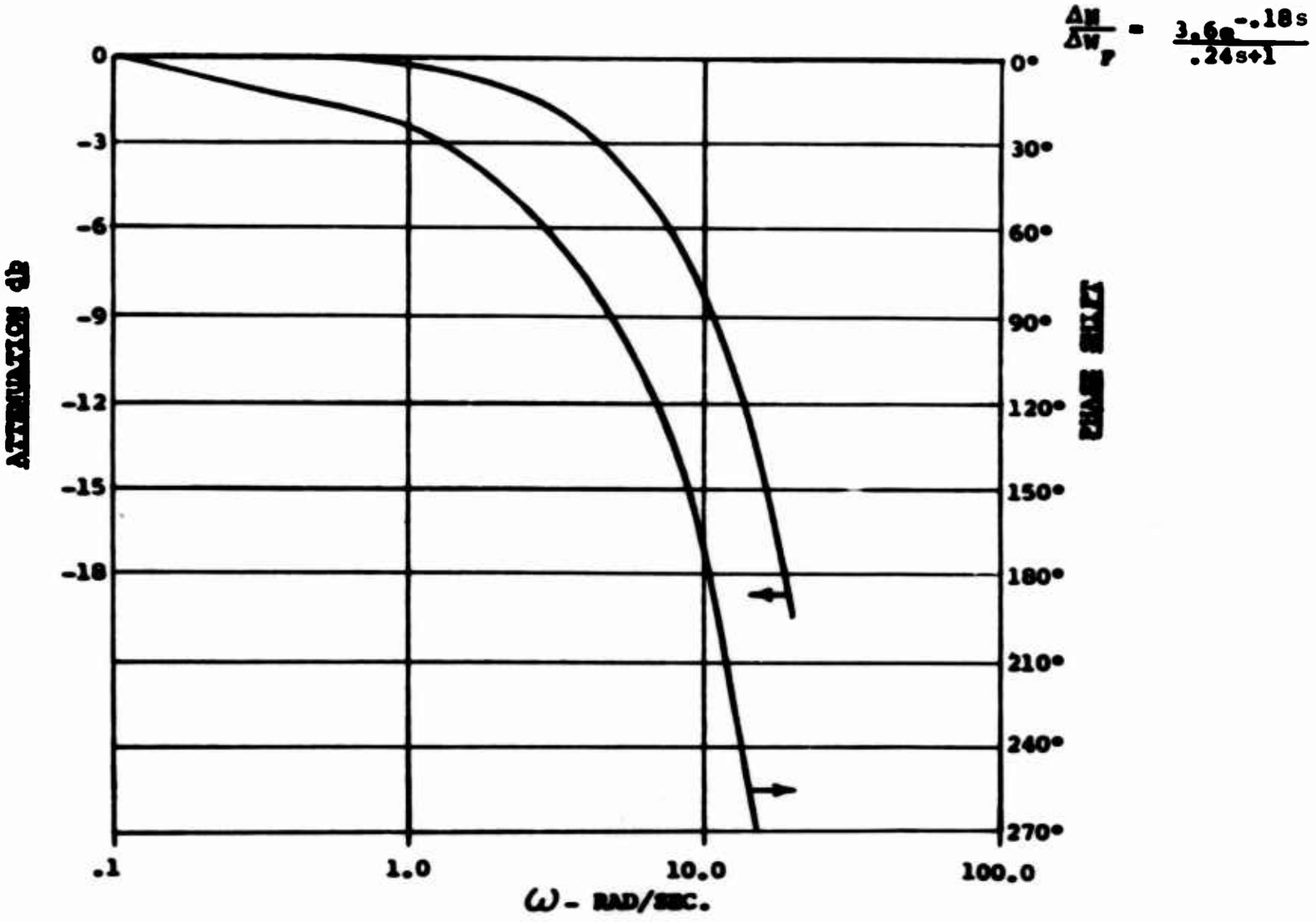

Fig. 45. Rotor Tip Fuel Control - Estimated Engine Response, Fuel Flow to Speed.

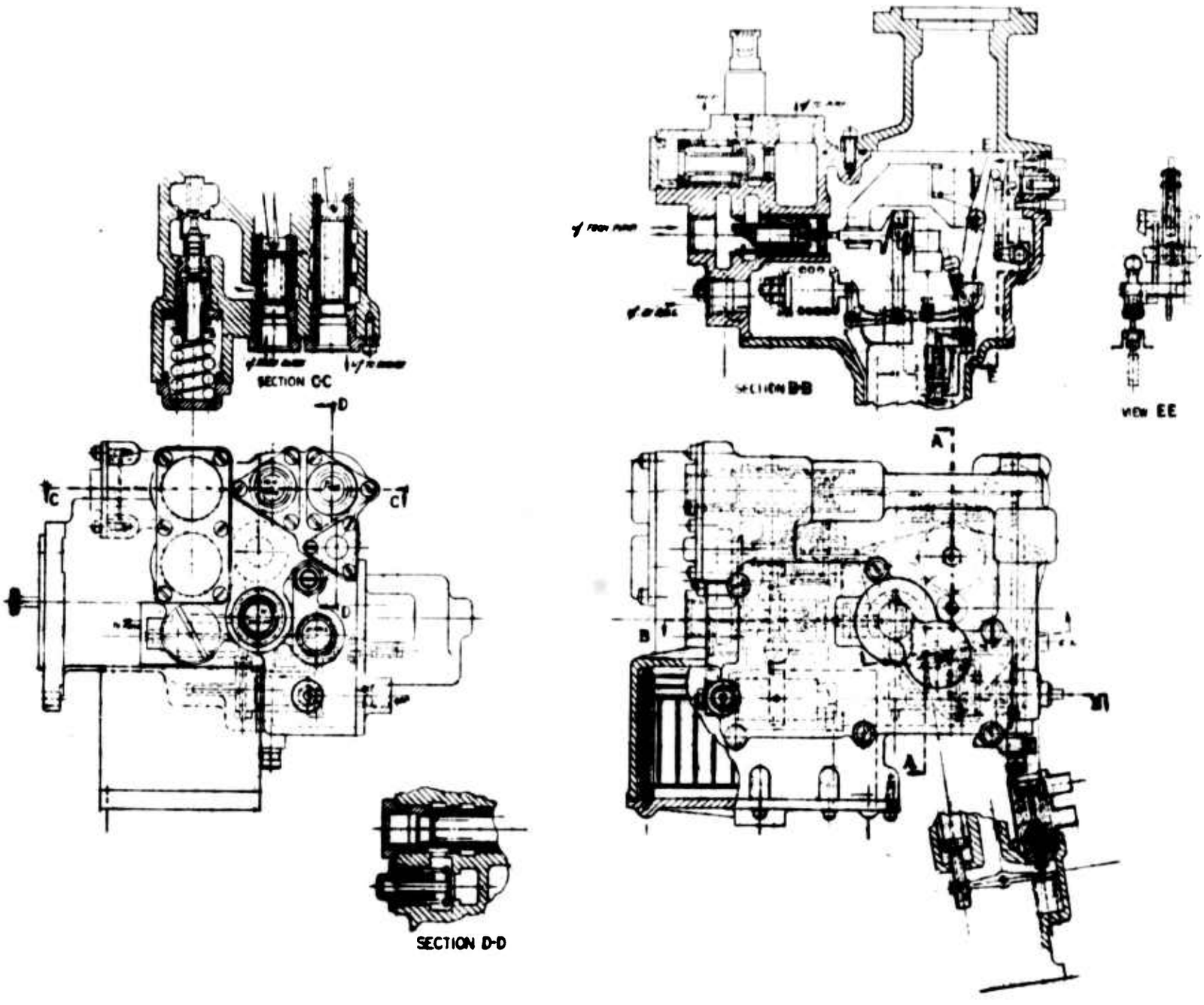

Fig. 46. Engine Fuel Control.

A

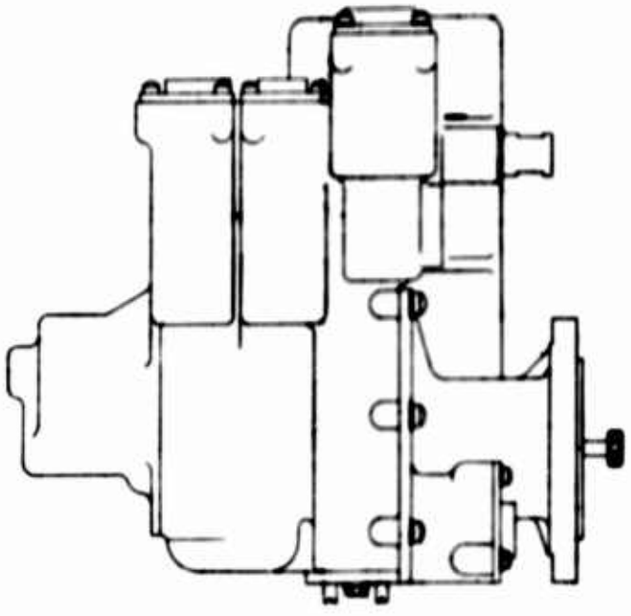

VIEW EE

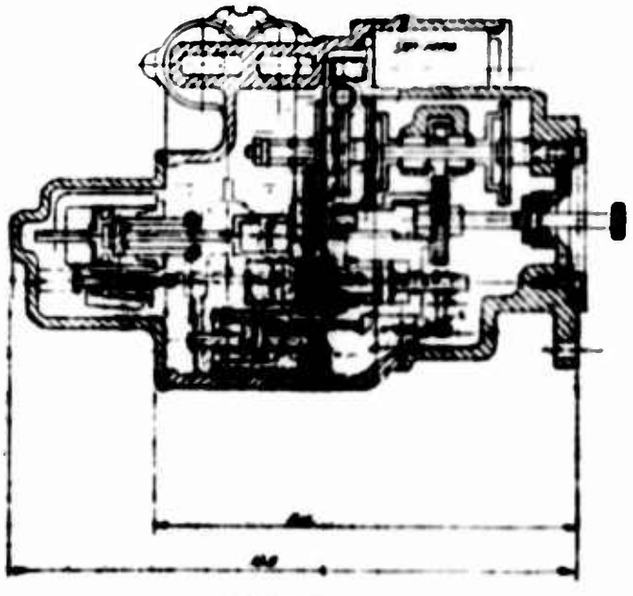

SECTION A-A

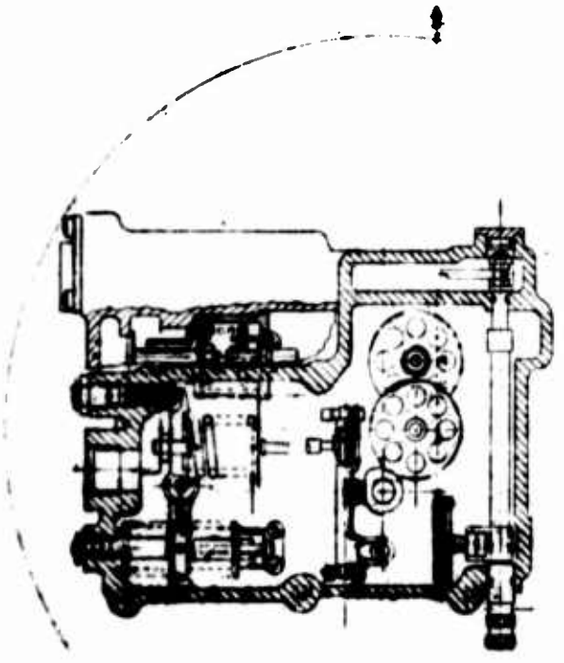

B

REFERENCES

1. Preliminary Purchase Specification No. 8-42, Fuel Control System for CAE Model 357-1 Turbojet Engine, Continental Aviation and Engineering Corporation, Detroit, Michigan, 6 August 1963.

2. Preliminary Purchase Specification No. 8-38, Fuel Control System for CAE Model 356-27 Turbojet Engine, Continental Aviation and Engineering Corporation, Detroit, Michigan, 15 April 1963.

3. Model Specification No. 2157-C, Engine, Aircraft, Turbojet: J69-T-29, Continental Model 356-7A, Continental Aviation and Engineering Corporation, Detroit, Michigan, 25 September 1958, revised 18 October 1960, with Amendment No. 1, dated 5 April 1961.

APPENDIX

g LOADING EFFECT ON SPRINGS AND BELLOWS

SPRINGS

Calculations were made to establish the effects of g loading directed laterally to the axis of the spring with regard to its axial deflections. The calculations were based on classical solutions which consider the spring as a beam with the bending moment at any section applied as either a torsion load or bending load depending upon angular location. Two extreme conditions were set up:

1. Consider the spring with fixed ends.

2. Consider the spring with pinned ends.

It is believed that the situation which will actually exist in the application will be something in between the two conditions. It is to be noted that the results of a sample calculation for a typical spring which could be used in the control is just within tolerable limits for the pinned end calculation, while well within the tolerable limits for a fixed end calculation.

Preliminary tests were conducted at CECO using several typical springs taken from our fuel controls to determine the effect of a load applied lateral to the spring axis. The spring was set in a spring testing machine and a lateral load applied at the center coil by means of a fish scale. The load was equivalent to three hundred times the weight of the spring. For a constant load there was no perceptible axial deflection of the spring. This test is actually more severe than that which exists under 300g since the load was concentrated. The results were the same for all of the springs tested, five in all.

The equations generated for the fixed end spring follow:

$$\text{Torsion Stress} = 2.09g \frac{R \rho N}{r} L^2 \qquad (1)$$

$$\text{Change in Axial Length} = 0.538 \left[g \frac{\rho}{E} \left(\frac{RN}{r} \right)^2 \right]^2 L^7 \qquad (2)$$

where g = number times gravity

R = coil radius, in.

r = wire radius, in.

ρ = wire density, lb/in.^{3}

E = wire modulus, p. s. i.

N = No. coils/inch

L = axial length

For a pinned end spring

$$\text{Torsion Stress} = 3.14g \frac{R \rho N}{r} L^2 \qquad (3)$$

$$\text{Change in Axial Length} = 13.9 \left[g \frac{\rho}{E} \left(\frac{RN}{r} \right)^2 \right]^2 L^7 \qquad (4)$$

$$\text{Change in End Slope} = 7.58g \frac{\rho}{E} \left(\frac{RN}{r} \right)^2 L^3 \qquad (5)$$

Assuming a spring of the following dimension

r = 0.075 in. N = 4.3

R = 0.54 in. ρ = 0.283 lb/in.^{3}

L = 1.4 in. E = 30 x 10^6 p. s. i.

with a 300g load applied, then

Additional stress = 16,000 p. s. i.

Axial deflection = 0.001 in.

Axial load change = 0.1 lb

Change in end slope = 0.055 radian

For the same spring with fixed ends

Additional stress = 10,700 p. s. i.

Axial deflection = 0.00004 in.

Axial load change = 0.004 lb

Change in end slope is zero.

Assume a spring to be rigidly attached to its spring supports and the spring supports mounted on a pair of ball bushings 0.5-inch long and having a 0.003-inch diametrical clearance with the shaft. Then, the largest change in end slope would be 0.006 radian. This is almost ten times less than that which would be obtained with a pinned end spring. Therefore, the performance of the springs will most nearly approach that for the fixed end calculations and the effect of the laterally applied g load will be nil.

Bellows

A similar set of calculations was performed on a bellows. However, only fixed ends were considered in this case due to the manner in which the bellows will be mounted. Also, if twc bellows are used in opposition to each other and relatively short strokes are experienced, the bellows, if affected by the g load at all, would have a cancelling effect upon one another.

The resulting equation follows:

$$f = \frac{W L^3}{24 PR_d^2}, \text{ inches} \qquad (6)$$

$$W = 2gt \quad (d + i), \text{ lb/in.} \qquad (7)$$

where

f = deflection at mid-section, inches

L = length of active portion of bellows, inches

P = length of one convolution (pitch), inches

R = spring rate per convolution, lb/in.

W = empirical loading due to acceleration (g), lb per inch of bellows length.

t = bellows wall thickness, inches

i = bellows inside diameter, inches

For a typical bellows design

Bellows OD = 0.750 inch, ID = 0.570 inch,
Effective area = 0.34 sq. inch

Pressure rating = 186 p.s.i.

Wall = 0.0025 in.

Stroke = 0.100 in.

Convolutions = 9, of 0.048 in. pitch = 0.432 active length

Spring rate of a single bellows = 41.6 lb/in.

Mass per unit length of the bellows = 0.0066 lb

Then the lateral deflection at 300g, using Equations 6 and 7, will be 0.00066 inch. This results in an axial deflection of 2.1×10^{-6} inches or a force change of 88×10^{-6} pounds; obviously a negligible amount.

Unclassified

Security Classification

DOCUMENT CONTROL DATA - R&D

(Security classification of title, body of abstract and indexing annotation must be entered when the overall report is classified)

1. ORIGINATING ACTIVITY (Corporate author) Hiller Aircraft Company, Inc. Continental Aviation & Engineering Corporation Chandler-Evans Corporation	2a. REPORT SECURITY CLASSIFICATION Unclassified 2b. GROUP

3. REPORT TITLE

Heavy-Lift Tip Turbojet Rotor System, "Fuel Pump and Control System Design" Volume XII

4. DESCRIPTIVE NOTES (Type of report and inclusive dates)

5. AUTHOR(S) (Last name, first name, initial)

6. REPORT DATE	7a. TOTAL NO. OF PAGES	7b. NO. OF REFS
October 1965	141	3

8a. CONTRACT OR GRANT NO.	9a. ORIGINATOR'S REPORT NUMBER(S)
DA 44-177-AMC-25(T) b. PROJECT NO. Task 1M121401D14412 c. d.	USAAVLABS Technical Report 64-68L 9b. OTHER REPORT NO(S) (Any other numbers that may be assigned this report) CAE Report No. 943

10. AVAILABILITY/LIMITATION NOTICES

Qualified requesters may obtain copies of this report from DDC.
This report has been furnished to the Department of Commerce for sale to the public.

11. SUPPLEMENTARY NOTES	12. SPONSORING MILITARY ACTIVITY
	US Army Aviation Materiel Laboratories Fort Eustis, Virginia

13. ABSTRACT

Volume XII of Heavy-Lift Tip Turbojet Rotor System discusses the proposal of a combination hydromechanical-electronic fuel control and fuel pump for control of a helicopter rotor tip mounted engine (CAE Model 357-1) which during normal operation is subjected to 235g of centrifugal force. The proposed preliminary design is submitted to meet the specification requirement of the engine in the tip turbojet hover mode of operation. Analytical design studies and preliminary test results show feasibility of this design for operation in a 235g field.

DD FORM 1 JAN 64 1473

Unclassified

Security Classification

Unclassified

Security Classification

14. KEY WORDS	LINK A		LINK B		LINK C	
	ROLE	WT	ROLE	WT	ROLE	WT
Fuel Pump Control System						

INSTRUCTIONS

1. **ORIGINATING ACTIVITY:** Enter the name and address of the contractor, subcontractor, grantee, Department of Defense activity or other organization *(corporate author)* issuing the report.

2a. **REPORT SECURITY CLASSIFICATION:** Enter the overall security classification of the report. Indicate whether "Restricted Data" is included. Marking is to be in accordance with appropriate security regulations.

2b. **GROUP:** Automatic downgrading is specified in DoD Directive 5200.10 and Armed Forces Industrial Manual. Enter the group number. Also, when applicable, show that optional markings have been used for Group 3 and Group 4 as authorized.

3. **REPORT TITLE:** Enter the complete report title in all capital letters. Titles in all cases should be unclassified. If a meaningful title cannot be selected without classification, show title classification in all capitals in parenthesis immediately following the title.

4. **DESCRIPTIVE NOTES:** If appropriate, enter the type of report, e.g., interim, progress, summary, annual, or final. Give the inclusive dates when a specific reporting period is covered.

5. **AUTHOR(S):** Enter the name(s) of author(s) as shown on or in the report. Enter last name, first name, middle initial. If military, show rank and branch of service. The name of the principal author is an absolute minimum requirement.

6. **REPORT DATE:** Enter the date of the report as day, month, year; or month, year. If more than one date appears on the report, use date of publication.

7a. **TOTAL NUMBER OF PAGES:** The total page count should follow normal pagination procedures, i.e., enter the number of pages containing information.

7b. **NUMBER OF REFERENCES:** Enter the total number of references cited in the report.

8a. **CONTRACT OR GRANT NUMBER:** If appropriate, enter the applicable number of the contract or grant under which the report was written.

8b, 8c, & 8d. **PROJECT NUMBER:** Enter the appropriate military department identification, such as project number, subproject number, system numbers, task number, etc.

9a. **ORIGINATOR'S REPORT NUMBER(S):** Enter the official report number by which the document will be identified and controlled by the originating activity. This number must be unique to this report.

9b. **OTHER REPORT NUMBER(S):** If the report has been assigned any other report numbers *(either by the originator or by the sponsor)*, also enter this number(s).

10. **AVAILABILITY/LIMITATION NOTICES:** Enter any limitations on further dissemination of the report, other than those imposed by security classification, using standard statements such as:

(1) "Qualified requesters may obtain copies of this report from DDC."

(2) "Foreign announcement and dissemination of this report by DDC is not authorized."

(3) "U. S. Government agencies may obtain copies of this report directly from DDC. Other qualified DDC users shall request through

_____."

(4) "U. S. military agencies may obtain copies of this report directly from DDC. Other qualified users shall request through

_____."

(5) "All distribution of this report is controlled. Qualified DDC users shall request through

_____."

If the report has been furnished to the Office of Technical Services, Department of Commerce, for sale to the public, indicate this fact and enter the price, if known.

11. **SUPPLEMENTARY NOTES:** Use for additional explanatory notes.

12. **SPONSORING MILITARY ACTIVITY:** Enter the name of the departmental project office or laboratory sponsoring *(paying for)* the research and development. Include address.

13. **ABSTRACT:** Enter an abstract giving a brief and factual summary of the document indicative of the report, even though it may also appear elsewhere in the body of the technical report. If additional space is required, a continuation sheet shall be attached.

It is highly desirable that the abstract of classified reports be unclassified. Each paragraph of the abstract shall end with an indication of the military security classification of the information in the paragraph, represented as *(TS)*, *(S)*, *(C)*, *or (U)*.

There is no limitation on the length of the abstract. However, the suggested length is from 150 to 225 words.

14. **KEY WORDS:** Key words are technically meaningful terms or short phrases that characterize a report and may be used as index entries for cataloging the report. Key words must be selected so that no security classification is required. Identifiers, such as equipment model designation, trade name, military project code name, geographic location, may be used as key words but will be followed by an indication of technical context. The assignment of links, rules, and weights is optional.

Unclassified

Security Classification

8304-68